Reliability of Shear-Critical Reinforced Concrete Members

by

Victor Hugo Aguilar Vidal

A dissertation submitted to the Graduate Faculty of
Auburn University
in partial fulfillment of the
requirements for the Degree of
Doctor of Philosophy

Auburn, Alabama
May 2, 2020

Keywords: one-way shear strength, reinforced concrete, reliability of structures, reliability-based calibration, strut-and-tie

Approved by

Andrzej S. Nowak, Committee Chair, Professor and Chair of Civil Engineering
Robert W. Barnes, Committee Co-chair, Associate Professor of Civil Engineering
J. Michael Stallings, Professor of Civil Engineering
Justin D. Marshall, Associate Professor of Civil Engineering
Jorge Valenzuela, Professor of Industrial and System Engineering

Abstract

Recent research on one-way shear strength and strut-and-tie design approach has led to updates in the *ACI 318 Building code requirements for structural concrete*. The changes in one-way shear design provisions in ACI 318-19 are significant enough to suspect that a new reliability-based calibration is warranted. For the case of strut-and-tie design procedure, a reliability-based calibration had never been done.

This dissertation is divided into three manuscripts connected by two broad topics: shear strength of concrete members and reliability of structures. Available databases and published literature were reviewed and used to quantify uncertainties in material properties, member dimensions, and analysis methods. Statistical tools were used to investigate the accuracy of recently published methods for one-way shear strength, as well as the accuracy of the strut-and-tie modeling approach. Reliability analysis was extensively applied to study the safety margins of concrete members and to calibrate strength reduction factors for available design procedures.

The findings of the work presented in this dissertation are expected to be useful for reinforced concrete designers and for code developers.

Acknowledgments

While navigating life, I met so many people that helped me right at the moment I needed it the most; I could write another hundred pages just listing them, let me say thanks to all the people who have supported me to complete my doctoral degree directly or indirectly.

I would like to express my special gratitude to my advisor, Professor Andrzej Nowak, for giving me the unique opportunity to pursue a Ph.D. degree at Auburn University. Thank you for supporting me and involving me in interesting projects. I am proud of being Dr. Nowak's 41st doctoral student. Besides my advisor, I received great help from my co-advisor, Dr. Robert Barnes, to whom I would like to express my sincere gratitude for his continuous support, his patience, his contributions to my work, and his immense knowledge. It was a great privilege and honor to work and study under their guidance.

I would also like to say thanks to my committee for their encouragement: Dr. Justin Marshall, Professor Mike Stallings, and Professor Jorge Valenzuela. I had the privilege of learning from Dr. Marshall's classes. I did my master's under the outstanding Professor Stallings, which in addition to be a great academic he is also a caring wonderful person. And I was lucky enough to meet Professor Valenzuela, who supported me in the admission process at the very beginning of this long and challenging path.

This research would have been impossible without the data received from the *Joint ACI-ASCE committee 445* shared by Dr. Karl-Heinz Reineck (University of Stuttgart, Germany). Also, Dr.

Nowak and Dr. Barnes's databases were of great help. So, your contributions are very much appreciated.

The Department of Civil Engineering at Auburn University is formed by a selected talented group of faculties that were always happy to provide encouragement, insightful comments, and excellent research questions. In addition, we count on a wonderful administrative staff that takes good care of us.

Once I first came to Auburn, Marek received me and guided me around while I was trying to do the check-in paperwork; without him, I might still be lost on campus. Later, I met Anjan, who helped me sort out so many things that were just impossible for me to understand. Eventually, we became roommates and great friends, and I hope we will keep our friendship forever. Along came Patrik Z., Golpar (Oh! What would it be of me if I did not meet you?), Lester and Megan, y'all were a great support when I had nobody to rely on. Living in Auburn for more than four years, I made many good friends that made Auburn a great place to be: Lester, Marek & family, Olga & Pavlo, Patryk & Navideh, Marta, Yalin, Haofan, Katy, MaryBeth, Debbie, Ivan, Gabriel and the Chileans that later came along. A special thanks to those that were the closest and stay the longest with me: Anjan, Mauricio, Golpar & Charles, Paty & Pablo, and Wu. And those that helped with the last push: Karina and Sylwia.

I am enormously grateful to my parents, Margarita and Hugo, and sister, Carla, for their love, prayers, caring, and sacrifices. Whom would have thought that a modest family as ours would manage to educate two civil engineers and one with a Ph.D. Since always, this has been a family effort that I am genuinely and sincerely grateful of having you. A kiss to my grandmother, Blanca, who is taking care of me from the Heavens, together with my grandfather, Guillermo.

Dedicated to my family

Table of Contents

List of Tables

List of Figures

Chapter 1

INTRODUCTION

1.1 MOTIVATION

When *Concrete International* dedicated a full issue[1] to present proposals for new one-way shear strength equations for the *ACI 318 Building code requirements for structural concrete*, several questions arise: why do we need a new one-way shear equation? Which of the prospective models is the best? Does the current strength reduction factors need an update? These questions guided the development of Chapter 2 and Chapter 3 of this dissertation. In 2019, the new ACI 318 building code requirements included a new set of empirical shear design equations not presented in the aforementioned *Concrete International* issue. However, the shear strength reduction factor was not modified, despite the fact that the new approach is more accurate than the traditional long-standing shear design equations. Once shear in reinforced concrete becomes of interest, it did not take long before the strut-and-tie topic came along. All strength reduction factors (also called resistance factors) in ACI 318-19[2] strut-and-tie design specifications are set as $\phi = 0.75$, regardless that the strength of nodes and struts depends on concrete compressive strength and tie strength depends on the steel yield stress, and those material properties have very different levels of variability. Therefore, all strength reduction factors being equal does not seem logical; moreover, in other design guides and codes[3,4], the specifications for nodes and struts strength as well as the resistance factors are significantly different from ACI 318. Thus, strut-and-tie is the focus of Chapter 4 of this document. Since 2014, the strut-and-tie method it is no longer just an appendix the ACI 318 building code requirements, it was included as part of the specification, which shows

the structural engineering community has an interest in this topic as well. The reader can notice that the strength reduction factors are the concern in one-way shear and strut-and-tie shear design. Load and resistance factors design are ideally calibrated based on probabilistic considerations of the load components, and the uncertainties involved in the resistance mechanism of the structural members. This probabilistic approach is known as reliability analysis, and it is the connecting concept of the topics of this dissertation: *reliability of shear-critical reinforced concrete members*. Chapter 2 studies the accuracy of several methods to predict the one-way shear strength of slender beams. Chapter 3 proposes a reliability-based set of strength reduction factors for the new ACI 318-19[2] one-way shear design specification. And, Chapter 4 is the first look at a reliability-based calibration of the strut-and-tie design method for the ACI 318 building code requirements.

1.2 PROBLEM STATEMENT

Three problems related to shear-critical structures and the reliability of those are identified and described in this section. These are then studied in the following chapter of the dissertation.

1. There are several one-way shear methods available in the literature as a result of an extensive research effort made by the Joint *ACI-ASCE Committees 445*, *ACI Subcommittee 318-E*, and many researchers. Unfortunately, those models in the literature lack documented studies about their accuracy, and therefore they cannot be used in practice. Some applications require a higher level of precision than traditional building design, e.g., structural evaluation of existing constructions and forensic engineering. Therefore, it is desirable to make the models developed by researchers available for use. Thus, different levels of model complexity and accuracy could be available for designers, and they can select the model that fits the best their analysis and design needs.

2. The one-way shear design equations for reinforced concrete members in the ACI 318 building code requirements had remained essentially unchanged since 1963, until the publication of ACI 318-19[2]. The new design method is more accurate that is predecessor; however, the strength reduction factor for shear design was maintained as it was. Therefore, the concrete industry is not taken full advantage of the new improved one-way shear equations, and a new reliability-based calibration is needed.

3. The strut-and-tie design approach has gained importance in reinforced concrete design practice in the US in the last two decades. Strut-and-tie has proven very useful for designing shear-critical structures where beam theory is not applicable. The resistance factors specified for the strut-and-tie method has not been calibrated based on reliability analysis. Therefore, the safety margin of structural members designed with ACI 318 strut-and-tie specifications is unknown. Moreover, the current resistance factors might favor non-ductile failure modes.

1.3 BACKGROUND

This dissertation deals with two broad topics: (1) Shear in reinforced concrete members and (2) reliability of structures. Shear can be further subdivided into two categories, shear in slender members and shear in deep members. This section provides the necessary background for the reader to be familiarized with the concepts used throughout the research.

1.3.1 Shear in slender reinforced concrete members

A simply supported beam subjected to a downward vertical load, like the one shown in **Fig. 1.1a** will develop internal bending moments and shear forces. Then, normal compression stresses occur above the neutral axis, whereas tensile stresses take place below the neutral axis. From principles

of classical mechanics of materials, the normal stress *(f)* cause by bending moment and the shear stress *(v)* caused by the shear force can be calculated as follows:

$$f = \frac{My}{I} \tag{1}$$

$$v = \frac{QV}{Ib} \quad Q = A'\bar{y}' \tag{2}$$

where M is the bending moment at a given cross section; y is the distance from the element to the neutral axis; and I is the moment of inertia of the cross-sectional area calculated about the neutral axis; and the neutral axis is the location of the fiber where f is equal to zero. V is the shear force at the cross section; b is the width of the member's cross section at the point where v is to be determined; A' is the area of the top or bottom portion of the member's cross section above or below the section plane where b is measured; and y' is the distance from the neutral axis to the centroid of A'.

The shear force *(V)* is the internal force resultant of all the vertical forces acting on a beam, at the section under consideration, and it tends to cut or shear the beam. The shear force creates both vertical and horizontal stresses. To clarity, consider the state of pure shear stress shown in **Fig. 1.2a.** The vertical shear stresses are equal and opposite on the two vertical faces because of equilibrium. If these were the only two stresses present, the element would rotate. Therefore, there must exist equal and opposite horizontal shear stresses on the horizontal faces and of the same magnitude as the vertical shear stresses.

Eq. (1) and **Eq. (2)** imply that all points along the length of the beam, where the shear and bending moment are not equal to zero, and at locations other than the extreme fiber or neutral axis are subjected to both shearing stresses and bending stresses. The typical distribution of stresses is shown in **Fig. 1.1b.**

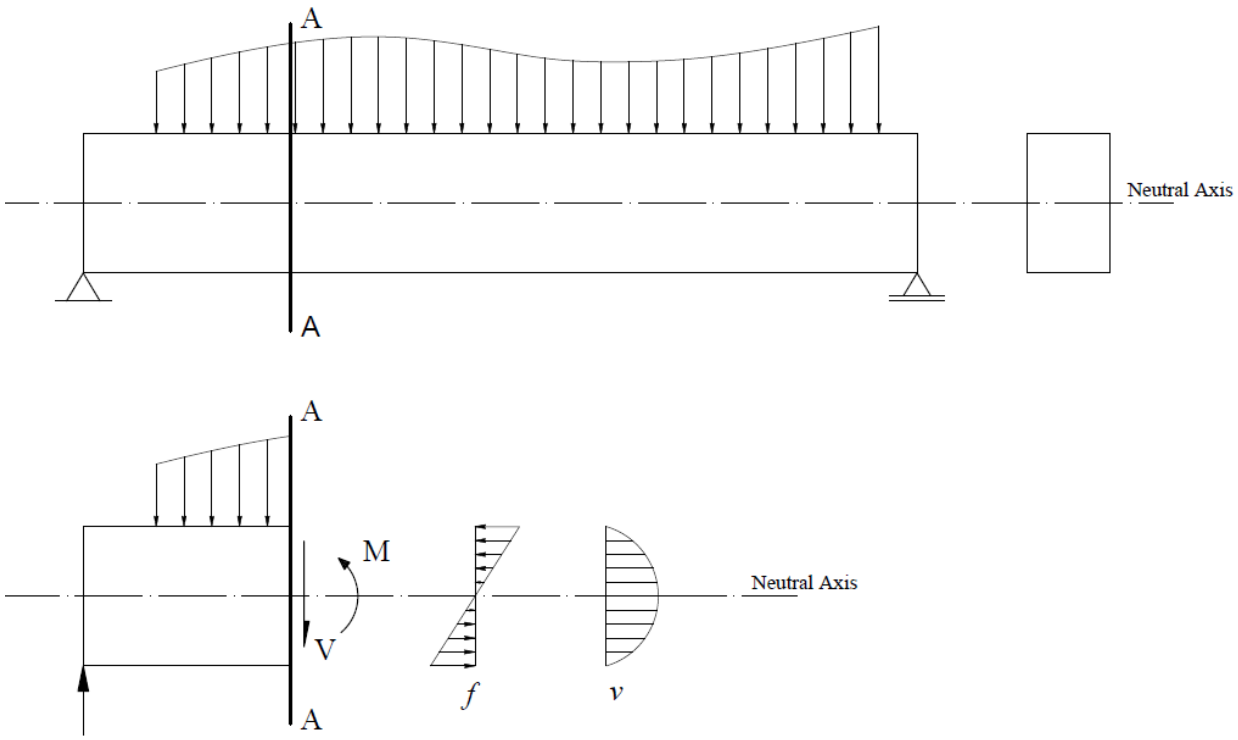

Fig. 1.1 Stress distribution for a typical homogeneous rectangular beam

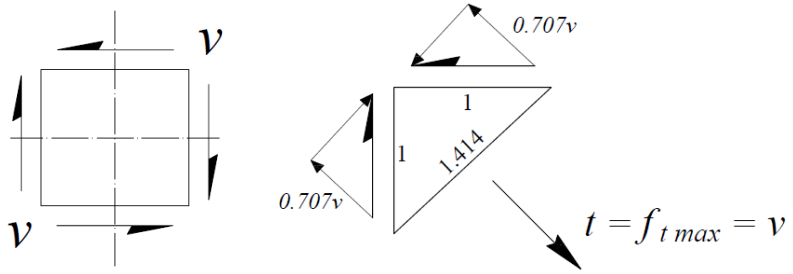

(a) (b)

Fig. 1.2 Equilibrium at 45° cut

For elements with both normal and shear stresses acting, an equivalent principal state of stress can be found. The maximum and minimum normal stresses exist on two perpendicular planes with no shear stress. These planes are called the principal planes, and the stresses acting on

them are called principal stresses. Using Mohr's circle analysis, it can be shown, that the principal stresses in a beam subjected to shear and bending may be calculated using the following equations:

$$f_{t\max} = \frac{f}{2} + \sqrt{\left(\frac{f}{2}\right)^2 + v^2} \tag{3}$$

$$f_{c\max} = \frac{f}{2} - \sqrt{\left(\frac{f}{2}\right)^2 + v^2} \tag{4}$$

where f_{tmax} is the principal tension stress; and f_{cmax} is the principal compression stress. The orientation of the principal planes may be calculated using the following formula:

$$\tan 2\alpha = \frac{2v}{f} \tag{5}$$

where α is the angle measured from the beam axis.

As the bending moment and the shear force vary along the length of the beam, the magnitude of the shearing stresses and bending stresses vary also, and they vary with distance from the neutral axis, as well. Therefore, the inclination of the principal planes, as well as the magnitude of the principal stresses will vary along the length of the beam and with high within the cross section.

Consider **Fig. 1.1** again, if a theoretical cut A-A is done, the internal forces and its corresponding stresses can be found. Let us insolate a small square unit element from above the neutral axis, at the neutral axis, and below the neutral axis. **Fig. 1.3** shows the stress state and the corresponding principal stresses.

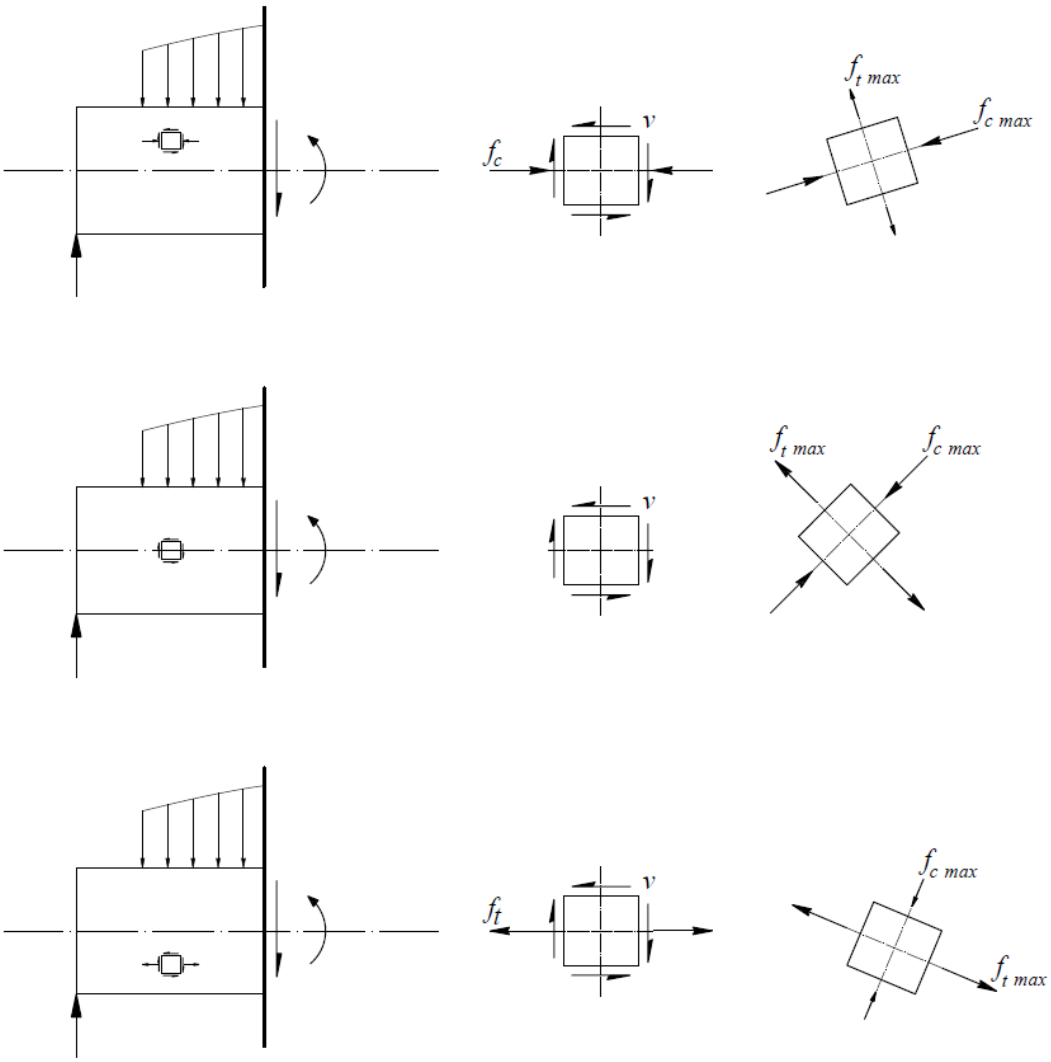

Fig. 1.3 Diagonal stresses in a homogenous beam

The principal tensile stress $f_{t\,max}$ is nearly equal to the longitudinal stress f_t if the shear stress is small. And, $f_{t\,max}$ is nearly equal to the shear stress v if the longitudinal tensile stress f_t is small. At the neutral axis, the principal stresses will occur at a 45° angle. This may be verified substituting $f = 0$, from which $\tan 2\alpha = \infty$ and $\alpha = 45^{\circ}$. In addition, the state of stress of pure shear at the neutral axis can be analyzed by creating a cut in 45° along the diagonal, as indicated in **Fig. 1.2b**. By equilibrium $1.414t = 0.707v + 0.707v \Rightarrow t = v$; therefore, at the neutral axis, the compressive

stress and tensile stress are equal in magnitude to the shearing stress. These stresses historically have been designated as diagonal compression and diagonal tension. The concrete can easily withstand the diagonal compression, but since concrete is weak in tension, when the diagonal tensile stress becomes excessive, it produces diagonal tensile crack. Thus, the principal tensile stress and the diagonal tension are correlated to the classical cracking pattern observed in concrete beams (see **Fig. 1.4)**.

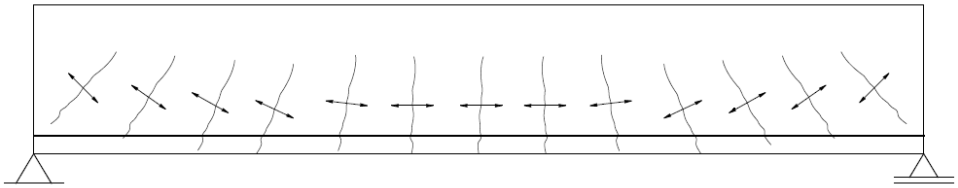

Fig. 1.4 Principal tensile stress and cracking (Adapted from Wang and Salmon[5])

1.3.1.1 Behavior of members without web reinforcement

In areas of large bending moment, when the principal tensile stress exceeds the rupture modulus $f_r = 7.5\sqrt{f_c'}$, cracks open almost perpendicular to the axis of the beam. These types of cracks are called flexural cracks. It is assumed that when the shear stress reaches the critical stress $2\sqrt{f_c'}$, the concrete cracks diagonally. Thus, high shear stress on a beam results in the opening of inclined cracks. In areas of high shear force, inclined cracks develop as an extension of the previously opened flexural cracks, and they are called flexural-shear cracks.

The distance between load and reaction is termed shear span *(a).* The behavior of beams failing in shear varies widely depending on the slenderness of the beam, that is, the shear span to depth ratio (*a/d*). Essentially, there are two types of failure that can occur: (1) diagonal tension

failure when *a/d* is between 2.5 and 6, and (2) shear failure mode that can be shear-compression or shear-tension failure when *a/d* is between 1.0 and 2.5 (these failures are discussed later, in the section about shear behavior of deep members). These are brittle failure modes, which have relatively small deflection at failure. Very slender beams, with *a/d* ratio larger than six, will normally fail in flexure prior to the formation of inclined cracks. **Fig. 1.5** shows the diagonal tension failure mode schematically. The diagonal tension failure requires ample room for a full diagonal crack to develop. Cracking starts with the development of a few fine vertical flexural cracks at areas of large bending moment, followed by the formation of more flexural cracks along the length of the beam. Flexural cracks destroy the bond between concrete and reinforcing steel; cracks also disrupt the horizontal shear flow from the longitudinal steel to the compression zone. Then, diagonal flexure-shear cracks open and widens into a principal diagonal tension crack that extends to the top compression fibers of the beam[5–7]. Wight and MacGregor[8] explain that beams without web reinforcement will fail when diagonal tension cracking occurs or shortly afterward. For this reason, the shear capacity of such members is taken equal to the shear force that causes inclined cracking. The inclined cracking load (shear strength) of a beam is affected by several variables as the tensile strength of concrete, the aggregate size, the longitudinal reinforcement ratio, and the size of the beam. The last two, which are the most controversial, are described in the following subsections, after a brief presentation of the shear resistance mechanism.

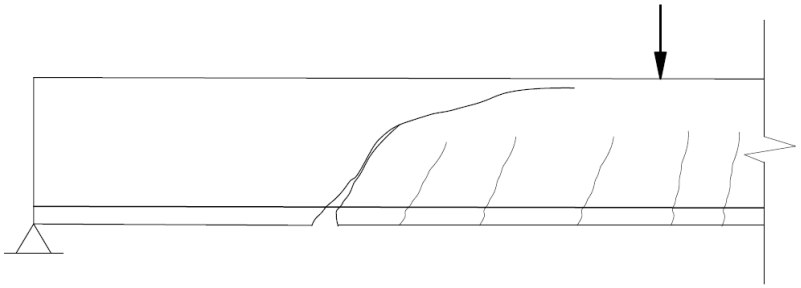

Fig. 1.5 Diagonal tension failure in a slender member

1.3.1.2 Resistance mechanism

Numerous factors affect the shear strength and the formation of diagonal cracks. A definitive conclusion regarding a shear resistance model is difficult to achieve. Over time, several shear resistance models have been proposed: e.g., the tooth model[9,10], modified compression field theory[11], multi-action model[12–14], fracture mechanics[15], and models based on the depth of the compression zone[16–18]. Nevertheless, it is accepted that the transfer of shear in reinforced concrete members without web reinforcement occurs by a combination of the following mechanisms[5,19]:

1. Shear resistance of the uncracked concrete.
2. Aggregate interlock force tangentially along the crack. Frictional force due to the irregular interlocking of the aggregate along the rough concrete surfaces on each side of the crack.
3. Dowel action, the resistance of the longitudinal reinforcement to transverse force.

Wang and Salmon[5] describe that for rectangular beams without web reinforcement after an inclined crack forms, about 20–40 percent of the shear is transferred by the uncracked compression zone, about 15–25 percent by doweling action of the flexural reinforcement, and about 33–50 percent by aggregate interlock along cracks.

1.3.1.3 Influence of longitudinal tension reinforcement ρ_w

Conceptually, when ρ_w is small, flexural cracks extend higher into the beam and open wider than would be in the case for large values of ρ_w. An increase in crack width causes a decrease in the maximum values of shear that is transferred across the inclined cracks by dowel action and by aggregate interlock[8]. Several experimental studies of the influence of the longitudinal

reinforcement ratio have been carried out[11,20–22]. Nevertheless, there is no consensus among researchers on how to consider the effect of the longitudinal reinforcement in the shear strength of beams. One-way shear models for slender reinforced concrete members developed by several research groups differ in the treatment of longitudinal reinforcement. Some models relate the shear strength directly to the geometric reinforcement ratio, while others consider the influence of reinforcement strain or stress[21]. Slenderness ratio (*a/d* or *M/Vd*) and ρ_w are commonly included in the one-way shear equations simultaneously. Since the bending moment determines the amount of longitudinal reinforcement needed, the bending moment acting at the cross section then is accounted for twice. ACI 318-14[23] empirical equations include both, slenderness ratio and longitudinal reinforcement ratio, while ACI 318-19[2], also empirical, does not include the slenderness ratio as a variable for determining the shear strength, and this is taken proportional to $\rho_w^{1/3}$. Bentz and Collins[24] proposal relies on the longitudinal strain, which depends on the bending moment, among other forces, and the amount of longitudinal reinforcement. Cladera et al.[14], Frosch et al.[25], Li et al.[26], and Park and Choi[17] utilize the depth of compression, which depends on the amount of longitudinal reinforcement. Reineck[10] proposal for shear prediction suggests that shear strength is proportional to $\rho_w^{1/3}$, and Cladera and Mari[27] state that shear strength is proportional to $\rho_w^{1/2}$, based on a trained neural network model.

1.3.1.4 Influence of beam size

The shear stress at failure of a reinforced concrete beam without web reinforcement decreases considerably as the overall depth of the beam increases. This effect is generally called the size effect. The influence of member size on shear strength is one of the most debated issues.

Experimental and theoretical studies on shear strength of large reinforced concrete beams have shown this effect repeatedly[22,28–34]. While there is now general agreement that there is a size effect in shear, the reason and the approaches to account for it are still controversial. Two different mechanisms have been offered to explain the size effect. One explanation is that the width of an inclined crack depends on the product of the strain in the reinforcement crossing the crack and the spacing of the cracks. Then, with an increasing beam depth, the crack spacing and the crack width tend to increase. This leads to a reduction in the maximum shear stress that can be transferred across the crack by aggregate interlock[8,19]. On the other hand, fracture mechanics theory proposes that the energy released in forming fracture bands of localized strain and damage depends on the size of the localization, which is proportional to d, in such a way that the shear strength is in inverse proportion to the square root of d[35–37].

Some authors have linked the size effect to other variables, as well. For example, Zararis and Papadakis[38] give an expression for taking into account the size effect that depends on the depth d, and the slenderness of the beam (a/d or M/Vd). Similarly, Cladera and Mari[27] propose an expression for size effect that considers the depth of the cross section and the concrete compressive strength.

Several approaches for considering the size effect can be found in the alternatives to update ACI 318 building code requirements that were published in Belarbi et al.[1] Frosch et al.[25] and Li et al.[26] use a size effect factor based on fracture mechanics that follows **Eq. (6)**. Furthermore, the same approach is adopted in Kuchma et al.[39] for the new ACI 318-19[2] one-way shear equation. Cladera et al.[14] proposal uses the combined size and slenderness factor in **Eq. (7)**. Reineck[10] does not address an independent size factor, instead, in this proposal the shear strength depends on a term that combines the longitudinal reinforcement ratio, the concrete compressive strength, and

the cross-section depth. Park and Choi[17] proposal uses a size factor that depends only on the depth, see **Eq. (8)**. Zararis and Papadakis[38] size effect approach was used by Choi and Park (2016) and previous editions of Cladera et al.[14], see **Eq. (9)**. Several equations for size effect are presented next.

$$\zeta = \frac{m}{\sqrt{1+\frac{d}{n}}} \leq 1.0 \tag{6}$$

$$\zeta = \frac{2}{\sqrt{1+\frac{d_0}{8}}}\left(\frac{d}{a}\right)^{0.25} = \frac{2}{\sqrt{1+\frac{d_0}{8}}}\left(\frac{Vd}{M}\right)^{0.25} \tag{7}$$

$$k_s = \left(\frac{12}{d}\right)^{0.25} \leq 1.1 \tag{8}$$

$$\zeta = 1.2 - \frac{1}{200}\left(\frac{M}{V}\right) \geq 0.65 \tag{9}$$

Where *m* and *n* are constant values. *m* is taken as 1, 1.4, or $\sqrt{2}$, and *n* is taken as 8 or 10 in. d_0 is the effective depth *d*, but not less than 4 in. *a* is the shear span taken as the ratio between *M* and *V*. For **Eq. (9)**, *M/V* ratio has to be in inches. **Fig. 1.6a** compares the size effect factor from the four approaches described for *M/Vd* = 3. **Fig. 1.6a** illustrates the effect of *M/Vd* ratio in Zararis and Papadakis[38] equation, and **Fig. 1.6c** shows the effect of *M/Vd* ratio in the combined size and slenderness in **Eq. (7)**. *M/Vd* was taken as 2.5, 3, 4, and 6 for **Fig. 1.6b** and **Fig. 1.6c.**

(a)

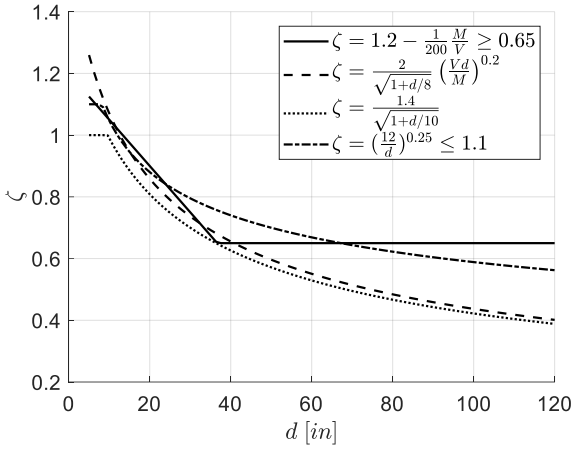

(b)

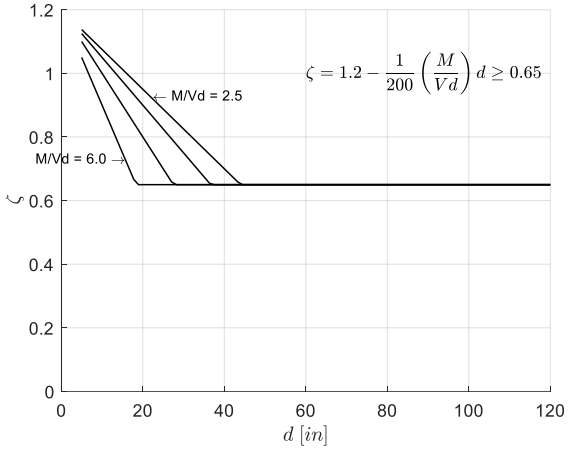

(c)

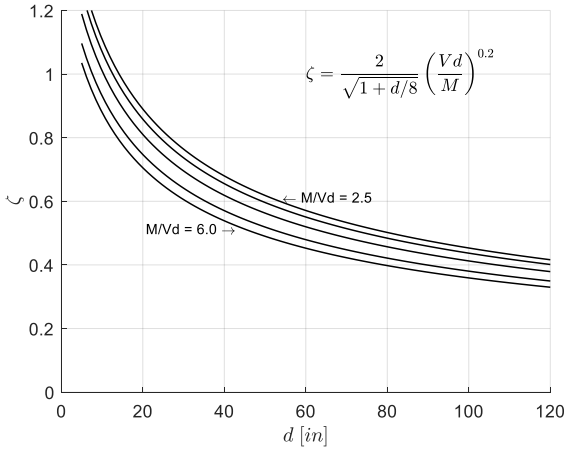

Fig. 1.6 (a) Comparison of size effect approaches *(M/Vd = 3)*; (b) Influence of shear span in size effect Eq. (9); (c) Influence of shear span in size effect Eq. (7)

1.3.1.5 Behavior of members with web reinforcement

An inclined crack causes the strength of beams to fall below the flexural capacity, in other words, a premature shear failure that does not allow the beam to reach its intended flexural strength. Thus, if shear stress exceeds the cracking strength of the concrete, it becomes necessary to provide steel reinforcement for the shear stress in excess of that the concrete alone could resist, this is called web reinforcement or shear reinforcement. The purpose of web reinforcement is to ensure that the full flexural strength can be developed. The basic idea then is to provide steel to cross the diagonal tension cracks and keep them from widening. Usually, web reinforcement or shear reinforcement, consists of vertical U-shape, closed-form, and occasionally W-shape stirrups.

Prior to diagonal cracking, the strain in the stirrups is equal to the corresponding strain of the concrete. Because concrete cracks at very small tensile strain, the stress in the stirrups prior to inclined cracking will not exceed 3 to 6 ksi. Thus, the vertical stirrups carry no significant stress until after a diagonal crack forms and they do not prevent inclined cracks from opening. They come into play after the cracks have formed. Once a diagonal crack opens, vertical stirrups act in tension to carry the load from one side of the crack to the other[7,8]. Wang and Salmon[5] explain that if the amount of web reinforcement is too little, it yields immediately at the formation of the inclined crack, and therefore the beam fails. In contrast, if the amount of web reinforcement is too high, there a shear-compression failure occurs before yielding of the web reinforcement. The optimum amount of shear reinforcement should allow the web reinforcement and the compression zone to continue to carry increasing shear force after the formation of the inclined crack, until yielding of the web reinforcement.

The web reinforcement has three key functions: (1) carry part of the shear force; (2) restrict the growth of the inclined crack so aggregate interlock is maintained; and (3) tie the longitudinal

bars in place and thereby increase their dowel capacity[5,8]. Thus, the external shear is resisted by the uncracked compression zone, the vertical component of the interface shear transfer along the cracks (aggregate interlock), the longitudinal reinforcement dowel action, and the shear carried by the stirrups across the cracks. In design, the first three contributions abovementioned are lumped together as the concrete contribution or shear carried by concrete, although the reader can understand this terminology is somewhat loose. The nominal one-way shear strength *(V_n)* is assumed as the sum of the concrete contribution *(V_c)* and the web reinforcement contribution *(V_s)*:

$$V_n = V_c + V_s \tag{10}$$

where V_c is the shear carried by concrete is taken equal to the failure capacity of a beam without web reinforcement, despite the actual failure mechanism of a beam with web reinforcement is different from the case of beams without stirrups; and V_s is the shear carried by the web reinforcement. Reineck[10] highlights that the failure of beams and slabs without web reinforcement is quite different from what has been observed in beams with web reinforcement. Hence, the shear strength cannot be expected to be the same in both cases.

Regarding the troublesome topic of the size effect in reinforced concrete beams. Wight and MacGregor[8] maintain that the reduction in shear strength due to increased size is not observed in beams with at least the minimum web reinforcement. This is because the web reinforcement holds the crack faces together so that the shear transfer across the cracks by aggregate interlock is not lost. ACI 318-19[2] shear design provisions do not include size effect factor for beams with at least minimum code specified web reinforcement. Notwithstanding, Bazant et al.[40] argue that web reinforcement does not eliminate the size effect. However, the size effect, in this case, is less significant than in members without web reinforcement. Consequently, Frosh et al.[25] method includes a size effect factor applicable to beams with web reinforcement and another factor for

beams without web reinforcement. Cladera et al.[14] and Li et al.[26] proposals for one-way shear design also include a size effect factor applicable to the concrete contribution, but the factor is the same for beams with and without web reinforcement.

1.3.2 Shear in deep reinforced concrete members

Shear strains have a predominant effect on the behavior of deep members. After an inclined crack opens, a deep beam tends to behave like an arch wherein the load is transferred from the application point to the supports by direct compression and by the tension in the longitudinal steel, see **Fig. 1.7**.

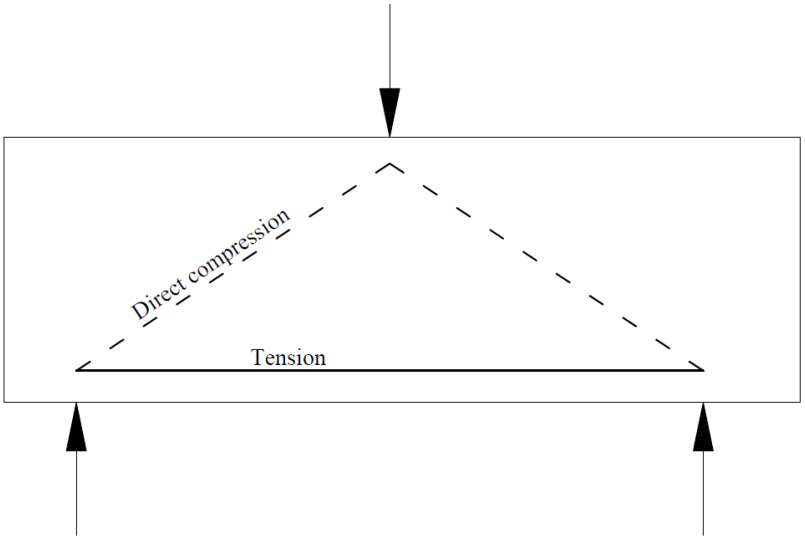

Fig. 1.7 Deep beam shear resistance mechanism

Deep beams have shear strength that exceeds the inclined cracking strength described in the section of shear in slender members; this is because when shear span is short, the load and reaction influence the diagonal crack formation in such a way that increases shear strength[7]. Two types of failures can occur in deep reinforced concrete members:

1. Shear-tension failure (**Fig. 1.8a**): After the flexure-shear crack forms, the crack extends further into the compression zone as the load increases. It also propagates as a secondary crack toward the tension reinforcement and then progresses horizontally along that reinforcement. Failure eventually results either by anchorage failure at the tension reinforcement or by crushing failure in the concrete near the compression face.

2. Shear-compression failure (**Fig. 1.8b**): After the flexure-shear crack forms, a steeply inclined crack suddenly develops and proceeds to propagate toward the neutral axis. This failure mode is less brittle than the diagonal tension failure due to the stress redistribution.

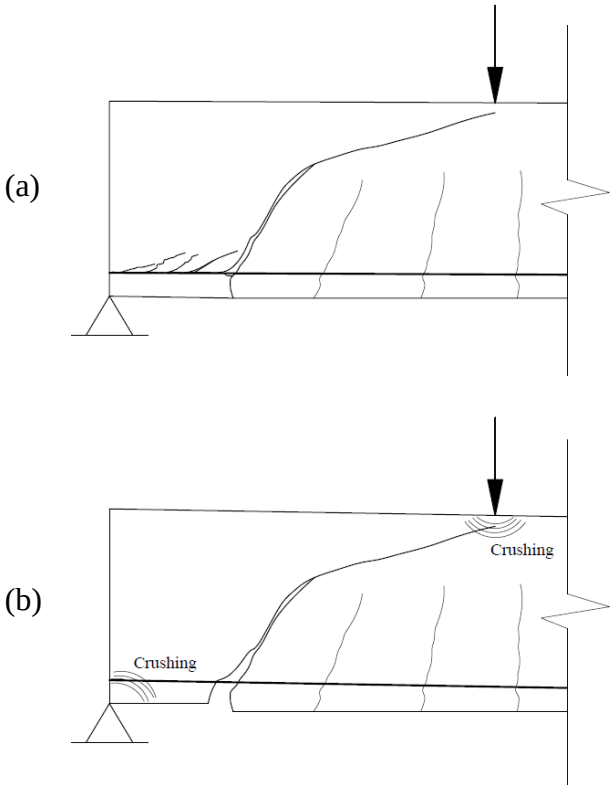

Fig. 1.8 Failure modes of a deep beam: (a) shear-tension failure; and (b) shear-compression failure (Adapter from Wang and Salmon[5] and Wight and MacGregor[8])

The assumption of plane sections remain plane after loading is no longer valid in deep beams due to significant shear deformations. Therefore, beam theory, which supports the shear strength description given for slender member, does not apply to deep beams. Thus, for the analysis and design of these members alternatives approaches are needed. For instance, since 2002 the ACI 318 requires that deep beams are designed using either nonlinear analysis or using the strut-and-tie method. This dissertation studies the strut-and-tie design specifications. The strut-and-tie modeling approach represents a complex stress field of a concrete structure as an equivalent truss, with elements in compression (struts) and elements in tension (ties); truss joints are called nodal zones (or nodes). The strength of struts and nodal zones control the dimensions of the concrete member, while the tie forces determine the amount of reinforcement required to resist a given load condition safely. The ties may be reinforcing bars, prestressing tendons, or concrete tensile stress fields. The strut-and-tie-models condense all stresses in compression and tension members and join them by nodes[41]. This approach has proven very useful for designing shear-critical structures where beam theory is not applicable, i.e., pile caps, corbels, beams with holes, walls with openings, anchorage zones, and the focus of Chapter 4, deep beams.

The strut-and-tie method includes the following four steps: (1) define and isolate a D-region; (2) calculate resultant forces at the D-region boundary; (3) select the model and compute the forces in the struts and ties to transfer the resultant forces across the D-region; and (4) design the strut and ties and nodal zones, so they have sufficient strength. Theoretical background on strut-and-tie modeling can be found elsewhere[3,8,41–45]; while examples of application have been provided by several researchers, as well[46–52].

The strut-and-tie method was formally published by Schlaich et al.[41], and it was introduced to the U.S. practice in the *AASHTO LRFD Bridge Design Specifications*[53] in 1994. Later it was

included for structural concrete design in Appendix A of ACI 318-02[54]. ACI 318-14[23] included the strut-and-tie method as a part of the main body. ACI 318-19[2] introduces several updates to the strut-and-tie design specifications. Thus, it is clear this approach has gained importance in concrete design practice.

1.3.3 Reliability of structures

Traditionally, the uncertainties in the calculations of loads and resistances were accounted for through a single global factor of safety. This approach is known as allowable stress design (ASD). Later, a partial factor of safety methodology was developed. This design approach includes load factors that amplify each load component (dead, live, wind, snow, earthquake, and so on), accounting for uncertainties associated with them, and the resistance factor (or strength reduction factor) that accounts for uncertainties associated with the load-carrying capacity. This methodology is called Load and Resistance Factors Design (LRFD). Nowadays, the latest editions of principal design and construction codes follow the LRFD philosophy. The objective of LRFD philosophy is to design more efficiently and manage risk in design and construction in a rational manner.

In addition to the evident variability in loads that affect structures, there are many sources of uncertainty inherent to structural design; for example, concrete compressive strength, yield strength, and material unit weight will never have exactly the same observed value under the same test conditions. Thus, parameters in the design are random variables. The concept of a random variable is closely related to the conducting of an experiment. If an experiment is performed repeatedly (with all conditions maintained as precisely as possible) and the measured results are identical, then the variables which are measured are said to be deterministic. However, if the

numerical results vary, the item is random[55]**.** Since random variables are inevitable, absolute safety (or zero probability of failure) cannot be achieved. Consequently, structures must be designed to serve their functions with a finite probability of failure[56].

How engineers treat the uncertainty in a given phenomenon depends upon the situation. If the degree of variability is small, and the consequences of any variability will not be significant, the uncertainty can be ignored by merely assuming that the variable will be equal to the best available estimate. This is typically done with the elastic constant of materials and the physical dimensions of precast structural components. If the uncertainty is significant, it is necessary to use a conservative estimate of the variable. This has been done in setting specified minimum strength properties of materials and members. Therefore, some questions arise: how can engineers maintain consistency in their conservatism from one situation to another? For instance, separate professional committees set the specified minimum concrete compressive strength and the specified minimum bending strength of wood[57]. How can engineers maintain consistency in their conservatism within the same construction project? For example, in a building, the specified minimum flexural and shear strength of beams, slabs, corbels, walls, and foundations should be consistent. Several procedures have been used to set a safety margin, and they are presented next.

1.3.3.1 Allowable stress design

The allowable stress design (ASD) approach has been used by civil engineers since the early 1800s and it is still found in practice. ASD is commonly used as an educational tool when engineering students learn concepts of mechanics of materials, and a design problem is discussed. Under ASD, the design load effect (Q), which consist of the estimated demand on the component, is compared

to the allowable load demand ($Q_{allowable}$), which is the resistance or strength (R) reduced by a factor of safety *(FS)*:

$$Q \leq Q_{allowable} = \frac{R}{FS} \tag{11}$$

at the limit, the factor of safety can be written as **Eq. (12)**:

$$FS = \frac{R}{Q} \tag{12}$$

when more than one source of load is acting, the load effect Q is calculated as the direct sum of the best estimation of the separate effect. Through experience, conventions have developed with regard to what values of a factor of safety are suitable for various situations. Factors of safety between 1.5 and 2.5 were common in structural design, and similar and higher values can be found in geotechnical practices.

This presentation of the factor of safety tends to give a false impression of certainty about these quantities. Notwithstanding, both resistance and loads are random variables. A possible clarification is to name this ratio as the nominal factor of safety (FS_n), which should be the nominal resistance (R_n) over the nominal load (Q_n). The term nominal is used for the value used in design:

$$FS_n = \frac{R_n}{Q_n} \tag{13}$$

another option is to define a central factor of safety as the mean resistance over the mean load:

$$\overline{FS} = \frac{\overline{R}}{\overline{Q}} \tag{14}$$

Eq. (13) and **Eq. (14)** imply a degree of uncertainty, and clearly, the definition of an appropriate factor of safety requires a probabilistic treatment. A critical drawback of this approach is that all uncertainty is lumped into one global factor, which leads to inconsistent margins of safety for

different scenarios. The same factor of safety can imply a very different safety margin in different cases. Consider for example the uncertainties involved in selecting a steel girder versus a concrete girder, or the uncertainties of precast versus cast-in-place concrete members.

1.3.3.2 Maximum probability of failure method

The maximum probability of failure method requires the definition of a performance function (also called limit state function) that represents the margin of safety, which intuitively is the difference between the resistance *(R)* and the load effect *(Q)* for a given component or system of interest:

$$g = R - Q \tag{15}$$

where a negative value of the function *g* means failure or unsatisfactory performance. *R* and *Q* are random variables; thus, *g* is also a random variable. For **Eq. (15),** the mean (μ) and standard deviation (σ) of *g* relates to the statistics of *R* and *Q* as follows:

$$\begin{aligned} \mu_g &= \mu_R - \mu_Q \\ \sigma_g^2 &= \sigma_R^2 + \sigma_Q^2 - 2\rho_{RQ}\sigma_R\sigma_Q \end{aligned} \tag{16}$$

where ρ_{RQ} is the correlation between *R* and *Q*; ρ_{RQ} is one if the variables are fully correlated and zero if they are independent.

The performance of a given design is measured in terms of the reliability index (β). β is defined as a function of the probability of failure *(P_F)* as follows:

$$\beta = -\Phi^{-1}\left(P_F\right) \tag{17}$$

where Φ^{-1} is the inverse standard normal distribution function. When P_F is normally distributed, and *R* and *Q* are independent and uncorrelated, the reliability index can also be expressed as follows.

$$\beta = \frac{\mu_g}{\sigma_g} = \frac{\mu_R - \mu_Q}{\sqrt{\sigma_R^2 + \sigma_Q^2}} \tag{18}$$

For structural components, *R* and *Q* can be usually considered as independent and uncorrelated.

This procedure is extended to give separate load factors and resistance factors for use in design, and it is the basis of current codes. The LRFD is presented as the following design requirement: the total factored nominal load effect being less or equal than the reduced nominal resistance, as stated in **Eq. (19)**:

$$\sum \gamma_i Q_{ni} \leq \phi R_n \tag{19}$$

where Q_{ni} is the nominal value of load component *i*; g_i is the load component *I*; R_n is the nominal value of resistance; and ϕ is the resistance factor or strength reduction factor. Loads and resistance factors are calibrated, so the limit state function meets a beforehand defined target reliability index (β_T). Compressive explanations are given by Nowak and Lind[58], Ellinwood et al.[59], and Nowak and Collins[56]. Examples of applications are calibration of the *AASHTO LRFD Bridge design specifications* by Nowak[60] (1999) and the *ACI 318 Building code requirements for structural concrete* by Szerszen and Nowak[61].

1.3.3.3 Minimum cost structure cost of failure

If the probability of failure of a structure can be estimated using the framework abovementioned, then the total cost of a structure with the inclusion of the cost of failure can be calculated, as well. Thus, the total lifetime cost of a structure can be represented as the sum of the construction cost, routine maintenance cost, failure cost, and repair or demolition costs. The failure cost is associated with the probability of failure and increases quickly as the probability of failure increases. This

computation provides an estimate of the optimum probability of failure, which leads to the reliability-based lifetime approach and has demonstrated the potential for cost savings and improved efficiency; nevertheless, this approach is not widely used yet.

1.4 METHODOLOGY

This dissertation explores the above-described problems using mainly the structural reliability approach and other statistical analysis techniques. This section describes the methodology used in each of the following chapters.

The first problem stated in section 1.2 is investigated in Chapter 2. The comparative assessment of one-way shear equations is done based on a database of reinforced concrete members loaded until failure with a clear shear failure mode. The database has been agreed upon by the Joint *ACI-ASCE Committees 445*. Test results are compared with predictions of available one-way shear equations. Central tendency parameters, goodness-of-fit, graphical tools, and comparison of statistical distributions are used as measurements of agreement between the predictions and the test data. The accuracy of each one-way shear equation is informed.

The second problem stated in section 1.2 is studied in Chapter 3. Statistical models for loads are taken from the published literature, while the statistical models for resistance are developed in this work. Reliability analysis is used to measure the probabilistic safety margin of past shear design practice. A data-driven quantification of the uncertainty in the analysis method is proposed. The past practice is used as a reference to suggest reliability-based resistance factors. Ductility of possible failure modes are taken into consideration to suggest different safety margins than past practice, and a different set of strength reduction factors is recommended.

Chapter 4 approaches the third problem stated in section 1.2. A data-driven quantification of the uncertainty in the analysis method is proposed. The reliability of deep beams designs according to ACI 318-19 strut-and-tie specification and the likelihood of a ductile failure mode are determined by means of reliability analysis. Reliability-based strength reduction factors are suggested to meet the safety margin defined by past practice of shear design in slender members, with consideration of failure modes.

1.5 ORGANIZATION

The next chapters of the dissertation are organized as follows. From Chapter 2 to Chapter 4, each chapter begins with an introduction of each topic, including motivation, previous work, and the research significance. The methodology briefly described in the previous section is presented in a comprehensive manner, including relevant supporting literature. Results are reported, followed by discussion and conclusions. A brief discussion of potential extensions and future research are also given. Tables and figures are located at the end of each chapter. Chapter 5 contains a summary of the findings and conclusions of these studies. At the end of the dissertation, appendixes with notation and supporting figures for Chapter 2 are included.

REFERENCES

1. Belarbi, A., Kuchma, D. A., and Sanders, D. H. "Proposals for New One-Way Shear Equations for the 318 Building Code," *Concrete International*, V. 39, No. 9, 2017, pp. 29–32.
2. ACI Committee 318. "Building code requirements for structural concrete: (ACI 318-19); and commentary (ACI 318R-19)," Farmington Hills, MI, American Concrete Institute, 2019.
3. FIP Commission 3. "Practical design of structural concrete," *The International Federation for Structural Concrete: FIB*, 1999.
4. AASHTO. "LRFD Bridge Design Specifications," 8th edition, Washington, DC, American Association of State Highway Transportation Officials, 2017.
5. Wang, C.-K., and Salmon, C. G. "Reinforced concrete design," 4th edition, New York, Harper & Row Publishers, 1985.
6. Nawy, E. "Reinforced concrete: A fundamental approach," Englewood Cliffs, New Jersey, Prentice Hall, Inc, 1985.
7. Ferguson, P. M. "Reinforced concrete fundamentals," 3rd edition, Canada, John Wiley & Sons, 1973.
8. Wight, J. K., and MacGregor, J. G. "Reinforced concrete: mechanics and design," 6th edition, New Jersey, Pearson Education, 2012.
9. Kani, G. N. J. "The riddle of shear failure and its solution." Journal Proceedings, vol. 61. 1964. pp. 441–468.
10. Reineck, K.-H. "Proposal for ACI 318 Shear Design," *Concrete International*, V. 39, No. 9, 2017, pp. 65–70.
11. Vecchio, F. J., and Collins, M. P. "The modified compression-field theory for reinforced concrete elements subjected to shear," *ACI J.*, V. 83, No. 2, 1986, pp. 219–231.
12. Marí, A., Cladera, A., Bairán, J., et al. "Shear-flexural strength mechanical model for the design and assessment of reinforced concrete beams subjected to point or distributed loads," *Frontiers of Structural and Civil Engineering*, V. 8, No. 4, 2014, pp. 337–353.
13. Mari, A., Bairán, J., Cladera, A., et al. "Shear-flexural strength mechanical model for the design and assessment of reinforced concrete beams," *Structure and Infrastructure Engineering*, V. 11, No. 11, 2015, pp. 1399–419.
14. Cladera, A., Marí, A., Bairán, J.-M., et al. "One-Way Shear Design Method Based on a Multi-Action Model," *Concrete International*, V. 39, No. 9, 2017, pp. 40–46.
15. Bažant, Z. P., and Oh, B. H. "Crack band theory for fracture of concrete," *Matériaux et construction*, V. 16, No. 3, 1983, pp. 155–177.
16. Wolf, T. S., and Frosch, R. J. "Shear Design of Prestressed Concrete: A Unified Approach," *Journal of Structural Engineering*, V. 133, No. 11, 2007, pp. 1512–9.
17. Park, H.-G., and Choi, K.-K. "Unified Shear Design Method of Concrete Beams Based on Compression Zone Failure Mechanism," *Concrete International*, V. 39, No. 9, 2017, pp. 59–63.
18. Tureyen, A. K., and Frosch, R. J. "Concrete shear strength: Another perspective," *Structural Journal*, V. 100, No. 5, 2003, pp. 609–615.

19. Kuchma, D. A., and Collins, M. P. “Advances in understanding shear performance of concrete structures,” *Progress in Structural Engineering and Materials*, V. 1, No. 4, 1998, pp. 360–9.
20. Tompos, E. J., and Frosch, R. J. “Influence of Beam Size, Longitudinal Reinforcement, and Stirrup Effectiveness on Concrete Shear Strength,” *ACI Structural Journal*, V. 99, No. 5, 2002.
21. Lubell, A. S., Bentz, E. C., and Collins, M. P. “Influence of longitudinal reinforcement on one-way shear in slabs and wide beams,” *Journal of Structural Engineering*, V. 135, No. 1, 2009, pp. 78–87.
22. Yu, L., Che, Y., and Song, Y. “Shear Behavior of Large Reinforced Concrete Beams without Web Reinforcement,” *Advances in Structural Engineering*, V. 16, No. 4, 2013, pp. 653–65.
23. ACI Committee 318. “Building code requirements for structural concrete: (ACI 318-14); and commentary (ACI 318R-14),” Farmington Hills, MI, American Concrete Institute, 2014.
24. Bentz, E. C., and Collins, M. P. “Updating the ACI Shear Design Provisions,” *Concrete International*, V. 39, No. 9, 2017, pp. 33–38.
25. Frosch, R. J., Yu, Q., Cusatis, G., et al. “A Unified Approach to Shear Design,” *Concrete International*, V. 39, No. 9, 2017, pp. 47–52.
26. Li, Y.-A., Hsu, T. T., and Hwang, S.-J. “Shear Strength of Prestressed and Nonprestressed Concrete Beams,” *Concrete International*, V. 39, No. 9, 2017, pp. 53–57.
27. Cladera, A., and Mari, A. R. “Shear design procedure for reinforced normal and high-strength concrete beams using artificial neural networks. Part I: beams without stirrups,” *Engineering Structures*, V. 26, No. 7, 2004, pp. 917–926.
28. Kani, G. “How safe are our large reinforced concrete beams?” Journal Proceedings, vol. 64. 1967. pp. 128–141.
29. Bhal, N. S. “The effect of beam depth on shear capacity of single-span reinforced concrete beams with and without shear reinforcement,” *Dr. Ing dissertation, Stuttgart University*, 1967.
30. Taylor, H. P. “Shear strength of large beams,” *Journal of the Structural Division*, V. 98, No. Proc Paper 9329, 1972.
31. Shioya, T., Iguro, M., Nojiri, Y., et al. “Shear strength of large reinforced concrete beams,” *Special Publication*, V. 118, 1990, pp. 259–280.
32. Collins, M. P., and Kuchma, D. “How Safe Are Our Large, Lightly Reinforced Concrete Beams, Slabs, and Footings?,” *ACI Structural Journal*, V. 96, No. 4, 1999.
33. Angelakos, D., Bentz, E. C., and Collins, M. P. “Effect of concrete strength and minimum stirrups on shear strength of large members,” *Structural Journal*, V. 98, No. 3, 2001, pp. 291–300.
34. Sherwood, E. G., Lubell, A. S., Bentz, E. C., et al. “One-way shear strength of thick slabs and wide beams,” *ACI Structural Journal*, V. 103, No. 6, 2006, p. 794.
35. Bažant, Z. P. “Fracturing Truss Model: Size Effect in Shear Failure of Reinforced Concrete,” *Journal of Engineering Mechanics*, V. 123, No. 12, 1997, pp. 1276–88.
36. Bažant, Z. P. “Size effect,” *International Journal of Solids and Structures*, V. 37, Nos. 1–2, 2000, pp. 69–80.

37. Bažant, Z. P., and Yu, Q. “Universal size effect law and effect of crack depth on quasi-brittle structure strength,” *Journal of engineering mechanics*, V. 135, No. 2, 2009, pp. 78–84.
38. Zararis, P. D., and Papadakis, G. Ch. “Diagonal Shear Failure and Size Effect in RC Beams without Web Reinforcement,” *Journal of Structural Engineering*, V. 127, No. 7, 2001, pp. 733–42.
39. Kuchma, D. A., Wei, S., Sanders, D. H., et al. “Development of the One-Way Shear Design Provisions of ACI 318-19 for Reinforced Concrete,” *ACI Structural Journal*, V. 116, No. 4, 2019.
40. Bažant, Z. P., Yu, Q., Gerstle, W., et al. “Justification of ACI 446 code provisions for shear design of reinforced concrete beams,” *ACI Structural Journal*, V. 104, No. 5, 2007, pp. 601–10.
41. Schlaich, J., Schafer, K., and Jennewein, M. “Toward a Consistent Design of Structural Concrete,” *PCI Journal*, V. 32, No. 3, 1987, pp. 74–150.
42. Collins, M. P., and Mitchell, D. “Prestressed concrete structures,” v. vol. 9, Prentice Hall Englewood Cliffs, NJ, 1991.
43. ACI Committee 445R. “ASCE/ACI Joint Committee 445 Recent Approaches to Shear Design of Structural Concrete, ACI 445R-99,” 1999.
44. Menn, C. “Prestressed concrete bridges,” 1997.
45. Muttoni, A., Schwartz, J., and Thürlimann, B. “Design of concrete structures with stress fields,” Springer Science & Business Media, 1996.
46. Colorito, A. B., Wilson, K. E., Bayrak, O., et al. “Strut-and-Tie Modeling (STM) for Concrete Structures, Design Examples,” 2017.
47. Kamara, M. E., Novak, L. C., and Rabbat, B. G. “Notes on ACI 318-08, Building Code Requirements for Structural Concrete: With Design Applications,” Portland Cement Assn, 2008.
48. Martin, B. T., Sanders, D. H., Wassef, W., et al. “Verification and implementation of strut-and-tie model in LRFD bridge design specifications,” *NCHRP Project*, 2007, pp. 20–07.
49. Nilson, A. H., Darwin, D., and Dolan, C. W. “Design of concrete structures 13th ed,” McGraw-Hill Higher Education, 2004.
50. Reineck, K.-H. “SP 208 (2002): Examples for the Design of Structural Concrete with Strut-and-Tie Models. Reineck, K,” *H. Editor, ACI SP-208, ACI, Farmington Hills, MI*, 2002.
51. Reineck, K.-H., and Novak, L. C. “Further Examples for the Design of Structural Concrete with Strut-and-Tie Models,” *ACI SP-273 (2010), ACI, Farmington Hills, MI*, 2010.
52. Williams, C. S., Deschenes, D., and Bayrak, O. “Strut-and-Tie Model (STM) Examples for Bridges,” 2012.
53. AASHTO. “LRFD Bridge Design Specifications,” 1st edition, Washington, D.C., American Association of State Highway and Transportation Officials, 1994.
54. ACI Committee 318. “Building code requirements for structural concrete (ACI 318-02); and commentary (ACI 318R-02),” Farmington Hills, MI, American Concrete Institute, 2002.
55. Hart, G. C. “Uncertainty analysis, loads, and safety in structural engineering,” Prentice Hall, 1982.
56. Nowak, A. S., and Collins, K. R. “Reliability of structures,” 2nd edition, Boca Raton, FL, CRC Press, 2013.

57. Benjamin, J. R., and Cornell, A. C. “Probability, Statistics and Decision for Civil Engineers,” New York, NY, McGraw-Hill, 1970.
58. Nowak, A. S., and Lind, N. C. “Practical code calibration procedures,” *Canadian Journal of Civil Engineering*, V. 6, No. 1, 1979, pp. 112–9.
59. Ellingwood, B., Galambos, T. V., MacGregor, J. G., et al. “Development of a Probability Based Load Criterion for American National Standard A 58,” *NBS Special Report 577, U. S. Department of Commerce, National Bureau of Standards*, 1980.
60. Nowak, A. S. “NCHRP report 368: Calibration of LRFD Bridge Design Code,” Washington, D.C, Transportation Research Board, National Research Council, 1999.
61. Szerszen, M. M., and Nowak, A. S. “Calibration of Design Code for Buildings (ACI 318) Part 2: Reliability Analysis and Resistance Factors,” *Ann Arbor*, V. 1001, 2003, pp. 48109–2125.

Chapter 2

COMPARATIVE ASSESSMENT OF ONE-WAY SHEAR STRENGTH EQUATIONS

ABSTRACT

An efficient yet safe method is always the goal for design purposes; however, a more accurate but complex approach may be warranted for forensic engineering or for the evaluation of existing structures. Several methods for prediction of one-way shear strength of reinforced concrete beams and one-way slabs are available in the literature as a result of an extensive research effort. These shear strength equations cannot be used by practitioners due to a lack of studies regarding their accuracy.

An assessment regarding the accuracy of several one-way shear strength methods for reinforced concrete members is described in this paper. Predictions of such methods are compared with a set of experimental results reported in the literature. The objective is to provide engineers guidance to select the most appropriate shear design method for a given structural application.

The results of this study are presented by measures of dispersion, goodness-of-fit indicators, and statistical distances. Almost all methods included in this analysis exhibit satisfactory predictions. The new ACI 318-19 shear design method is the simplest of the methods reviewed, and it gives reasonably accurate predictions for members with and without shear reinforcement. For members without shear reinforcement, the ACI 318-14 shear strength equations are not recommended.

Keywords: reinforced concrete, one-way shear strength, building code, database, shear design, accuracy

2.1 INTRODUCTION

The traditional shear design equations for reinforced concrete members in the *ACI 318-14 Building code requirements for structural concrete*[1] were developed in the early 1960s. The provisions were based on the test results available at the time with the goal of providing simplified design equations that conservatively estimate the one-way shear strength. However, over the past few decades, several drawbacks were identified in the work done for the ACI subcommittee *318-E Section and Member Strength*, and the *Joint ACI-ASCE Committees 445 Shear and Torsion and 446 Fracture Mechanics of Concrete*. Both procedures in ACI 318-14[1], i.e., the simplified and the detailed methods, have shortcomings: the equation to estimate the concrete contribution to shear strength (V_c) is the same for beams with or without shear reinforcement despite the failure mechanism is being notoriously different; the influence of axial tension in reducing V_c has been considered too great; provisions can be severely unconservative for beams with light longitudinal reinforcement and when applied to the design of large beams; the specifications do not allow the use of $\sqrt{f_c'}$ larger than 100 psi. Other concerns are the large number and variety of equations specified in ACI 318-14[1]. Hence, there was a high potential for improvements to the shear provisions in the code. This led to a call by the *Joint ACI-ASCE Committee 445* and *ACI Subcommittee 318-E* for proposals for new one-way shear equations for the ACI 318 building code requirements. As a result, six proposals based on various failure mechanisms were presented[2]. However, none of those proposals made it to the new code; instead, ACI 318-19[3] replaced the one-way shear design specifications with a new set of empirical equations, the development of which is described by Kuchma et al.[4] Because of this research effort, there are several alternatives to predict the one-way shear strength of reinforced concrete members that are not in use by practitioners. These shear

strength equations cannot be used by practitioners due to a lack of studies regarding their accuracy and range of application.

Although for design purposes a safe and efficient method is the goal, a more accurate but complex approach may be warranted for forensic engineering or for evaluation of existing structures. An assessment of the accuracy of methods to estimate the one-way shear strength of reinforced concrete members is described in this paper. This study includes six proposals recently publised[2], the traditional ACI 318-14[1] methods, and the ACI 318-19[3] new method. Predictions of such methods are compared against experimental results reported by Reineck[5,6] and later updates. The experimental database includes specimens built with and without shear reinforcement. The objective is to provide engineers guidance to select the most appropriate shear design method for a given structural application.

2.2 RESEARCH SIGNIFICANCE

Many researchers have proposed design equations that address the identified shortcomings in the ACI 318 traditional shear design provisions. The accuracy of a selection of methods currently available to estimate the one-way shear strength of reinforced concrete beams, including the six proposals recently published[2], and the ACI 318-14[1] and ACI 318-19[3] methods, is informed in this research. Hence, engineers can use these results for selecting the method that fits better their purpose according to the intended application.

2.3 REVIEW OF SELECTED SHEAR DESIGN METHODS

The methods studied in this paper are described in this section. In all cases, it is assumed that the nominal shear strength of a member *(V_n)* is the sum of the contributions of the concrete *(V_c)* and the shear reinforcement *(V_s)*:

$$V_n = V_c + V_s \tag{1}$$

Maximum and minimum values of V_n or the individual contribution *(V_c* or *V_s)* are often specified to prevent undesired failure modes. For example, the ACI 318 building code requirements attempt to prevent shear failure due to crushing of the web and excessive cracking at service loads by limiting the shear reinforcement contribution to $V_{s,\max} = 8\sqrt{f_c'}b_w d$. Also, a maximum value of $\sqrt{f_c'} = 100$ psi is specified as a limit. For this evaluation, those kind of limits in ACI 318 and other methods were not applied, as the intention of this work is to study the accuracy and range of application of the methods.

2.3.1 ACI 318 building code requirements

The set of equations for predicting the one-way shear strength of reinforced concrete members, given in the ACI 318 building code requirements, are empirical relationships based on fundamental mechanics adjusted to fit available test results. The ACI 318-14[1] building code requirements comprise a total of ten equations grouped into the simplified methods and the detailed method. The ACI 318-19[3] replaced these methods by a new set of empirical equations that addressed some of the shortcomings of the traditional methods. The traditional simplified method, detailed method, and the new method are described below.

2.3.1.1 ACI 318-14 simplified method

In accordance with the ACI 318-14[1] simplified method, the contribution of concrete and shear reinforcement can be estimated as follows:

$$V_c = 2\lambda\sqrt{f_c^{'}}b_w d \tag{2}$$

$$V_s = A_v f_{yt}\left(\frac{d}{s}\right) \tag{3}$$

when axial load is present, the concrete contribution is determined as indicated in **Eq. (4)**. When a compressive axial load is acting on the member V_c increases, while a tensile axial load decreases V_c.

$$V_c = \begin{cases} 2\left[1+\dfrac{N_u}{2000A_g}\right]\lambda\sqrt{f_c^{'}}b_w d & \text{if } N_u > 0 \text{ (compression)} \\ 2\left[1+\dfrac{N_u}{500A_g}\right]\lambda\sqrt{f_c^{'}}b_w d & \text{if } N_u < 0 \text{ (tension)} \end{cases} \tag{4}$$

2.3.1.2 ACI 318-14 detailed method

In accordance with the ACI 318-14[1] detailed method, the contribution of concrete is computed by **Eq. (5),** and the shear reinforcement contribution remains the same as **Eq. (3)**:

$$V_c = Lesser\ of \begin{cases} \left[1.9\lambda\sqrt{f_c^{'}} + 2500\rho_w\dfrac{V_u d}{M_u}\right]b_w d \\ \left[1.9\lambda\sqrt{f_c^{'}} + 2500\rho_w\right]b_w d \\ 3.5\lambda\sqrt{f_c^{'}}b_w d \end{cases} \tag{5}$$

when axial load is present, the concrete contribution is calculated as the lesser of the expressions in **Eq. (6).**

$$V_c = Lesser\ of \begin{cases} \left[1.9\lambda\sqrt{f_c^{'}} + 2500\rho_w \dfrac{V_u d}{M_u - N_u \dfrac{(4h-d)}{8}} \right] b_w d \\ 3.5\lambda\sqrt{f_c^{'}} b_w d \sqrt{1 + \dfrac{N_u}{500 A_g}} \end{cases} \quad (6)$$

2.3.1.3 ACI 318-19

In accordance with the ACI 318-19[3], for beams without shear reinforcement and slabs the concrete contribution is estimated as follows:

$$V_c = \left[8\lambda_s \lambda \rho_w^{\frac{1}{3}} \sqrt{f_c^{'}} + \frac{N_u}{6A_g} \right] b_w d \quad (7)$$

where λ_s is the size effect factor defined in **Eq. (8)**.

$$\lambda_s = \frac{1.4}{\sqrt{1 + \dfrac{d}{10}}} \leq 1.0 \quad (8)$$

For beams with shear reinforcement, the concrete contribution is given by either of the lines in **Eq. (9)**. The first line of **Eq. (9)** is the classical shear equation, while the second line is **Eq. (7)** without the size effect factor. This evaluation considers the second line of **Eq. (9)**.

$$V_c = Either\ of \begin{cases} \left[2\lambda\sqrt{f_c^{'}} + \dfrac{N_u}{6A_g} \right] b_w d \\ \left[8\lambda\rho_w^{\frac{1}{3}} \sqrt{f_c^{'}} + \dfrac{N_u}{6A_g} \right] b_w d \end{cases} \quad (9)$$

The shear reinforcement contribution is taken as the same as in previous provisions, see **Eq. (3)**.

2.3.2 Bentz and Collins

Bentz and Collins[7] proposal is based on the modified compression field theory developed by Vecchio and Collins[8]. The full derivation of this proposal is given by Bentz and Collins[9]. Two versions of this model have been proposed by Bentz and Collins[7], i.e., detailed and simplified.

2.3.2.1 Bentz and Collins detailed

In accordance with Bentz and Collins[7] detailed method, the concrete contribution is estimated with **Eq. (10)**, this equation is applicable to all members with and without shear reinforcement:

$$V_c = 2\sqrt{f_c'}\,\frac{2.25}{(1+1500\varepsilon_x)}\,\frac{50}{(38+s_x)}\,b_w d \tag{10}$$

where ε_x is the longitudinal strain of concrete at mid-depth at shear failure, and it can be determined with **Eq. (11)**:

$$\varepsilon_x = \frac{\frac{M_u}{0.9d} + V_u + 0.5N_u}{2A_s E_s} \geq -0.2\times10^{-3} \tag{11}$$

where M_u and V_u are always positive, and N_u is positive for tension and negative for compression. Thus, the limiting strain is a compressive strain. Also, the bending moments should not be taken less than $0.9V_u d$. s_x is the crack spacing, and it is estimated as indicated in **Eq. (12).** If $f_c' > 9{,}000\,psi$, d_{agg} is taken equal to zero.

$$s_x = \begin{cases} 12\ \text{in.} & \text{if} \quad A_v \geq A_{v\min} \\ \dfrac{1.25d}{0.65+d_{agg}} & \text{if} \quad A_v < A_{v\min} \text{ and } d_{agg} < 1\ \text{in.} \\ 0.75d & \text{if} \quad A_v < A_{v\min} \text{ and } d_{agg} \geq 1\ \text{in.} \end{cases} \tag{12}$$

For the shear reinforcement contribution, an estimate of the inclination angle of the principal compression stress on the web concrete is needed, and it can be obtained as:

$$\theta = 29^\circ + 7000\varepsilon_x \tag{13}$$

thus, the web reinforcement contribution is taken as follows.

$$V_s = A_v f_y \left(\frac{0.9d}{s}\right)\cot\theta \tag{14}$$

This method requires iterations. First, a reasonable value of ε_x needs to be assumed (i.e., $\varepsilon_x = f_y / 2E_s$). Then, V_n can be calculated, and ε_x is updated until convergence is obtained.

2.3.2.2 Bentz and Collins simplified

A more straightforward procedure is desirable for design; therefore, Bentz and Collins[7] also proposed a simplified method. If it is assumed that for 60 ksi steel $\varepsilon_x = f_y / 2E_s \approx 0.85\times10^{-3}$, then for members without stirrups the concrete contribution is:

$$V_c = \frac{100}{38 + s_x}\sqrt{f_c'}\,b_w d \tag{15}$$

while for members with stirrups, a constant of $s_x = 12$ in. is used; therefore, the traditional longstanding **Eq. (2)** for V_c is obtained.

The shear reinforcement contribution can also be simplified from **Eq. (14)**. Using the same assumptions as before, **Eq. (16)** is obtained.

$$\begin{aligned} &\theta = 29^\circ + 7000\varepsilon_x = 35^\circ \Rightarrow V_s = A_v f_y 0.9\left(\frac{d}{s}\right)\cot 35^\circ \\ &\Rightarrow V_s = 1.285 A_v f_y \left(\frac{d}{s}\right) \end{aligned} \tag{16}$$

2.3.3 Cladera, Mari, Bairan, Oller, and Ribas

The method proposed by Cladera et al.[10] is based on the multi-action shear model, which is explained in detail elsewere[11–13]. The concrete contribution, for members with and without web reinforcement is given by **Eq. (17)**:

$$V_c = 6\lambda\zeta \frac{c}{d}\sqrt{f_c'}\, b_{veff}\, d \tag{17}$$

where c is the neutral axis depth; ζ is the combined size and slenderness effect; and b_{veff} is the effective flange width for shear strength, which depends on where the neutral axis is located, in the web or in the flange. This proposal includes a combined size and slenderness ratio based on the work of Bazant[14] expressed in **Eq. (18)**:

$$\zeta = \frac{2}{\sqrt{1+\frac{d_0}{8}}}\left(\frac{d}{a}\right)^{0.25} \tag{18}$$

where a is taken as $a = \frac{M_{u\max}}{V_{u\max}}$.

The shear strength provided by the shear reinforcement is given by **Eq. (19)**:

$$V_s = 1.20 A_v f_{yt}\left(\frac{d}{s}\right) \tag{19}$$

2.3.4 Frosch, Yu, Cusatis, and Bazant

The method proposed by Frosch et al.[15] assumes a simplified distribution shear stress over the compression zone depth and it includes the size effect factor proposed by Bazant[14]. The early development of this method is presented elsewhere[16,17]. In accordance with this model, the

concrete contribution for members with and without shear reinforcement is given by **Eq. (20)**, with the size effect factor defined in **Eq. (21)**:

$$V_c = \left(5\lambda\sqrt{f_c'}b_w c\right)\gamma_d \tag{20}$$

$$\gamma_d = \frac{1.4}{\sqrt{1+\frac{d}{d_o}}} \le 1.0 \tag{21}$$

where d_o changes for beams with and without shear reinforcement as specified in **Eq. (22)**.

$$d_0 = \begin{cases} 10 \text{ in.} & \text{if } A_v < A_{v\min} \\ 100 \text{ in.} & \text{if } A_v \ge A_{v\min} \end{cases} \tag{22}$$

The shear strength provided by the shear reinforcement is given by **Eq. (3).**

2.3.5 Li, Hsu, and Hwang

The method proposed by Li et al.[18] includes an arch action function of the shear-to-moment ratio, and a size effect factor adopted from Bazant[14]. The development of this method can be found elsewhere[19–21]. In accordance with this model, the concrete contribution for members with and without shear reinforcement is given by **Eq. (23).** The shear strength provided by the shear reinforcement is given by **Eq. (3).**

$$V_c = 17\lambda\left(\frac{V_u d}{M_u}\right)^{0.7}\sqrt{f_c'}b_w c\frac{1}{\sqrt{1+\frac{h}{11.8}}} \tag{23}$$

This proposal is very sensitive to the ratio $V_u d/M_u$. In this evaluation the arch action factor is taken the geometric d/a.

2.3.6 Park and Choi

The method proposed by Park and Choi[22] is based on the compression zone failure mechanism. In accordance with this model, the concrete contribution for members with and without web reinforcement is given by **Eq. (24)**:

$$V_c = k_s f_t b_w c_s \cot\phi \tag{24}$$

where k_s is a size effect factor given by **Eq. (25)**; f_t is the concrete tensile strength calculated as in **Eq. (26)**; c_s is the depth of the compression zone at shear failure; and ϕ is the inclined crack angle in the compression zone at the shear critical section given by **Eq. (27)**.

$$k_s = \left(\frac{12}{d}\right)^{0.25} \leq 1.1 \tag{25}$$

$$f_t = 2.2\lambda\sqrt{f_c'} \tag{26}$$

$$\cot\phi = \sqrt{1 + \frac{\overline{\sigma_{ct}}}{f_t}} \tag{27}$$

In **Eq. (27)**, $\overline{\sigma_{ct}}$ is the average normal stress developed by bending moment at the inclined cracking surface. The values of $\overline{\sigma_{ct}}$ and c_s are determined from sectional analysis considering bending moment, axial force, and assuming linear strain distribution. The authors of this proposal provided equations and graphical aids to estimate these parameters, and details of the model can be found elsewhere[23–25]. The shear strength provided by the shear reinforcement is given by **Eq. (3)**.

2.3.7 Reineck

The method proposed by Reineck[26] is based on the tooth model. The early development of this model can be found elsewhere[27–30]. The approach for calculating the shear strength is different for members with and without shear reinforcement. In accordance with this model, the concrete contribution for members without shear reinforcement is evaluated with **Eq. (28)**, while for members with shear reinforcement it is taken as **Eq. (29)**:

$$V_c = \left[71\lambda \left(\rho_w \frac{f_c^{'}}{d} \right)^{1/3} - 0.23\sigma_c \right] b_w d \tag{28}$$

$$V_c = 0.066 f_{cwu} b_w z \tag{29}$$

where σ_c is the normal stress caused by axial load on the gross section; $\sigma_c = N / A_g$ (negative for compressive stress and positive for tensile stresses); $f_{cwu} = 0.70 f_c^{'}$ is the compressive strength of inclined struts in the web, and *z* is the inner lever arm.

The contribution of the shear reinforcement is given by **Eq. (30)**:

$$V_s = Either\ of \begin{cases} \dfrac{A_v}{s} f_{yt} z \cot \beta_r \\ \dfrac{A_v}{s} f_{yt} z \cot \theta \end{cases} \tag{30}$$

where β_r is the crack inclination angle given by **Eq. (31)**; and θ is the inclination angle of the struts given by **Eq. (32)**. The first line of **Eq. (30)** and **Eq. (31)** were used in this evaluation.

$$\cot \beta_r = 1.20 - 1.40 \frac{\sigma_c}{f_c^{'}} \tag{31}$$

$$1 \le \cot \theta = \frac{\cot \beta_r}{1 - \dfrac{V_c}{V_u}} \le 3 \tag{32}$$

2.4 DATABASE FOR ONE-WAY SHEAR IN REINFORCED CONCRETE BEAMS

A significant amount of experimental work has been carried out to study the shear response of concrete beams with and without shear reinforcement. Over the last 15 years, the *Joint ACI-ASCE Committee 445*, in collaboration with the German Committee of reinforced concrete (DAbStb), has built a database of slender beams ($a/d > 2.4$) with a clear shear failure. The datasets used in this research include reinforced concrete members without shear reinforcement (784 samples), and reinforced concrete members with shear reinforcement (large dataset: 170 samples and small dataset: 87 samples). The ranges of the most relevant input parameters in the databases are shown in **Table 2.1,** and their distributions are drawn in **Fig. 2.1.** The criteria for collecting the experimental information and a full description of the data is given elsewhere[5,6]. For members with shear reinforcement, there are two databases: the large database and the small database. The small database is a subset of the large database where there is certainty that the shear reinforcement yielded before the shear failure occurred.

2.4.1 Data exploring

As a first step to explore the data, the average shear stress in the concrete at failure ($v_c = V_c/b_w d$) was plotted against relevant variables, for beams without shear reinforcement and for beams with shear reinforcement (small database). For members with shear reinforcement, V_c was estimated as $V_c = V_{exp} - V_s$, where V_{exp} stands for experimental test result, and V_s was taken from **Eq. (3)**. The results are shown in **Fig. 2.2** and **Fig. 2.3**, respectively.

Scatter plots do not allow a straightforward interpretation of the data because of the significant dispersion and poor distribution of the test parameters (see **Fig. 2.1**). Therefore, box plots are also presented. The central mark inside the box indicates the median, and the bottom and

top edges of the box indicate the 25th and 75th percentiles, respectively. The whiskers indicate the most extreme data points: minimum and maximum.

For members without shear reinforcement, **Fig. 2.2** shows a positive correlation between v_c and $\sqrt{f_c'}$ in the box plot, which is not evident from the corresponding scatter plot. The dependency of v_c on d is clearly seen in scatter and box plots. If one looks to the scatter plot, the ratio a/d seems to be relevant for v_c; however, the box plot clarifies that the correlation between v_c and a/d is negative but weak. A strong positive correlation is seen between v_c and ρ_w.

For members with shear reinforcement, **Fig. 2.3** shows a strong correlation among v_c and ρ_w and ρ_v; however, correlations among v_c and $\sqrt{f_c'}$, a/d, and d are not clear.

2.4.2 Coefficients of correlation and significance test

The correlation coefficient, r, is a measure of the strength and direction of the linear relationship between v_c and a variable of interest ($\sqrt{f_c'}$, d, a/d, ρ_w, d_{agg} or ρ_v), and an estimate of the unknown population correlation coefficient, ρ. However, the ability to infer about the population based on a sample depends on the database size. A significance test of the correlation coefficient was conducted to determine if the evidence collected from the available datasets is enough to infer about the linear correlation in the population[31] (see **Table 2.2** and **Table 2.3**). The null hypothesis is H_o: $\rho = 0$, while the alternate hypothesis is H_a: $\rho \neq 0$. Sample size (N), degrees of freedom (df), significance level (α), and critical values of the two-tailed Student's t-distribution (t_c) are given in each table.

According to **Table 2.2**, for members without shear reinforcement, H_o is rejected in favor of H_a at 0.05 significance level for all variables considered. Therefore, the evidence is sufficient

to say that the population correlation coefficient, ρ, is different from zero in all cases. Therefore, one can conclude that v_c is influenced by $\sqrt{f_c'}$, d, a/d, ρ_w, and d_{agg}. As indicated in **Table 2.3**, for members with shear reinforcement, H_o is rejected in favor of H_a at 0.05 significance level for $\sqrt{f_c'}$, ρ_w, and ρ_v. Therefore, the evidence is sufficient to conclude that ρ between v_c and $\sqrt{f_c'}$, ρ_w, and ρ_v is different from zero. The correlation between v_c and d, a/d, and d_{agg} is negligible and not statistically significant; therefore, it is fair to say that there is not enough evidence to suspect d, a/d, or d_{agg} influences of the resistance mechanism of members with shear reinforcement. A non-linear correlation could exist and further analysis could be done on that regard.

2.5 COMPARISON OF PREDICTIONS AND EXPERIMENTAL RESULTS

The described methods in section 2.3 were analyzed to study their accuracy in predicting shear strength using several criteria. Four categories of comparison were defined: graphical, central tendency, statistical goodness-of-fit, and statistical distances. The V_{exp}/V_{pred} ratio is used for comparing, where V_{exp} is the experimentally obtained shear strength and V_{pred} is the predicted shear strength. For the V_{exp}/V_{pred} ratio, a value close to one means that the prediction is accurate. A V_{exp}/V_{pred} ratio greater than one indicates that the prediction is conservative. If the V_{exp}/V_{pred} ratio is less than one means that the shear strength was overestimated, and the prediction is unconservative. Box plots are used to visualize the predictive accuracy of each method; these plots are presented in **Appendices B** and **C**. Statistical central tendency and dispersion measures of V_{exp}/V_{pred} were calculated. Goodness-of-fit and statistical dispersion measures were plotted together so the more accurate methods are easily identified. Radar plots were used to produce a

single visual indicator of the overall performance of each method with respect to all the evaluation criteria.

2.5.1 Graphical comparison

Fig. 2.4 contains box plots of the V_{exp}/V_{pred} ratios obtained for all shear strength methods reviewed.

Fig. 2.4a shows the results for beams without shear reinforcement. A large dispersion and extreme values are observed in the ACI 318-14[1] simplified and Bentz and Collins[7] simplified methods. Also, severely unconservative predictions resulted from the application of the ACI 318-14[1] simplified and detailed methods. The ACI 318-19[3] new method is a significant improvement relative to both ACI 318-14[1] design alternatives. Bentz and Collins[7] detailed, and Li et al.[18] methods show outstanding performance. ACI 318-19[3], Frosch et al.[15] and Reineck[26] equations are also good predictors for members without shear reinforcement.

Fig. 2.4b shows the results for beams with shear reinforcement. The extreme values are much closer to one and the dispersion observed (box' sizes) is similar to the dispersion in the case of beams without shear reinforcement. Bentz and Collins[7] detailed and Frosch et al.[15] methods exhibit the least dispersion, while Reineck[26] proposal shows the largest dispersion of the group for members with shear reinforcement.

The median values of the methods plotted in **Fig. 2.4** are different, indicating that each method was developed or calibrated for a nonsystematic margin of safety defined by the judgment and experience of each developer(s). In this analysis, the empirical safety margin observed for each method is not a parameter of interest. In general, safety should be managed by a reliability assessment that includes resistance and load uncertainty. Therefore, further analysis of each predictor is focused on its accuracy and variability, rather than its safety margin.

2.5.2 Central tendency and dispersion measures

Central tendency and dispersion measures, i.e., mean, coefficient of variation (COV), percentage of unconservative predictions, and 5th percentile values (the 5th percentile value indicates the V_{exp}/V_{pred} ratio that 95 percent of the data exceed), are used to evaluate the performance of each method. **Table 2.4** summarizes the results. Based on the V_{exp}/V_{pred} ratios, the central tendency measures, and dispersion measures reported in **Table 2.4**, the reader can have an idea of the overall accuracy of each method and the empirical level of safety of each method analyzed. The lowest coefficients of variation are observed in the proposal from Li et al.[18] and Park and Choi[22] for members without and with shear reinforcement, respectively.

The database of members without shear reinforcement is composed of 734 specimens loaded with concentrated loads, and 50 specimens loaded with uniformly distributed loads. In general, the mean V_{exp}/V_{pred} ratio is between 4–17 percent less for the case of tests under uniform loads than for tests under concentrated loads.

2.5.3 Statistical goodness-of-fit

The least-square linear regression line $V_{pred}*=kV_{pred}$ was found for each method to fit V_{exp} as close as possible. Thus, $V_{pred}*$ is the best possible fit between prediction and experimental data. Then, goodness-of-fit indicators between V_{exp} and $V_{pred}*$ were calculated: coefficients of determination (R^2), and root of mean squared errors (*RMSE*). Additionally, the percentage of predictions that were within 20 percent of the corresponding experimental values was also calculated and denoted "acceptable predictions" (*AP*). See results in **Table 2.5**.

2.5.4 Statistical distances

The two-sample Kolmogorov-Smirnov test[32] was used to examine whether the two datasets (V_{exp} and V_{pred}*) come from the same distribution. This test is based on the maximum distance between two cumulative distribution functions (CDF) as indicated in **Eq. (33)**.

$$D_{ks} = \max_{V} \left| CDF(V_{\exp}) - CDF(V^{*}_{pred}) \right| \tag{33}$$

A distance, D_{ks}, was calculated between the V_{exp} and V_{pred}* distributions for each method. The average distance between the two distributions, D_{kss}, was also calculated and used as an indicator of the difference between the V_{exp} distribution and the V_{pred}* distribution. This can be expressed as **Eq. (34):**

$$D_{kss} = \frac{1}{N} \sum_{i=1}^{N} \left| CDF(V_{\exp i}) - CDF(V^{*}_{pred\,i}) \right| \tag{34}$$

where N is the number of pair samples. **Fig. 2.5** shows two example distributions and indicates the maximum distance between V_{exp} and V_{pred}* (D_{ks}), and one pair at which $CDF(V_{exp})$ minus $CDF(V_{pred}*)$ can be calculated. **Table 2.5** shows the results of the statistical distances of both categories of concrete members.

The statistical analysis on the accuracy of each method, reported in **Table 2.5**, highlights the performance of Cladera et al.[10] and Frosch et al.[15] proposals in the prediction of V_c for members without shear reinforcement since these show the greatest R^2. Similarly, Bentz and Collins[7] detailed method shows the highest R^2 in the prediction of shear strength for members with shear reinforcement.

2.6 RESULTS AND DISCUSSION

There are three significant changes between ACI 318-14[1] and ACI319-19[3] shear equations: (1) the moment-to-shear ratio (*M/Vd*) dependency was removed; (2) a size effect factor was incorporated for members without shear reinforcement; and (3) the shear strength depends on the cube root of the longitudinal steel ratio (ρ_w), instead of linearly as before. The new ACI 318-19[3] shear design provisions overcome some of the identified drawbacks, and overall it represents a more robust one-way shear strength model. In addition, the ACI 318-19[3] new provisions simplify the process of shear strength calculations and improve the accuracy of the shear strength prediction. ACI 318-19[3] is also the simplest of all methods reviewed, and it gives reasonably accurate predictions for members with and without shear reinforcement.

The available methods for predicting shear strength of reinforced concrete members have different levels of complexity. ACI 318-14[1], ACI319-19[3], and Reineck[26] methods can be directly applied if the basic geometric and mechanical information of the member is known. ACI 318-14[1] contains a large number of equations, and the detailed procedure requires the designer to look for the most critical *M/Vd* ratio along the length of the member. Bentz and Collins[7] detailed approach requires an iterative process and searching for the most critical *M/Vd* ratio. Cladera et al.[10], and Li et al.[18] proposals require the *a/d* ratio, and not the most critical *M/Vd* ratio. Frosch et al.[15], Cladera et al.[10], Li et al.[18], and Park and Choi[22] equations require the calculation of the neutral axis depth at each critical section.

The effect of the amount of longitudinal reinforcement and the size effect are considered in different ways in the methods reviewed. The only two approaches that explicitly include a dependency on the amount of longitudinal steel are ACI 318-19[3] and Reineck[26]. In both cases, V_c is a function of $\rho_w^{1/3}$. All methods use a hyperbolic approach to model the size effect. ACI 318-

19[3], Cladera et al.[10], Frosch et al.[15], and Li et al.[18] use a size effect factor that depends on the square root of *d* or *h*. Park and Choi[22] proposal uses a size effect factor that depends on the fourth root of *d*, and Reineck[26] equation includes a size factor that depends on the cube root of *d*.

The shear strength is often considered a function of the tensile strength of the concrete, which depends on $\sqrt{f_c'}$ or $\left(f_c'\right)^{1/3}$. In the proposal by Reineck[26] V_c depends on $\left(f_c'\right)^{1/3}$ for members without shear reinforcement and depends directly on f_c' for members with shear reinforcement.

Fig. 2.6 contains plots of *COV* vs. normalized *RMSE* and *COV* vs. *AP* in such a way that methods located close to the bottom left corner of the plots are those that exhibit the best performance. Hollow markers are used to represent the results obtained from the analysis of members without shear reinforcement, and solid markers are used to plot the results from the analysis of member with shear reinforcement. A line connects the two markers corresponding to each method; thus, a shorter line indicates that a method has more consistent performance for both reinforcement cases (with and without). If one looks at members without shear reinforcement (hollow markers), the proposal from Frosch et al.[15], Li et al.[18], and Reineck[26] show the best performance. If one focuses on members with shear reinforcement (solid markers) the proposal from Frosch et al.[15], Li et al.[18], Park and Choi[22], and Bentz and Collins[7] detailed exhibit the best performance. Consistent performance across both types of members is found in the application of Li et al.[18], Frosch et al.[15], and ACI 318-19[3]. The performance of ACI 318-19[3] is far better than the traditional provisions in ACI 318-14[1].

Fig. 2.7 contains radar plots with all parameters used for comparing performance. In the radar plots, there is one axis per parameter, and all results are plotted on the same scale. Each axis is set so the larger the value, the better the performance. The most interior pentagram is the

minimum value of the axis, and the exterior pentagram is the maximum value the axis. For each method, each parameter defines a point along the corresponding axis, thus a polygon can be drawn for each method. The larger the polygon, the better the method. **Fig. 2.7a** shows the results for members without shear reinforcement, and it clearly indicates that ACI 318-14[1] methods are the least suitable for predicting V_c, while Cladera et al.[10], Frosch et al.[15], Reineck[26], and Li et al.[18] are in excellent agreement with the database. **Fig. 2.7b** includes the results for members with shear reinforcement, and it indicates that Park and Choi[22], and Frosch et al.[15] proposals show the best agreement with the database.

The selection of a particular method depends on the intended purpose (size of the member, amount of longitudinal and shear reinforcement, compressive strength of concrete, and others) and the chosen level of analysis complexity. Figures contained in **Appendices B** and **C** inform the reader how the median V_{exp}/V_{pred} ratio varies as a function of relevant variables. The drawbacks of the ACI 318-14[1] methods, and how much better the ACI 318-19[3] method is, are clearly seen in **Fig. B1–B3**. Frosch et al.[15] and Reineck[26] proposals tend to give more conservative predictions for low *a/d* ratios, while Li et al.[18] show the opposite trend (see **Fig. B7, B8, and B10**). Unconservative predictions can be observed in **Appendix C** for a large amount of shear reinforcement for all methods. These are very few data points that represent beams heavily reinforced with stirrups that do not represent typical construction.

2.7 CONCLUSIONS

The accuracy of several methods to predict one-way shear strength was evaluated. Each method's ability to predict shear strength in members with and without shear reinforcement was studied by comparing predictions against experimental results available in the literature. The results were

informed by measures of dispersion, goodness-of-fit indicators, and statistical distances. The accuracy of each method is reported in tables and plots, so they serve as a guide for practitioners to select a suitable one-way shear strength method for a given structural application.

The analysis described in this paper resulted in the following conclusions:

1. The new ACI 318-19[3] shear design method is the simplest of the methods reviewed, and it gives reasonably accurate predictions for members with and without shear reinforcement.
2. For members without shear reinforcement, the ACI 318-14[1] shear strength equations are not recommended. All other available methods analyzed are similar regarding their level of accuracy in this category. The methods evaluated predict between 4–17 percent larger strength for members uniformly loaded than for members under concentrated loads.
3. For members with shear reinforcement, the ACI 318-14[1] simplified, Reineck[26], and Cladera et al.[10] methods are the least suitable for predicting one-way shear strength of all alternatives considered. All other available methods analyzed are similar regarding their level of accuracy in this category.

2.8 FURTHER RESEARCH

The effect of flanges and compressive steel reinforcement needs to be evaluated because of its influence in the depth of the neutral axis that is a significant component in the shear strength mechanism. The method proposed for Cladera et al.[10] includes the concept of effective with for T-beams and L-beams. The effect of the degree of accuracy on the neutral axis depth calculation can also be important to look at. A comparison among methods could be helpful in understanding the differences for a wide range of parameters.

REFERENCES

1. ACI Committee 318. “Building code requirements for structural concrete: (ACI 318-14); and commentary (ACI 318R-14),” Farmington Hills, MI, American Concrete Institute, 2014.
2. Belarbi, A., Kuchma, D. A., and Sanders, D. H. “Proposals for New One-Way Shear Equations for the 318 Building Code,” *Concrete International,* V. 39, No. 9, 2017, pp. 29–32.
3. ACI Committee 318. “Building code requirements for structural concrete: (ACI 318-19); and commentary (ACI 318R-19),” Farmington Hills, MI, American Concrete Institute, 2019.
4. Kuchma, D. A., Wei, S., Sanders, D. H., et al. “Development of the One-Way Shear Design Provisions of ACI 318-19 for Reinforced Concrete,” *ACI Structural Journal,* V. 116, No. 4, 2019.
5. Reineck, K.-H., Kuchma, D. A., Kim, K. S., et al. “Shear Database for Reinforced Concrete Members without Shear Reinforcement,” *ACI Structural Journal*, V. 100, No. 2, 2003.
6. Reineck, K.-H., Bentz, E., Fitik, B., et al. “ACI-DAfStb Databases for Shear Tests on Slender Reinforced Concrete Beams with Stirrups,” *ACI Structural Journal,* V. 111, No. 5, 2014.
7. Bentz, E. C., and Collins, M. P. “Updating the ACI Shear Design Provisions,” *Concrete International,* V. 39, No. 9, 2017, pp. 33–38.
8. Vecchio, F. J., and Collins, M. P. “The modified compression-field theory for reinforced concrete elements subjected to shear,” *ACI J.*, V. 83, No. 2, 1986, pp. 219–231.
9. Bentz, E. C., and Collins, M. P. “Development of the 2004 Canadian Standards Association (CSA) A23.3 shear provisions for reinforced concrete,” *Canadian Journal of Civil Engineering*, V. 33, No. 5, 2006, pp. 521–34.
10. Cladera, A., Marí, A., Bairán, J.-M., et al. “One-Way Shear Design Method Based on a Multi-Action Model,” *Concrete International,* V. 39, No. 9, 2017, pp. 40–46.
11. Mari, A., Bairán, J., Cladera, A., et al. “Shear-flexural strength mechanical model for the design and assessment of reinforced concrete beams,” *Structure and Infrastructure Engineering*, V. 11, No. 11, 2015, pp. 1399–419.
12. Cladera, A., Marí, A., Ribas, C., et al. “Predicting the shear–flexural strength of slender reinforced concrete T and I shaped beams,” *Engineering Structures,* V. 101, 2015, pp. 386–98.
13. Mari, A., Bairán, J. M., Cladera, A., et al. “Shear Design and Assessment of Reinforced and Prestressed Concrete Beams Based on a Mechanical Model,” *Journal of Structural Engineering*, V. 142, No. 10, 2016, p. 04016064.
14. Bažant, Z. P., Yu, Q., Gerstle, W., et al. “Justification of ACI 446 Proposal for Updating ACI Code Provisions for Shear Design of Reinforced Concrete Beams,” *ACI Structural Journal*, V. 104, No. 5, 2007.
15. Frosch, R. J., Yu, Q., Cusatis, G., et al. “A Unified Approach to Shear Design,” *Concrete International,* V. 39, No. 9, 2017, pp. 47–52.
16. Tureyen, A. K., and Frosch, R. J. “Concrete shear strength: Another perspective,” *Structural Journal,* V. 100, No. 5, 2003, pp. 609–615.

17. Tureyen, A. K., Wolf, T. S., and Frosch, R. J. “Shear strength of reinforced concrete T-beams without transverse reinforcement,” *ACI structural journal*, V. 103, No. 5, 2006, p. 656.
18. Li, Y.-A., Hsu, T. T., and Hwang, S.-J. “Shear Strength of Prestressed and Nonprestressed Concrete Beams,” *Concrete International*, V. 39, No. 9, 2017, pp. 53–57.
19. Laskar, A., Hsu, T. T. C., and Mo, Y. L. “Shear Strengths of Prestressed Concrete Beams Part 1: Experiments and Shear Design Equations,” *ACI Structural Journal,* V. 107, No. 03, 2010.
20. Hsu, T. T. C., Laskar, A., and Mo, Y. L. “Shear Strengths of Prestressed Concrete Beams Part 2: Comparisons with ACI and AASHTO Provisions,” *ACI Structural Journal*, V. 107, No. 03, 2010.
21. Kuo, W. W., Hsu, T. T. C., and Hwang, S. J. “Shear Strength of Reinforced Concrete Beams,” *ACI Structural Journal*, V. 111, No. 4, 2014.
22. Park, H.-G., and Choi, K.-K. “Unified Shear Design Method of Concrete Beams Based on Compression Zone Failure Mechanism,” *Concrete International*, V. 39, No. 9, 2017, pp. 59–63.
23. Choi, K.-K., Park, H.-G., and Wight, J. “Unified Shear Strength Model for Reinforced Concrete Beams—Part I: Development,” *ACI Structural Journal*, V. 104, No. 2, 2007.
24. Choi, K.-K., and Park, H.-G. “Unified Shear Strength Model for Reinforced Concrete Beams—Part II: Verification and Simplified Method,” *ACI Structural Journal*, V. 104, No. 2, 2007.
25. Choi, K.-K., Kim, J.-C., and Park, H.-G. “Shear Strength Model of Concrete Beams Based on Compression Zone Failure Mechanism,” *ACI Structural Journal*, V. 113, No. 5, 2016.
26. Reineck, K.-H. “Proposal for ACI 318 Shear Design,” *Concrete International*, V. 39, No. 9, 2017, pp. 65–70.
27. Kani, G. N. J. “The riddle of shear failure and its solution.” Journal Proceedings, vol. 61. 1964. pp. 441–468.
28. Kani, G. N. J. “Basic facts concerning shear failure.” Journal Proceedings, vol. 63. 1966. pp. 675–692.
29. Fenwick, R. C., and Pauley, T. “Mechanism of shear resistance of concrete beams,” *Journal of the Structural Division*, V. 94, No. 10, 1968, pp. 2325–2350.
30. Taylor, H. P. J. “Investigation of the forces carried across cracks in reinforced concrete beams in shear by interlock of aggregate,” 1970.
31. Wonnacott, T. H., and Wonnacott, R. J. “Introductory Statistics,” 5th edition, Canada, Wiley, 1990.
32. Massey, F. J. “The Kolmogorov-Smirnov Test for Goodness of Fit,” *Journal of the American Statistical Association*, V. 46, No. 253, 1951, pp. 68–78.

Table 2.1–Range of the main input parameters in the databases

Parameter	Without shear reinforcement Range	With shear reinforcement Range
f_c' *(psi)*	1,530–19,820	1,598–17,827
d (in)	2.3–118.1	6.3–53.9
ρ_w	0.0014–0.664	0.0050–0.1561
a/d	2.4–8.1	2.4–7.1
ρ_v	N/A	0.0007–0.0387

Table 2.2–Correlation coefficients and test of significance for members without shear reinforcement. ***N=784, df=783,*** α***=0.05,*** t_c***=1.96***

Variable	*r*	*t-stat*	$\lvert t_{stat}\rvert > \lvert t_c\rvert$	Conclusion
$\sqrt{f_c'}$	0.43	13.14	TRUE	Reject H_o
d	-0.45	-14.13	TRUE	Reject H_o
a/d	-0.11	-3.08	TRUE	Reject H_o
ρ_w	0.66	24.68	TRUE	Reject H_o
d_{agg}	-0.17	-4.83	TRUE	Reject H_o

Table 2.3–Correlation coefficients and test of significance for members with shear reinforcement (small database). ***N=87, df=86,*** α ***=0.05,*** t_c***=1.99***

Variable	*r*	t_{stat}	$\lvert t_{stat}\rvert > \lvert t_c\rvert$	Conclusion
$\sqrt{f_c'}$	0.23	2.18	TRUE	Reject H_o
d	0.03	0.28	FALSE	Fail to reject H_o
a/d	0.05	0.42	FALSE	Fail to reject H_o
ρ_w	0.76	10.95	TRUE	Reject H_o
d_{agg}	-0.14	-1.33	FALSE	Fail to reject H_o
ρ_v	0.66	8.06	TRUE	Reject H_o

Table 2.4–Measures of central tendency and dispersion of V_{exp}/V_{pred} ratio

Method	Without shear reinforcement				With shear reinforcement (large)			
	MEAN	COV (%)	$V_{exp}/V_{pred} < 1$ (%)	P_{5th}	MEAN	COV (%)	$V_{exp}/V_{pred} < 1$ (%)	P_{5th}
ACI 318-14 simplified	1.494	39	15	0.69	1.476	23	2	0.89
ACI 318-14 detailed	1.096	30	39	0.64	1.227	21	4	0.79
ACI 318-19	1.410	22	7	0.96	1.321	21	2	0.89
Bentz and Collins detailed	1.034	24	55	0.78	1.115	20	6	0.74
Cladera et al.	1.247	26	13	0.92	1.034	23	10	0.68
Frosch et al.	1.501	20	2	1.12	1.201	20	4	0.81
Li et al.	1.446	19	3	1.07	1.397	20	1	1.00
Park and Choi	1.360	23	6	0.98	1.367	19	2	0.97
Reineck	1.376	20	4	1.02	1.127	30	8	0.64

Table 2.5–Measures of goodness-of-fit and statistical distance between V_{exp} and V_{pred}*

Method	Without shear reinforcement					With shear reinforcement (large)				
	R^2	*RMSE (kip)*	*AP (%)*	D_{ks}	D_{kss}	R^2	*RMSE (kip)*	*AP (%)*	D_{ks}	D_{kss}
ACI 318-14 simplified	0.63	17	4	0.50	0.0330	0.89	26	51	0.17	0.0115
ACI 318-14 detailed	0.71	15	5	0.44	0.0270	0.90	25	67	0.10	0.0079
ACI 318-19	0.91	8	65	0.09	0.0064	0.91	24	61	0.15	0.0107
Bentz and Collins detailed	0.92	8	73	0.11	0.0067	0.93	21	66	0.13	0.0093
Cladera et al.	0.95	6	76	0.05	0.0028	0.90	25	46	0.28	0.0149
Frosch et al.	0.95	6	73	0.06	0.0030	0.91	23	68	0.08	0.0067
Li et al.	0.94	7	72	0.08	0.0049	0.90	25	65	0.10	0.0085
Park and Choi	0.93	8	67	0.12	0.0077	0.90	24	69	0.11	0.0074
Reineck	0.93	7	76	0.09	0.0050	0.76	38	44	0.18	0.0178

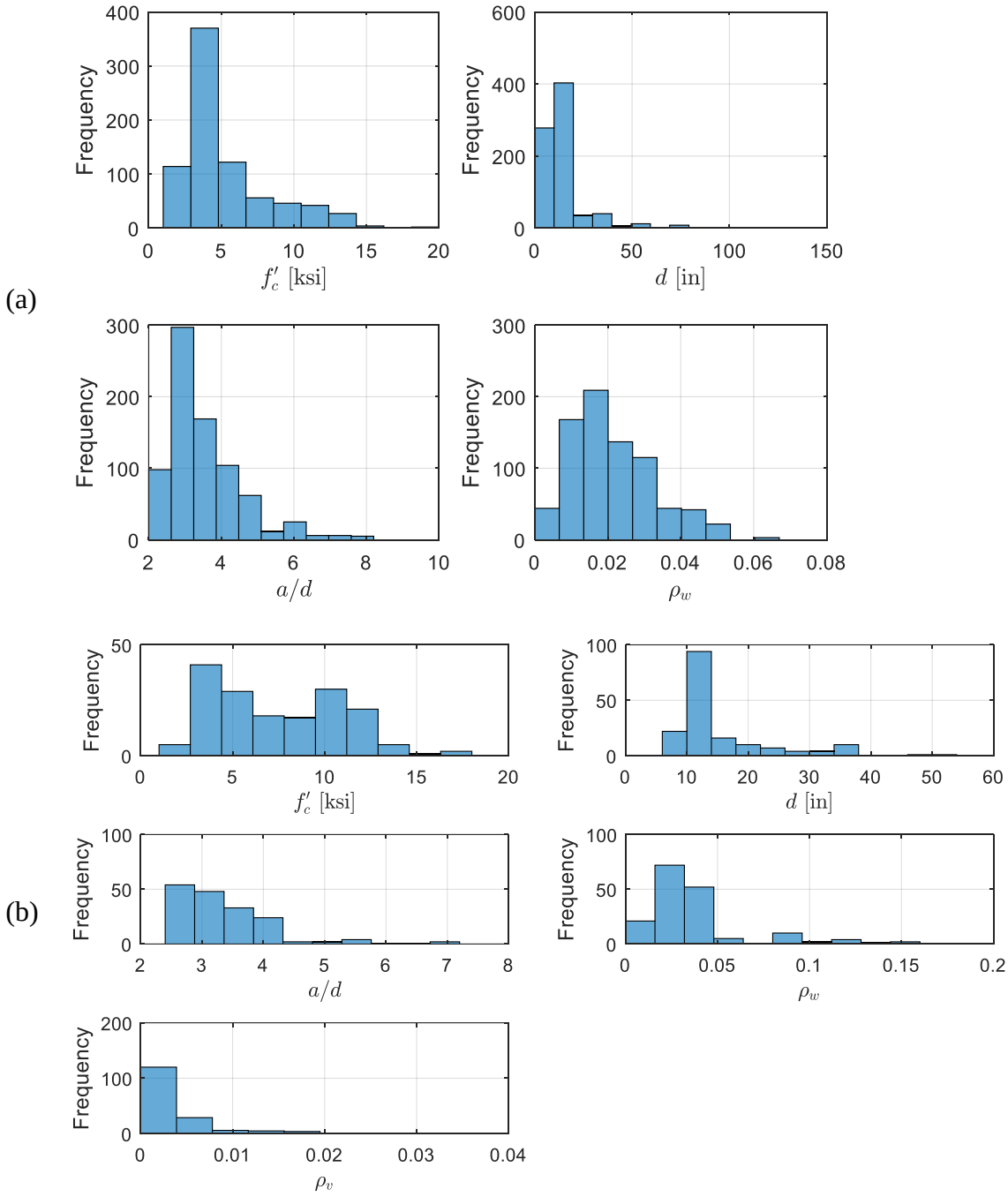

Fig. 2.1–Distribution of the main input parameters in the databases: (a) members without shear reinforcement; and (b) members with shear reinforcement

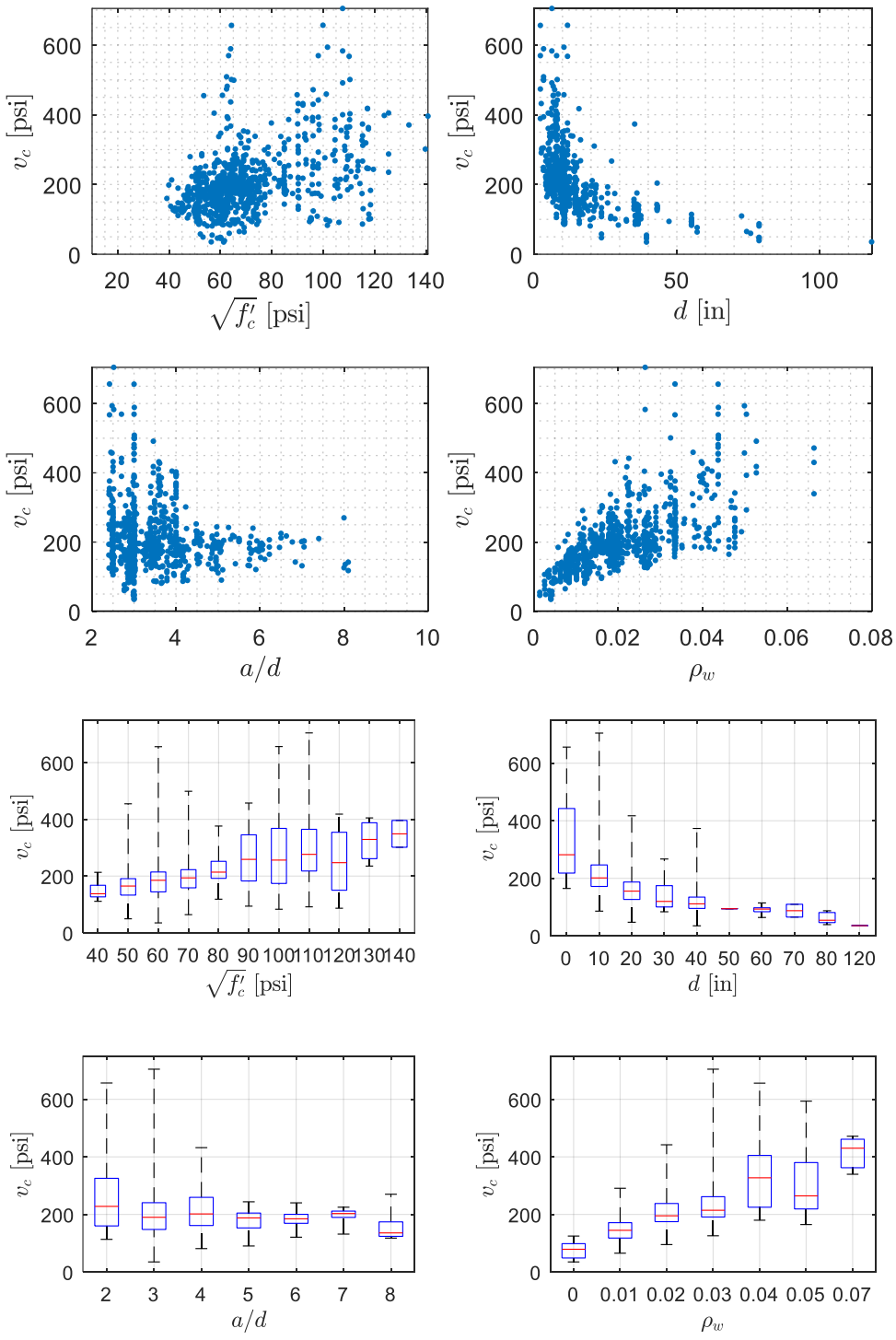

Fig. 2.2–Average shear stress at failure as function of relevant input parameters for members without shear reinforcement

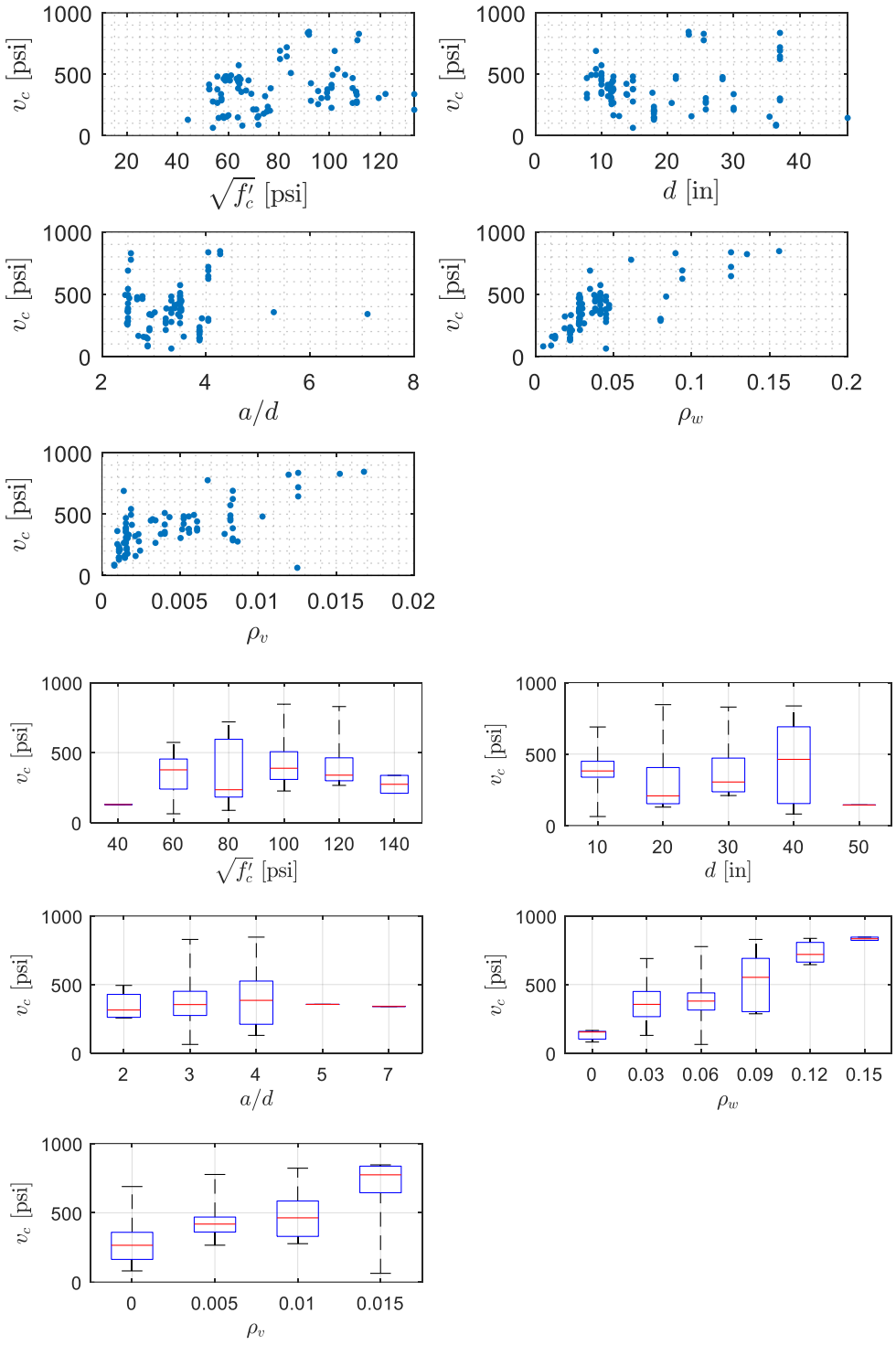

Fig. 2.3–Average shear stress in the concrete at failure as function of relevant input parameters for members with shear reinforcement (small database)

(a)

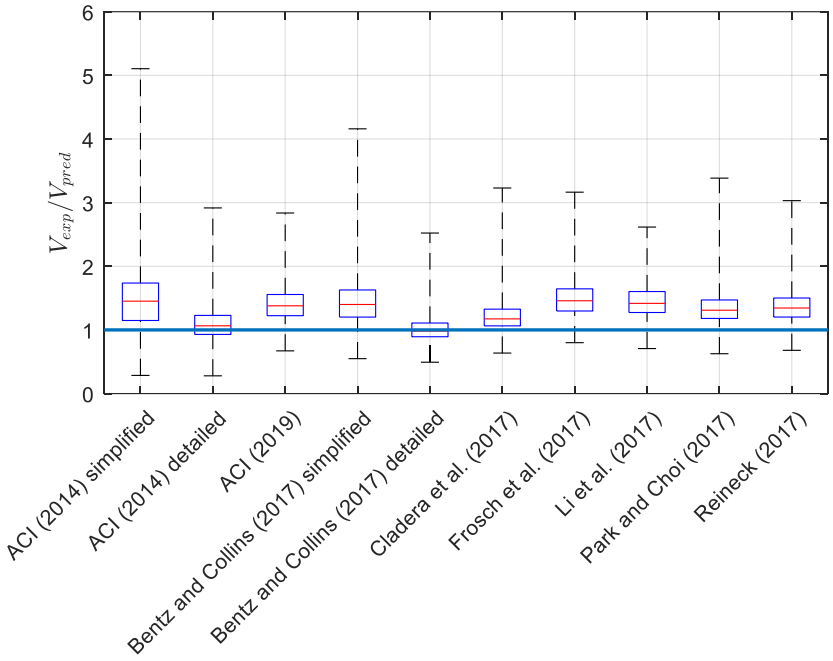

(b)

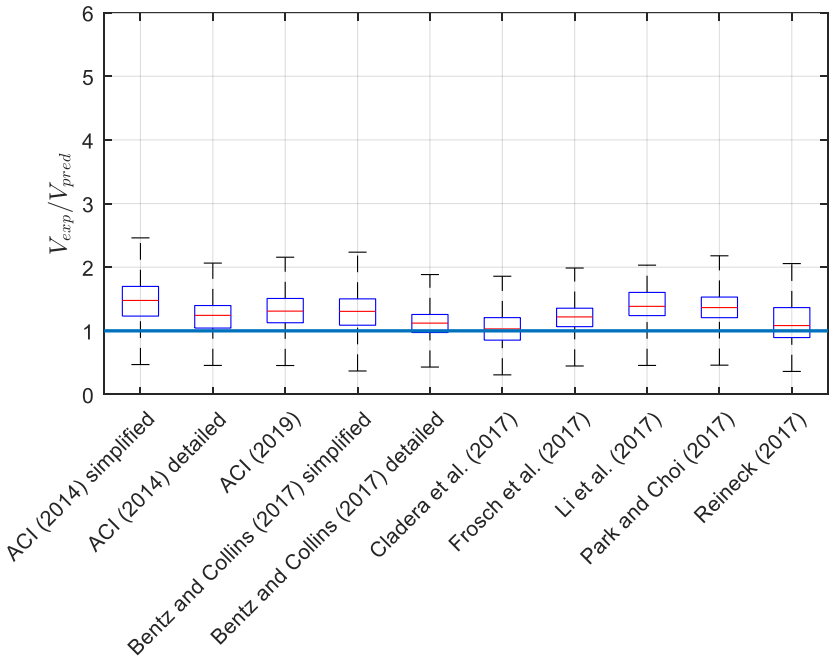

Fig. 2.4–Performance of methods based on V_{exp}/V_{pred} ratio: (a) members without shear reinforcement; (b) members with shear reinforcement

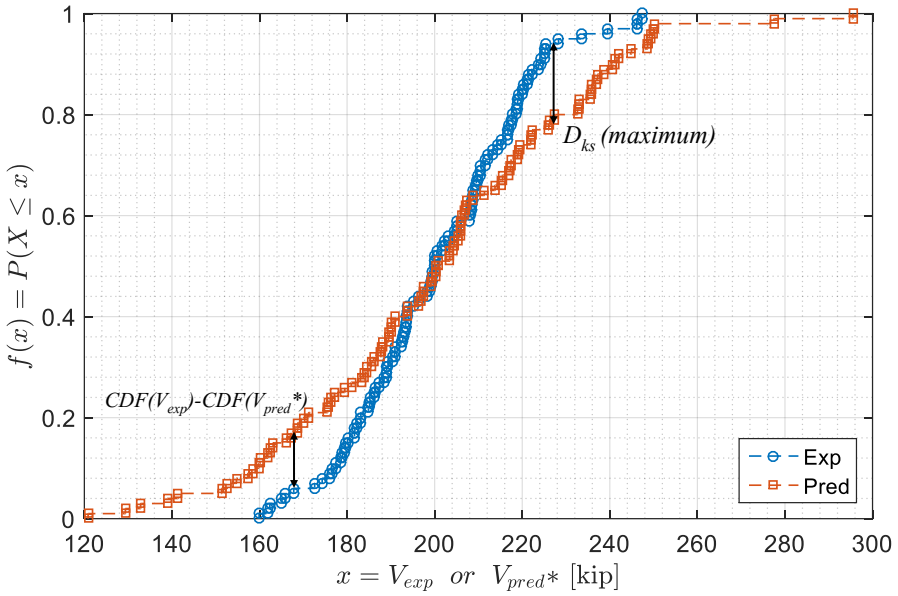

Fig. 2.5–Graphical explanation of statistical distances

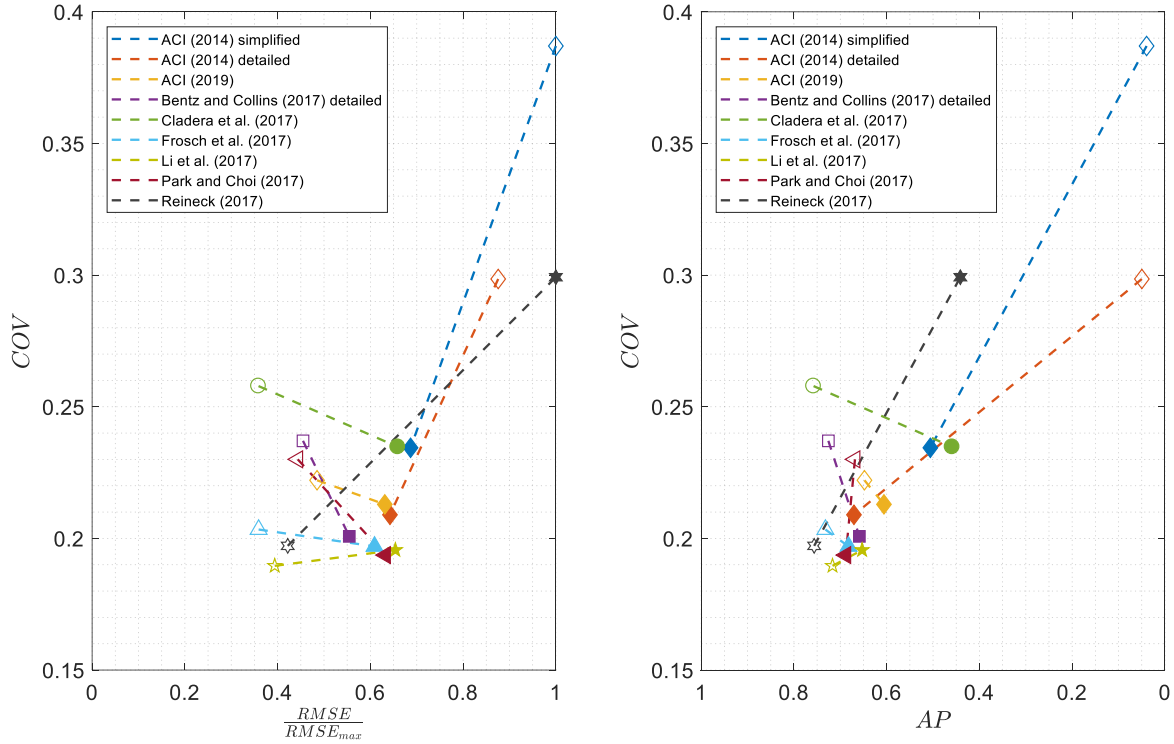

Fig. 2.6–Summary of results for members without shear reinforcement (hollow markers) and members with shear reinforcement (solid markers)

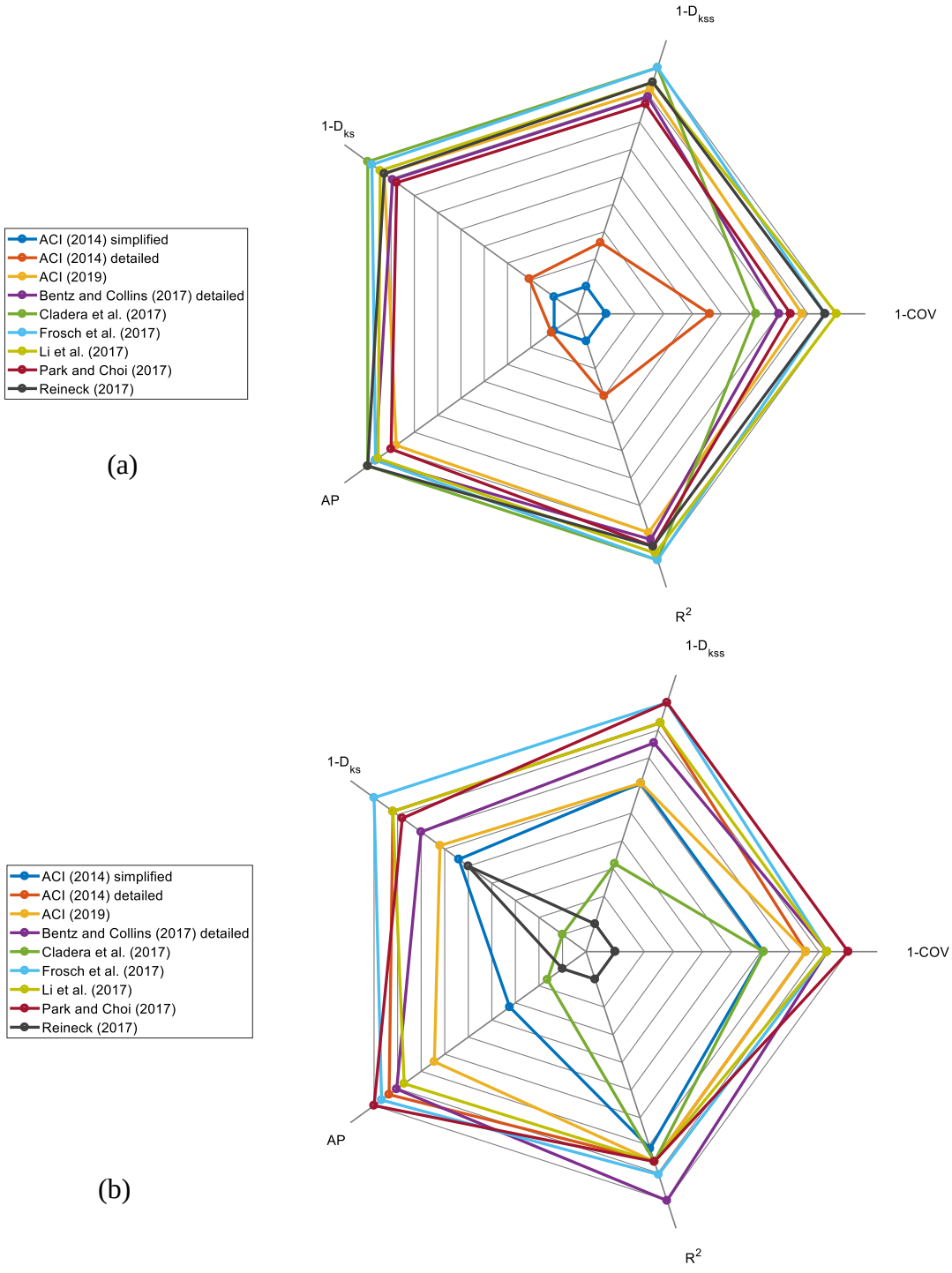

Fig. 2.7–Radar plot for (a) members without shear reinforcement and (b) with shear reinforcement

Chapter 3

STATISTICAL MODELS AND STRENGTH REDUCTION FACTORS FOR THE ACI 318-19 NEW ONE-WAY SHEAR EQUATIONS

ABSTRACT

The one-way shear design equations for reinforced concrete members in the *ACI 318 Building code requirements for structural concrete* remained essentially unchanged from 1963, until the publication of ACI 318-19. Since the one-way shear equations have now been improved, there is an opportunity for updating the strength reduction factor aiming for more efficient shear designs.

Statistical models for one-way shear resistance are developed, including uncertainty in material, fabrication, and analysis. On this last source of uncertainty, uncertainty in analysis or professional factor, this research proposes data-driven professional factors that update the experience-based professional factor used in previous reliability-based calibrations. The statistical models of resistance developed are then used to obtained reliability-based strength reduction factors for one-way shear design. Reinforced concrete slabs and beams with and without web reinforcement are included in this calibration.

Two sets of strength reduction factors are suggested. One set is defined to assure an equivalent safety margin as in past satisfactory practice, and a second set is defined with the objective of reducing the likelihood of brittle failure modes.

Keywords: reliability; one-way shear; reinforced concrete; design

3.1 INTRODUCTION

The traditional shear design equations for reinforced concrete beams in the *ACI 318-14 Building code requirements for structural concrete*[1] provisions were developed in 1963. Over the past few decades, several drawbacks of these provisions were identified by the work done for the *ACI Subcommittee 318-E Section and Member Strength*, and the *Joint ACI-ASCE Committees 445* and *446 Shear and Torsion and Fracture Mechanics of Concrete*. It has been repetitively shown that those shear design provisions may be dangerously unconservative when applied to the design of large or lightly longitudinally reinforced beams. ACI 318-19[2] has replaced the traditional one-way shear design method with a new set of empirical equations while maintaining the strength reduction factor for shear as $\phi = 0.75$. The new equations are more accurately predict one-way shear strength; therefore, there is an opportunity for improving the efficiency of reinforced concrete shear design by updating the strength reduction factor (or resistance factor). Thus, the concrete industry can take full advantage of the new improved shear model.

The available statistical parameters describing the variability of material properties, construction or fabrication uncertainties, and analysis model performance allow for the determination of statistical parameters for the traditional one-way shear strength provisions in ACI 318-14[1] and the new one-way shear strength provisions in ACI 318-19[2]. This is the first reliability analysis of the ACI 318-19[2] new shear design method. The objective of this study is to evaluate if any change in strength reduction factors for the shear design for future editions of the ACI 318 building code requirements is warranted. The resulting proposed strength reduction factors for one-way shear strength design are based on reliability analysis and statistical simulations supported on the *Joint ACI-ASCE Committees 445* database of shear test results. The proposed strength reduction factors maintain consistency with the former code calibration; also,

considerations to reduce the likelihood of brittle failure modes are suggested.

3.2 RESEARCH SIGNIFICANCE

The contributions of this study are: (1) the update of statistical model for analysis uncertainty based on available experimental data (data-driven professional factor); (2) the determination of the probabilistic safety margin of members designed for one-way shear according to ACI 318-14[1] specifications; (3) the development of statistical models for one-way shear resistance; and (4) the reliability-based calibration of strength reduction factors for the new ACI 318-19[2] one-way shear design method.

3.3 PROCEDURE OVERVIEW

The procedure followed to determine resistance factors, i.e., strength reduction factors, was developed by Nowak[3,4] for the calibration of the *AASHTO LRFD Bridge design specifications*. The considered load components include dead load and live load, and their statistical models are based on the available literature[5,6]. The structural types considered are reinforced concrete slabs and beams with and without web transverse reinforcement. The statistical models for one-way shear resistance developed in this paper are based on available data for material properties and fabrication tolerances documented by Nowak et al.[7] In the past, the uncertainty in the one-way shear prediction, i.e., the analytical uncertainty or professional factor, has been estimated relying on professional judgment and experience of experts by previous researchers dealing with reliability-based calibrations. The research described in this paper is focused on determining data-driven professional factors for one-way shear strength predictions.

The statistical models for resistance are developed for components with representative dimensions and reinforcement ratios. Resistance parameters are then used for the determination of appropriate resistance factors to reach a target probabilistic safety margin expressed in terms of a target reliability indexes. The reliability indexes are calculated for a practical range of load ratios expressed as $D_n/(D_n+L_n)$.

The selection of target reliability index—the target safety margin or performance in probabilistic terms—comprises the consideration of consequences of failure and cost of increasing the safety margin by a unit. This is a complicated task since it requires consensus among users, designers, builders, and other stakeholders. Instead, traditionally this target is defined based on past successful practice. The target reliability indexes in this research were estimated based on the reliability indexes calculated for slabs and beams made of ordinary concrete (concrete compressive strength ranging from 3,000 psi to 6,000 psi) designed according to ACI 318-14[1] building code requirements. A different separate set of target reliability indexes was defined based on considerations for reducing the likelihood of brittle failures.

The final step in the calibration is the selection of strength reduction factors (ϕ) for the shear strength limit state to correspond with the load factors specified in ASCE/SEI 7-16[8]. The acceptance criterion is closeness to the preselected target reliability index, where the strength reduction factors are rounded to the nearest 0.05. The reliability indexes are calculated for the proposed resistance factors and compared with the target values for each structural component considered.

3.4 RELIABILITY ANALYSIS BACKGROUND

There are many sources of uncertainty inherent to the design of concrete structures, e.g., the concrete compressive strength, yield stress, unit weight, flexural and shear load-carrying capacity will never have exactly the same observed value under the same test conditions. These, among other parameters in structural design, are random variables. To clarify the concept of the random variable, consider an experiment repeatedly performed, with all conditions maintained as precisely constant as possible, and the measured results are identical, then the variable that is measured is said to be deterministic. On the contrary, if the outcomes vary, the variable is called random or stochastic. Random variables are inevitable in structural design; therefore, absolute safety or zero probability of failure cannot be achieved. Consequently, structural members must be designed to serve their functions with a finite probability of failure[6]. The objective of reliability analysis is to incorporate the uncertainties involved in load and resistance in the design process to determine a probabilistic safety margin. This probabilistic approach has been extensively used to calibrate design procedures in modern structural design codes[3,9–12]. In the reliability analysis, load and resistance are treated as random variables, and the limit state function is defined as the difference between resistance and load—in other words, the safety margin. The strength limit state function considered in this case and its corresponding design condition are stated in **Eq. (1)**:

$$\begin{aligned} g &= R-(D+L) \\ \phi R_n &\geq 1.2D_n + 1.6L_n \end{aligned} \tag{1}$$

where D, L, and R are random variables corresponding to dead load effect, live load effect, and corresponding resistance, respectively; ϕ is the strength reduction factor; D_n, L_n, and R_n are the nominal values of the dead load effect, live load effect, and corresponding resistance, respectively. The term nominal is used to refer to value used for design purposes. One can see that a positive

value of g represents satisfactory performance, and a negative value of g corresponds to failure. If g is assumed normally distributed, the probability of failure can be written as **Eq. (2)**:

$$P_F = P\left(g < 0\right) = \Phi\left(-\frac{\mu_g}{\sigma_g}\right) \tag{2}$$

where μ_g is the mean of g; σ_g is the standard deviation of g; and Φ is the standard normal cumulative distribution function. The reliability index β is a probabilistic measure of the safety margin, and it is defined in **Eq. (3)**:

$$\beta = \frac{\mu_g}{\sigma_g} \tag{3}$$

thus, the reliability index (β) is a function of the probability of failure (p_f), and as the probability of failure decreases the reliability index increases. The acceptable safety margin, in terms of a reliability index, must be established upfront in order to calibrate strength reduction factors. The target reliability index for individual beams or girders for strength limit states have been selected as $\beta_T = 3.5$ in previous reliability-based calibrations[9]. This is equivalent to a probability of failure $p_f = 0.233\times10^{-3}$. Lower values of reliability index are specified for service limit state since the consequences of exceedance a service limit state are not nearly as dangerous as if a strength limit state is reached. Consequently, larger values of reliability index are desired for structural members which failure could represent severe consequences. In addition, larger values of reliability index are preferred for strength limit states that correspond to non-ductile failures, as is the case of shear failure.

The following sections present the statistical models for loads and resistance used to perform the reliability analysis and reliability-based calibration.

3.5 LOADS AND LOAD COMBINATION

The fundamental load case for calibration is a combination of dead load and live load. The statistical parameters of the load components used in this study are taken from the literature[5,6]. For the distribution of dead load effect (*D)*, the bias factor (λ = mean/nominal) is λ = 1.05, and the coefficient of variation (*COV* = standard deviation/mean) is *COV* = 0.10 for cast-in-place concrete. Precast concrete members have better statistical parameters than cast-in-place members (i.e., lower λ and *COV*); consequently, cast-in-place is used as a reference for calibration. For the distribution of live load effect *(L)*, the statistical parameters depend on the type of occupancy and the influence area for a given structural member. For the maximum 50 years live load, the bias factor is λ = 1.0, and *COV* ranges from 0.10 to 0.20, depending on the influence area. In this study, λ = 1.0 and *COV* = 0.18 were assumed to represent the live load in statistical terms. The statistical parameters of the total load effect ($Q = D+L$) depend on the amount of dead load relative to total load. According to a previous ACI 318 calibration[9], $D_n/(D_n+L_n)$ ranges typically from 0.3 to 0.6 for slabs, and from 0.3 to 0.7 for beams.

3.6 RESISTANCE MODELS FOR ACI 318 ONE-SHEAR STRENGTH EQUATIONS

The objective of this section is to develop statistical models for one-way shear resistance for (1) the traditional simplified equations in ACI 318-14[1] (which has been widely used since 1963), and (2) the new one-way shear equation included in ACI 318-19[2]. The resistance models are developed for structural members made with concrete compressive strength ranging from 3,000 psi to 12,000 psi, with representative dimensions, and typical reinforcement ratios.

The load-carrying capacity of a member, in this case, the one-way shear strength, is a function of material characteristics, the cross-sectional dimensions, and the analytical model.

Although these quantities are treated as deterministic in design, there is uncertainty associated with each of them. Therefore, the resistance (R) is a random variable. The sources of uncertainty in resistance can be grouped into three categories: (1) The material factor *(M)* is the uncertainty in the material properties (concrete compressive strength, concrete tensile strength, steel yield stress); (2) The fabrication factor *(F)* is the uncertainty in the dimensions of the member (width, depth, reinforcement size, location and spacing); and (3) The analysis or professional factor *(P)*, which is the uncertainty resulting from approximation built into the methods of analysis and design. Each factor is represented by a statistical distribution, and therefore the resistance can be expressed as indicated in **Eq. (4)**:

$$R = R_n MFP \tag{4}$$

where R_n is the nominal value of the resistance; and M, F, and P are statistical distributions that represent the uncertainties described. To find the statistical parameters of R, each category is quantified separately and then combined by simulating possible outcomes using the Monte Carlo simulation technique. The statistical parameters for M, F, and P were previously considered by various researchers, and the results were summarized by Ellingwood et al.[5] The statistical information reported in Ellingwood et al.[5] was collected in the 1960s and 1970s. Since then, concrete and steel technology and associated regulations have changed considerably, and contemporary concrete technology has led to different and more reliable material properties. New concrete data have been documented and used for reliability-based calibrations[7,9,13–15]. However, statistical parameters for F and P have not been updated. The focus of this research is the professional factor *(P)*. The professional factors reported in Ellingwood et al.[5] were defined based on the experience and judgment of experts. Now, there are experimental data available to support data-driven professional factors.

The following sections present the statistical parameters used to simulate each of the aforementioned sources of uncertainty.

3.6.1 Material and fabrication factors

The statistical parameters reported in **Table 3.1** are used in the development of resistance models for one-way shear strength. The full description of the material data and fabrication uncertainty can be found elsewhere[7]. The statistical parameters of concrete compressive strength were determined based on cylinder tests. However, the concrete compressive strength in-place is presumably less than determined by cylinder tests. As has been done in former calibrations[3,13], in this study, a five percent reduction in tensile strength was assumed. On the other hand, the concrete tensile strength, which is closely related to the determination of the shear strength, has a higher degree of variation than the concrete compressive strength. In the past, the coefficient of variation of concrete tensile strength has been increased 0.05 relative to the *COV* of the concrete compressive strength[3,13]. Another approach has been to assume the coefficient of variation of shear strength is larger than the coefficient of variation for corresponding concrete compressive strength by 20 percent[7,14]. This study takes the *COV* of the concrete compressive strength from cylinder tests and combines it with the *COV* associated with the prediction of the modulus of rupture. Legeron and Paultre[16] defined an upper and lower bound for modulus of rupture of concrete based on 395 data points, as $f_{r\min} = 1.20\sqrt{f_c'}$ and $f_{r\max} = 0.68\sqrt{f_c'}$ with an average value of $f_r = 0.94\sqrt{f_c'}$ (SI units). If it is assumed that the uncertainty in the estimation of the modulus of rupture follows a normal distribution, the difference between the maximum and minimum values is equivalent to approximately six standard deviations of the distribution (see 3σ rule of thumb[17,18]). This

assumption was used to estimate the *COV* associated with the modulus of rupture prediction, which is approximately 0.10. Therefore, if the concrete tensile strength is a function of the uncertainty of the concrete compressive strength and the analytical model for modulus of rupture, the *COV* for concrete tensile strength can be estimated as $COV_{\sqrt{f_c'}} = \sqrt{COV_{f_c'}^2 + 0.10^2}$, if the sources of uncertainty are assumed normally distributed.

3.6.2 Professional factor

The professional factor is the uncertainty in the analytical model itself. The equation or set of equations for predicting the one-way shear strength of reinforced concrete members, given in the ACI 318 building code requirements, are empirical relationships based on fundamental mechanics adjusted to fit available test results. The analytical model includes simplifications from classical assumptions of structural analysis and reinforced concrete behavior; moreover, the curve fitting to select coefficients also included simplifications and professional judgment. Hence, there is uncertainty in the analytical model itself that arises from those approximations.

Shear force at failure measured from tests conducted in laboratories are compared to predictions made with the ACI 318 one-way shear models. The most precise information of material properties and dimensions, loading, and support conditions reported by researchers are used to predict the strength and then define the statistical parameters of *P*. The ratio V_{test}/V_{pred} is an indication of the accuracy of the analytical model, but it is not the complete answer. Even in the laboratory environment, not all materials are tested, and there are sources of uncertainty such as equipment calibration, fabrication tolerances, imperfections, etc. Therefore, the professional

factor is estimated based on the distribution of V_{test}/V_{pred} discounting the degree of variation in the laboratory testing (COV_{Lab}).

3.6.3 Professional factor assumed in previous calibrations

In previous reliability-based calibration, the professional factor for flexural strength of reinforced beams was assumed to have a normal distribution with λ = 1.02 and COV = 0.06. Rakoczy and Nowak[14] collected experimental data from 14 studies (a total of 45 test results) and computed the mean and COV of the ratio between flexural strength determined from tests and the predicted flexural strength (M_{test}/M_{pred}) are 1.01 and 0.04, respectively. Thus, experimental data validate the assumed professional factor for the flexural strength of reinforced concrete beams.

For one-way shear, the professional factor was previously assumed as having a normal distribution with λ = 1.16 and COV = 0.11 for slabs and beams without web reinforcement, and λ = 1.075 and COV = 0.10 for beams with web reinforcement. However, Kuchma et al.[19] evaluated the performance of the ACI 318-14[1] one-way shear method against the available database[20,21], and the mean and COV of the ratio V_{test}/V_{pred} are 1.51 and 0.38 for beams without web reinforcement, and 1.47 and 0.24 for beams with web reinforcement. These values of COV, obtained from experimental experiences, indicate that the professional factor assumed in the past was too optimistic regarding the dispersion. Moreover, several researchers have found that the accuracy of the ACI 318-14[1] one-way shear model varies significantly with effective depth and longitudinal reinforcement ratio. This non-uniform level of accuracy has not been incorporated in the professional factor so far. For these reasons, the professional factors for one-way shear need revision.

3.6.4 Development of data-driven professional factors for ACI 318

This section provides a description of the ACI 318-14[1] simplified method and the new ACI 318-19[2] method, a comparison between them against available experimental databases, and the determination of data-driven professional factors for reliability-based calibration.

3.6.4.1 ACI 318-14 simplified method

In accordance with ACI 318-14[1] code, the calculation of the nominal one-way shear capacity (V_n) of a non-prestressed member is based on the sum of the contribution of the concrete *(V_c)* and the web reinforcement *(V_s)* as follows,

$$V_n = V_c + V_s \leq V_c + 8\sqrt{f_c'}\, b_w d \tag{5}$$

Concrete contribution in reinforced concrete,

$$V_c = 2\lambda\sqrt{f_c'}\, b_w d \tag{6}$$

and the reinforcement contribution is calculated as follows.

$$V_s = \frac{A_v f_{yt} d}{s} \tag{7}$$

3.6.4.2 ACI 318-19 method

The new shear design method is overall a more robust one-way shear strength model. It follows the same idea stated in **Eq. (5)**. In accordance with ACI 318-19[2], if minimum web reinforcement is not provided the concrete contribution is estimated as follows:

$$V_c = \left[8\lambda_s \lambda \rho_w^{\frac{1}{3}} \sqrt{f_c'} + \frac{N_u}{6A_g} \right] b_w d \tag{8}$$

where λ_s is the size effect factor defined in **Eq. (9)**.

$$\lambda_s = \frac{1.4}{\sqrt{1+\frac{d}{10}}} \leq 1.0 \tag{9}$$

If minimum web reinforcement is provided, the concrete contribution is given by **Eq. (10)**. For cases with no axial load, the first line of **Eq. (10)** is the same as **Eq. (6)**. The second line of **Eq. (10)** is the same as **Eq. (8)** without the size effect factor. This second line is used for further analysis in this work.

$$V_c = Either\ of \begin{cases} \left[2\lambda\sqrt{f_c'} + \frac{N_u}{6A_g}\right] b_w d \\ \left[8\lambda\rho_w^{\frac{1}{3}}\sqrt{f_c'} + \frac{N_u}{6A_g}\right] b_w d \end{cases} \tag{10}$$

The shear reinforcement contribution is taken as the same as in **Eq. (7)**.

3.6.5 Comparison between ACI 318-14 and ACI 318-19

There are three significant changes between ACI 318-14[1] and ACI319-19[2] one-way shear equations: (1) the moment-to-shear ratio (*M/Vd*) dependency was removed; (2) a size effect factor was incorporated for members without shear reinforcement; and (3) the shear strength depends on the cube root of the longitudinal steel (ρ_w), instead of linearly. **Table 3.2** shows the mean and *COV* of the ratio V_{test}/V_{pred} for each method from two sources: the values computed in this study and the values previously reported by Kuchma et al.[19] The database used for this comparison includes reinforced concrete members without shear reinforcement (784 specimens), and reinforced concrete members with shear reinforcement (170 specimens). A full description of the data is given elsewhere[20,21]. **Table 3.2** shows that the new ACI 318-19[2] method is much more accurate than ACI

318-14[1] for beams without web reinforcement. The ACI 318-19[2] method is slightly more accurate than ACI 318-14[1] for beams with web reinforcement. In both types of members, the mean of the ratio V_{test}/V_{pred} obtained for ACI 318-19[2] method is less than for ACI 318-14[1]; therefore, the new ACI 318-19[2] shear model is, on average, less conservative than the ACI 318-14[1] traditional shear model.

Fig. 3.1 shows box plots with the performance of each method for beams without web reinforcement. One can clearly see the ACI 318-14[1] dependency on the effective depth and longitudinal reinforcement ratio. Also, **Fig. 3.1** shows the improved consistency in the performance of ACI 318-19[2] method. Similarly, **Fig. 3.2** shows the comparison of the two methods for beams with web reinforcement, where no significant difference is apparent.

3.6.6 Data-driven professional factor

The professional factor can be defined by comparing test results and predictions made based on the analytical method used. Cumulative distribution functions (CDF) for the data presented in **Table 3.2**, **Fig. 3.1**, and **Fig. 3.2** are plotted on normal probability scale in **Fig. 3.3** and **Fig. 3.4**. The specimens are divided into three groups based on their effective depths. Test specimens with $d \leq 12$ in. are considered representative of slabs and beams in buildings. Specimens with $12 < d \leq 40$ in. are considered representative of beams in buildings. Specimens with $d > 40$ in. are less common in buildings, yet they might be common in foundations. From the reliability analysis point of view, the main interest is to quantify the probability of overload and understrength; hence, the lower tail of the distribution is of paramount importance. Thus, normal distributions were fitted each dataset focusing on the lower tail with. Thus, λ_P and COV_P are obtained for each combination of method and structural member group and are indicated in each graph.

Fig. 3.3a shows the normal distributions fitted to each size group for the simplified method in ACI 318-14[1], and how the professional factor changes significantly with the size of the member. **Fig. 3.3b** shows the normal distribution fitted to all the data for all sizes for the ACI 318-19[2] method. **Fig. 3.3c** shows how the all-sizes fitted normal distribution in **Fig. 3.3b** exhibits good agreement for different specimen sizes, except for $d > 40$ in., where the all-sizes fitted distribution is on the conservative side. These parameters are useful to determine a professional factor. The distribution of V_{test}/V_{pred} is, in essence, the professional factor, if the material and dimensional knowledge were complete. However, even in well-controlled environments such as a research laboratory, there is variability in material, fabrication, and testing procedures. In order to obtain estimations of the variability in shear strength measurement in the laboratory, non-unique specimens with more than three replicates were identified in the database. The *COV*s for these replicate cases were calculated and are 0.04, 0.06, 0.11, 0.12, and 0.14. Also, Bentz and Collins[22] quantified variability in shear strength measurement as 0.06. Hence, two potential levels of variability in shear strength measurement were assumed for further analysis, i.e., $COV_{Lab} = 0.06$ and $COV_{Lab} = 0.10$.

Following the same logic used in the definition of the statistical model of resistance, one can assume that the shear resistance obtained from test is a function of the predicted resistance value (R_{pred}), the variability in the laboratory regarding material control *(M')*, fabrication tolerance *(F')*, testing procedures *(Tp)*, and the professional factor *(P)*, as shown in **Eq. (11)**. The statistical parameters reported in **Fig. 3.3** and **Fig. 3.4** correspond to λ_{test} and COV_{test}, from which the COV_P for the professional factor can be obtained from **Eq. (12)** if the COV_{Lab} is known. **Table 3.3** summarizes the formerly assumed professional factor, and the new recommended data-driven

professional factors. The professional factor is reported for each method for the two laboratory variability levels assumed.

$$R_{test} = R_{pred}\left(M'F'Tp\right)_{Lab} P \tag{11}$$

$$COV_{test}^2 = COV_{Lab}^2 + COV_P^2 \tag{12}$$

3.6.7 Resistance models

The resistance models are given in terms of bias factors (λ_R) and coefficient of variations (COV_R) for different structural components as a function of the concrete compressive strength. For this purpose, the one-way shear strength for each structural component considered, i.e., slabs, beams without web reinforcement, and beams with web reinforcement, was simulated based on the appropriate expression—**Eq. (7)** to **Eq. (11)**—and the statistical parameters listed in **Table 3.1** and **Table 3.3**. The CDF of the simulated resistances were obtained by generating one million values of R for each considered design case for each structural component. The CDFs were plotted on normal probability scale, and a normal distribution was fitted to the lower tail of the simulated distribution of R. Then, mean (μ_R), standard deviation (σ_R), bias factor (λ_R), and coefficient of variation (COV_R) or R were found for each design case and each concrete compressive strength. A curve that described λ_R and COV_R variation as a function of the concrete compressive strength was fitted to the results for each design case for each structural component. The statistical parameters of resistance for each structural member are summarized in **Tables 3.4**–**3.9**. The resistance parameters are given for the two cases considered regarding COV_{Lab}. One can observe that λ_R deceases as the concrete compressive strength increases, following the trend of the statistics for the concrete compressive strength. In addition, COV_R is heavily influenced by the COV_P, since the

professional factor is the largest source of uncertainty in members without web reinforcement. Likewise, COV_R is uniform and almost equal to COV_P across the range of concrete compressive strength for beams with web reinforcement.

3.7 RELIABILITY ANALYSIS RESULTS

The reliability index was calculated with **Eq. (3)** for a number of design scenarios (i.e., combinations of structural member, load ratio, concrete compressive strength, member size, amount of longitudinal and transverse reinforcement, and shear strength method) based on the load and resistance statistical models presented in previous sections. The reliability indexes obtained for slabs, beams without web reinforcement, and beams with web reinforcement, designed according to ACI 318-14[1] and ACI 318-19[2], are presented in **Table 3.10**, for two different assumed values of laboratory variability (COV_{Lab}). For slabs, the range of the reliability index for ACI 318-19[2] is about 0.25 higher than for ACI 318-14[1]. The ACI 318-19[2] shear design equation is more consistently accurate than the ACI 318-14[1] method, but it is also less conservative on average (see professional factors in **Table 3.3**). Hence, the reliability index increase is not as pronounced as might be expected. For beams with web reinforcement, the range of the reliability index for ACI 318-14[1] and ACI 318-19[2] does not change significantly. This is because the ACI 318-19[2] method is not substantially better than the ACI 318-14[1] method for these structural members. The most noteworthy difference is observed in the reliability ranges obtained for beams without web reinforcement with $d > 12$ in. This is consistent with the fact that the major improvement of the ACI 318-19[2] relative to the ACI 318-14[1] is the addition of a size correction factor that allows for a more consistent level of accuracy in one-way shear strength prediction across a wide range of beam sizes. Therefore, to maintain an effective safety margin roughly equivalent to the past

practice, the strength reduction factor for beams with web reinforcement may remain as $\phi = 0.75$. On the other hand, the design of slabs and beams without web reinforcement might incorporate an increased resistance factor and maintain a safety margin equivalent to past practice.

The reliability indexes obtained for slabs, beams without web reinforcement, and beams with web reinforcement, made of ordinary concrete (3,000 psi to 6,000 psi), designed according to ACI 318-14[1] are presented in **Table 3.11** and **Table 3.12**, for two different assumed values COV_{Lab}. The range of reliability index is used to define a target reliability index that corresponds to the safety margin inherent in past shear design practice. These target reliability indexes for beams were selected as β_T = 3.0–3.25 based on members with minimum web reinforcement for beams with web reinforcement; And as β_T = 3.9–4.0 based on members with $d \leq 12$ in. for beams without shear reinforcement. The reliability index range obtained for past practice for members with $d > 12$ in. without web reinforcement designed according to ACI 318-14[1] indicates that these designs are very unconservative (β from 2.24 to 2.79), as expected; therefore, this range was deemed inappropriate as a target value. These target reliability index for slabs were selected as β_T = 2.75–3.00.

3.8 STRENGTH REDUCTION FACTORS CALIBRATION FOR ACI 318-19

Strength reduction factors can be obtained based on the statistical models described and the selected target reliability indexes. **Table 3.13** contains the reliability index range obtained for the selected ϕ, $\phi - 0.05$, and $\phi + 0.05$. Since this target reliability index is determined by comparison with past practice, the value assumed for COV_{Lab} does not have influence.

Reliability indexes can be targeted to decrease the probability of less desireable nonductile failure modes relative to the probability of ductile failure modes. A flexural failure is a ductile failure mode, and the target reliability index for the flexural strength limit state has been selected as β_T = 3.5 in former calibrations[9,15]. Shear failure of a beam without shear web reinforcement is a very brittle failure mode; therefore, β_T = 4.0 is suggested ($\beta = 4.0$ means a p_f almost ten times lower than $\beta = 3.5$). Shear failure of a beam with web reinforcement is less brittle than a sudden failure of a beam without web reinforcement; thus, β_T = 3.75 is suggested for shear failure of beams with web reinforcement. For one-way slabs, a flexural or shear failure is likely to influence a relatively small potion of the structure, without a global collapse of the member; therefore, the target reliability for shear is taken as the same as for flexure in one-way slabs of shallow depth, i.e., β_T = 3.50. **Table 3.14** contains the reliability index range obtained for the selected ϕ, $\phi - 0.05$, and $\phi + 0.05$. The two different values assumed for COV_{Lab} lead to a difference in the resulting resistance factors of 0.05–0.10.

3.9 DISCUSSION

The new ACI 318-19[2] one-way shear design equation is a significant improvement relative to the traditional shear design equations in former editions of the ACI 318 building code requirements. Nevertheless, its contribution from the reliability point of view is only relevant for the design of one-way slabs and beams without web reinforcement.

The probabilistic safety margin of members designed according to ACI 318-14[1] specifications was determined, and it is reported in terms of reliability indexes. The ACI 318-14[1] shear design method was found unconservative for beams with d > 12 in. On the contrary, the ACI

318-14[1] one-way shear equation is overly conservative for beams with $d \leq 12$ in. and one-way slabs. On the other hand, the new ACI 318-19[2] one-way shear strength equations provide a consistent level of conservatism for a wide range of effective depth. Hence, the ACI 318-19[2] is more conservative than ACI 318-14[1] for members with $d > 12$ in. and less conservative for members with $d \leq 12$ in. Therefore, despite the increased overall accuracy of the new ACI 318-19[2] one-way shear equation, the diminished level of conservatism for slabs and beams with small cross sections ($d \leq 12$ in.) leads to a similar overall safety margin as for the former ACI 318-14[1] design specifications.

The most significant contribution of the new ACI 318-19[2] one-way shear equation is in the design of beams without shear reinforcement. The increase in reliability for beams without stirrups with $d > 12$ in. is very significant: from an undesirably $\beta = 2.1$ to $\beta = 4.0$ and more.

For beams with web reinforcement, both methods have a similar level of accuracy and conservatism. Therefore, the inclusion of the new ACI 318-19[2] one-way shear equation for design does not affect the reliability of these members. Hence, keeping the resistance factor as $\phi = 0.75$ is justified to maintain the safety margin of past practice. It is worth notice, that as the amount of web reinforcement increases, the reliability index also increases. This indicates that partial strength reduction factors could help to reach a more uniform reliability index for various amount of web reinforcement.

3.10 FURTHER RESEARCH

The major assumption made throughout this work was the variability of test results so that it can be discounted from the test to prediction comparison and obtain the uncertainty in the analytical model only. Thus, experimental research in this line is advised. Lightweight concrete nor

prestressed concrete were included in this work. The effect of the axial load was also left out of the scope of this research. Similar reliability-based calibration with data-driven professional factors is recommended for two-way shear and torsion.

3.11 CONCLUSIONS

This study dealt with the development of statistical models for one-way shear resistance of reinforced concrete slabs and beams with and without web reinforcement (see **Tables 3.4**–**3.9**). The statistical models for one-way shear resistance were developed with consideration of the uncertainty in the analytical model (professional factor) based on available experimental information instead of experts' judgment as has been done in past reliability-based calibrations (see **Table 3.3**). Furthermore, this work also suggests strength reduction factors for the ACI 318 new one-way shear design specifications based on reliability analysis (see **Table 3.13** and **Table 3.14**).

The results of the reliability-based calibration allow to conclude the following:

1. To assure the same safety margin than in past satisfactory practice, the strength reduction factor can be increased to ϕ = 0.80 for slabs and beams without web reinforcement, and it should be maintained as ϕ = 0.75 for beams with web reinforcement.

2. Target reliability indexes with consideration of failure modes were defined and used to suggest a second set of strength reduction factors. Assuming that the laboratory variability is about 10 percent, the recommended resistance factors are ϕ = 0.60 for slabs, ϕ = 0.80 for beams without web reinforcement, and ϕ = 0.60 for beams with web reinforcement. Assuming that the laboratory

variability is about 6 percent, the recommended resistance factor are $\phi = 0.55$ for slabs, $\phi = 0.75$ for beams without web reinforcement, and $\phi = 0.50$ for beams with web reinforcement.

REFERENCES

1. ACI Committee 318. “Building code requirements for structural concrete: (ACI 318-14); and commentary (ACI 318R-14),” Farmington Hills, MI, American Concrete Institute, 2014.
2. ACI Committee 318. “Building code requirements for structural concrete: (ACI 318-19); and commentary (ACI 318R-19),” Farmington Hills, MI, American Concrete Institute, 2019.
3. Nowak, A. S. “NCHRP report 368: Calibration of LRFD Bridge Design Code,” Washington, D.C, Transportation Research Board, National Research Council, 1999.
4. Nowak, A. S., and Lind, N. C. “Practical code calibration procedures,” *Canadian Journal of Civil Engineering*, V. 6, No. 1, 1979, pp. 112–9.
5. Ellingwood, B., Galambos, T. V., MacGregor, J. G., et al. “Development of a Probability Based Load Criterion for American National Standard A 58,” *NBS Special Report 577, U. S. Department of Commerce, National Bureau of Standards*, 1980.
6. Nowak, A. S., and Collins, K. R. “Reliability of structures,” 2nd edition, Boca Raton, FL, CRC Press, 2013.
7. Nowak, A. S., Rakoczy, A. M., and Szeliga, E. K. “Revised statistical resistance models for r/c structural components,” *Special Publication*, V. 284, 2012, pp. 1–16.
8. ASCE. “Minimum Design Loads and Associated Criteria for Buildings and Other Structures,” 2016.
9. Szerszen, M. M., and Nowak, A. S. “Calibration of Design Code for Buildings (ACI 318) Part 2: Reliability Analysis and Resistance Factors,” *Ann Arbor*, V. 1001, 2003, pp. 48109–2125.
10. Nowak, A. S., and Ritter, M. A. “Load and Resistance Factor Design Code for Wood Bridges,” n.d., p. 8.
11. Paikowsky, S. G. “LRFD design and construction of shallow foundations for highway bridge structures,” v. vol. 651, Transportation Research Board, 2010.
12. Paikowsky, S. G., Birgisson, B., McVay, M., et al. “NCHRP report 507: Load and resistance factor design (LRFD) for deep foundations,” Washington, D.C., Transportation Research Board, National Research Council, 2004.
13. Nowak, A. S., and Szerszen, M. M. “Calibration of Design Code for Buildings (ACI 318) Part 1: Statistical Models for Resistance,” *Ann Arbor*, V. 1001, 2003, pp. 48109–2125.
14. Rakoczy, A. M., and Nowak, A. S. “Resistance Model of Lightweight Concrete Members,” *ACI Materials Journal*, 2013, p. 9.
15. Rakoczy, A. M., and Nowak, A. S. “Resistance Factors for Lightweight Concrete Members,” *ACI Structural Journal*, 2014, p. 17.
16. Legeron, F., and Paultre, P. “Prediction of modulus of rupture of concrete,” *Materials Journal*, V. 97, No. 2, 2000, pp. 193–200.
17. Dai, S.-H., and Wang, M.-O. “Reliability analysis in engineering applications,” Van Nostrand Reinhold, 1992.
18. Duncan, J. M. “Factors of safety and reliability in geotechnical engineering,” *Journal of geotechnical and geoenvironmental engineering*, V. 126, No. 4, 2000, pp. 307–316.

19. Kuchma, D. A., Wei, S., Sanders, D. H., et al. “Development of the One-Way Shear Design Provisions of ACI 318-19 for Reinforced Concrete,” *ACI Structural Journal*, V. 116, No. 4, 2019.
20. Reineck, K.-H., Kuchma, D. A., Kim, K. S., et al. “Shear Database for Reinforced Concrete Members without Shear Reinforcement,” *ACI Structural Journal*, V. 100, No. 2, 2003.
21. Reineck, K.-H., Bentz, E., Fitik, B., et al. “ACI-DAfStb Databases for Shear Tests on Slender Reinforced Concrete Beams with Stirrups,” *ACI Structural Journal*, V. 111, No. 5, 2014.
22. Bentz, E. C., and Collins, M. P. “The Toronto Size Effect Series,” *Special Publication*, V. 328, 2018, pp. 2–1.

Table 3.1–Statistical parameters for material and fabrication factors[7]

Material factor		λ_M	COV_M
	3,000	1.31	0.170
	4,000	1.24	0.150
	5,000	1.19	0.135
f'_c (psi)	6,000	1.15	0.125
	8,000	1.11	0.110
	10,000	1.09	0.110
	12,000	1.08	0.110
f_y (psi)	60,000	1.13	0.030
Fabrication factor		λ_F	COV_F
b_w		1.01	0.04
d beams		0.99	0.04
d slabs		0.92	0.12
s stirrups		1.00	0.04
A_s		1.00	0.015
A_v		1.00	0.015

Table 3.2–Mean and COV of V_{test}/V_{pred} ratio

Method	Members without web reinforcement		Members with web reinforcement		Source
	MEAN	*COV*	MEAN	*COV*	
ACI 318-14 simplified	1.49	0.39	1.48	0.23	This study
	1.51	0.38	1.47	0.24	Kuchma et al. (2019)
ACI 318-19	1.41	0.22	1.31	0.21	This study
	1.44	0.22	1.32	0.20	Kuchma et al. (2019)

Table 3.3–Professional factors for one-way shear methods in ACI 318

Professional factor	Source
Previous factor based on expert's judgment	
Members without web reinforcement	
λ_P = 1.16 and COV_P = 0.11	Refs. 5–7
Members with web reinforcement	
λ_P = 1.075 and COV_P = 0.10	
Data-driven for ACI 318-14 assuming COV_{Lab} = *0.10*	
Members without web reinforcement	
$d \leq 12$ in. λ_P = 1.57 and COV_P = 0.19	This study
$12 < d \leq 40$ in. λ_P = 1.13 and COV_P = 0.28	This study
$d > 40$ in. λ_P = 0.61 and COV_P = 0.21	This study
Members with web reinforcement	
λ_P = 1.48 COV_P = 0.19	This study
Data-driven for ACI 318-14 assuming COV_{Lab} = *0.06*	
Members without web reinforcement	
$d \leq 12$ in. λ_P = 1.57 and COV_P = 0.21	This study
$12 < d \leq 40$ in. λ_P = 1.13 and COV_P = 0.29	This study
$d > 40$ in. λ_P = 0.61 and COV_P = 0.22	This study
Members with web reinforcement	
λ_P = 1.48 and COV_P = 0.21	This study
Data-driven for ACI 318-19 assuming COV_{Lab} = *0.10*	
Members without web reinforcement	
λ_P = 1.38 and COV_P = 0.16	This study
Members with web reinforcement	
λ_P = 1.31 and COV_P = 0.17	This study
Data-driven for ACI 318-19 assuming COV_{Lab} = *0.06*	
Members without web reinforcement	
λ_P = 1.38 and COV_P = 0.18	This study
Members with web reinforcement	
λ_P = 1.31 and COV_P = 0.19	This study

Table 3.4–Resistance parameters for one-way shear in slabs designed according to ACI 318-14

Statistical parameters	Concrete compressive strength						
	3,000 psi	4,000 psi	5,000 psi	6,000 psi	8,000 psi	10,000 psi	12,000 psi
λ_R for COV_{Lab} = 0.10	1.42	1.38	1.35	1.33	1.29	1.27	1.24
λ_R for COV_{Lab} = 0.06	1.42	1.38	1.36	1.33	1.30	1.28	1.26
COV_R for COV_{Lab} = 0.10	.207	.200	.196	.194	.193	.194	.193
COV_R for COV_{Lab} = 0.06	.214	.210	.207	.206	.205	.206	.206

Table 3.5–Resistance parameters for one-way shear in slabs designed according to ACI 318-19

Statistical parameters	Concrete compressive strength						
	3,000 psi	4,000 psi	5,000 psi	6,000 psi	8,000 psi	10,000 psi	12,000 psi
λ_R for COV_{Lab} = 0.10	1.42	1.36	1.31	1.28	1.23	1.22	1.21
λ_R for COV_{Lab} = 0.06	1.38	1.32	1.28	1.25	1.22	1.21	1.18
COV_R for COV_{Lab} = 0.10	.198	.186	.177	.172	.168	.169	.169
COV_R for COV_{Lab} = 0.06	.201	.193	.187	.183	.181	.181	.181

Table 3.6–Resistance parameters for one-way shear in beams without web reinforcement designed according to ACI 318-14

Statistical parameters	Concrete compressive strength						
	3,000 psi	4,000 psi	5,000 psi	6,000 psi	8,000 psi	10,000 psi	12,000 psi
λ_R for COV_{Lab} = 0.10							
$d \leq 12$ in.	1.60	1.55	1.52	1.50	1.46	1.43	1.40
$12 < d \leq 40$ in.	1.22	1.18	1.16	1.14	1.11	1.09	1.07
$d > 40$ in.	0.62	0.60	0.55	0.58	0.57	0.56	0.55
λ_R for COV_{Lab} = 0.06							
$d \leq 12$ in.	1.59	1.55	1.52	1.50	1.46	1.44	1.41
$12 < d \leq 40$ in.	1.24	1.21	1.18	1.16	1.13	1.11	1.09
$d > 40$ in.	0.62	0.61	0.60	0.59	0.58	0.57	0.56
COV_R for COV_{Lab} = 0.10							
$d \leq 12$ in.	0.205	0.199	0.194	0.192	0.190	0.191	0.191
$12 < d \leq 40$ in.	0.282	0.282	0.282	0.282	0.282	0.282	0.282
$d > 40$ in.	0.214	0.210	0.207	0.206	0.206	0.208	0.208
COV_R for COV_{Lab} = 0.06							
$d \leq 12$ in.	0.214	0.210	0.207	0.206	0.205	0.205	0.205
$12 < d \leq 40$ in.	0.293	0.293	0.293	0.293	0.293	0.294	0.294
$d > 40$ in.	0.221	0.221	0.221	0.220	0.220	0.219	0.219

Table 3.7–Resistance parameters for one-way shear in beams without web reinforcement designed according to ACI 318-19

Statistical parameters	Concrete compressive strength						
	3,000 psi	4,000 psi	5,000 psi	6,000 psi	8,000 psi	10,000 psi	12,000 psi
λ_R for COV_{Lab} = 0.10	1.51	1.44	1.38	1.34	1.30	1.29	1.27
λ_R for COV_{Lab} = 0.06	1.46	1.40	1.36	1.33	1.29	1.28	1.26
COV_R for COV_{Lab} = 0.10	0.199	0.186	0.178	0.172	0.168	0.168	0.167
COV_R for COV_{Lab} = 0.06	0.201	0.192	0.186	0.182	0.180	0.180	0.179

Table 3.8–Resistance parameters for one-way shear in beams with web reinforcement designed according to ACI 318-14

Statistical parameters	Concrete compressive strength						
	3,000 psi	4,000 psi	5,000 psi	6,000 psi	8,000 psi	10,000 psi	12,000 psi
λ_R for COV_{Lab} = 0.10							
Minimum A_v	1.58	1.55	1.53	1.51	1.48	1.46	1.44
Average A_v	1.64	1.63	1.61	1.60	1.59	1.58	1.57
Maximum A_v	1.65	1.64	1.63	1.62	1.61	1.60	1.60
λ_R for COV_{Lab} = 0.06							
Minimum A_v	1.59	1.56	1.53	1.52	1.49	1.47	1.45
Average A_v	1.65	1.63	1.62	1.61	1.59	1.58	1.57
Maximum A_v	1.65	1.64	1.63	1.62	1.61	1.60	1.59
COV_R for COV_{Lab} = 0.10				0.191			
COV_R for COV_{Lab} = 0.06				0.206			

Table 3.9–Resistance parameters for one-way shear in beams with web reinforcement designed according to ACI 318-19

Statistical parameters	Concrete compressive strength						
	3,000 psi	4,000 psi	5,000 psi	6,000 psi	8,000 psi	10,000 psi	12,000 psi
λ_R for COV_{Lab} = 0.10							
Minimum A_v	1.42	1.39	1.38	1.36	1.34	1.32	1.31
Average A_v	1.46	1.45	1.44	1.43	1.42	1.41	1.41
Maximum A_v	1.47	1.46	1.45	1.45	1.43	1.43	1.42
λ_R for COV_{Lab} = 0.06							
Minimum A_v	1.42	1.39	1.37	1.35	1.33	1.31	1.30
Average A_v	1.47	1.45	1.44	1.43	1.42	1.40	1.39
Maximum A_v	1.47	1.46	1.45	1.44	1.43	1.42	1.42
COV_R for COV_{Lab} = 0.10							
Minimum A_v				0.175			
Average A_v				0.173			
Maximum A_v				0.173			
COV_R for COV_{Lab} = 0.06							
Minimum A_v				0.190			
Average A_v				0.190			
Maximum A_v				0.190			

Table 3.10–Reliability index for one-way shear design for ACI 318-14 and ACI 318-19 specifications

Structural member	Assumed COV_{Lab}	β range ACI 318-14	β range ACI 318-19
Slabs	0.10	2.75–3.06	2.98–3.33
	0.06	2.61–2.92	2.97–3.26
Beams without web reinforcement ($\phi V_c \geq 2V_u$)			
$d \leq 12$ in.	0.10	3.97–4.31	4.03–4.72
	0.06	3.80–4.00	3.96–4.40
$12 < d \leq 40$ in.	0.10	2.56–2.79	4.03–4.72
	0.06	2.48–2.69	3.96–4.40
$d > 40$ in.	0.10	2.18–2.65	4.03–4.72
	0.06	2.11–2.57	3.96–4.40
Beams with web reinforcement			
Minimum A_v	0.10	3.04–3.45	3.07–3.52
	0.06	2.84–3.22	2.82–3.26
Average A_v	0.10	3.23–3.52	3.30–3.62
	0.06	3.00–3.28	2.98–3.33
Maximum A_v	0.10	3.26–3.53	3.31–3.64
	0.06	3.02–3.28	3.03–3.33

Table 3.11–Target reliability index based on satisfactory past practice if COV_{Lab} = 0.10

Structural member	β range	β_T
Slabs	2.85–3.06	3.00
Beams without web reinforcement ($\phi V_c \geq 2V_u$)		
$d \leq 12$ in.	3.97–4.29	4.00
$12 < d \leq 40$ in.	2.62–2.79	-
$d > 40$ in.	2.34–2.65	-
Beams with web reinforcement		
Minimum A_v	3.15–3.45	3.25
Average A_v	3.26–3.52	-
Maximum A_v	3.29–3.53	-

Table 3.12–Target reliability index based on satisfactory past practice if COV_{Lab} = 0.06

Structural member	β range	β_T
Slabs	2.73–2.92	2.75
Beams without web reinforcement ($\phi V_c \geq 2V_u$)		
$d \leq 12$ in.	3.80–4.00	3.90
$12 < d \leq 40$ in.	2.54–2.69	-
$d > 40$ in.	2.24–2.57	-
Beams with web reinforcement		
Minimum A_v	2.94–3.22	3.00
Average A_v	3.04–3.28	-
Maximum A_v	3.06–3.28	-

Table 3.13–Suggested resistance factors for ACI 318-19 one-way shear design based on target reliability index selected from past practice

Structural member	Assumed COV_{Lab}	ϕ	β range ACI 318-19	β_T
Slabs	0.10	0.75	2.98–3.33	3.00
		0.80	**2.84–3.16**	
		0.85	2.66–2.84	
	0.06	0.75	2.79–3.10	2.75
		0.80	**2.61–2.94**	
		0.85	2.43–2.78	
Beams without web reinforcement ($\phi V_c \geq 2V_u$)	0.10	0.75	4.03–4.72	4.00
		0.80	**3.96–4.64**	
		0.85	3.90–4.55	
	0.06	0.75	3.96–4.40	3.90
		0.80	**3.89–4.33**	
		0.85	3.82–4.25	
Beams with web reinforcement				
Minimum A_v	0.10	0.70	3.25–3.67	3.25
		0.75	**3.07–3.52**	
		0.80	2.90–3.37	
	0.06	0.70	2.98–3.40	3.00
		0.75	**2.82–3.26**	
		0.80	2.66–3.13	
Average A_v	0.10	0.70	3.46–3.77	3.25
		0.75	**3.30–3.62**	
		0.80	3.13–3.48	
	0.06	0.70	3.13 - 3.46	3.00
		0.75	**2.98 - 3.33**	
		0.80	2.83 - 3.22	
Maximum A_v	0.10	0.70	3.48–3.78	3.25
		0.75	**3.31–3.64**	
		0.80	3.15–3.49	
	0.06	0.70	3.18–3.46	3.00
		0.75	**3.03–3.33**	
		0.80	2.88–3.20	

Table 3.14–Suggested resistance factors for ACI 318-19 one-way shear design based on target reliability index selected with consideration of failure modes

Structural member	Assumed COV_{Lab}	ϕ	β range ACI 318-19	β_T
Slabs	0.10	0.55	3.54–4.02	3.50
		0.60	**3.40–3.84**	
		0.65	3.26–3.67	
	0.06	0.50	3.58–3.90	
		0.55	**3.44–3.74**	
		0.60	3.29–3.58	
Beams without web reinforcement ($\phi V_c \geq 2V_u$)	0.10	0.75	4.03–4.72	4.00
		0.80	**3.96–4.64**	
		0.85	3.90–4.55	
	0.06	0.70	4.03–4.48	
		0.75	**3.96–4.40**	
		0.80	3.89–4.33	
Beams with web reinforcement				
Minimum A_v	0.10	0.55	3.78–4.12	3.75
		0.60	**3.60–3.97**	
		0.65	3.43–3.82	
	0.06	0.45	3.80–4.08	
		0.50	**3.64–3.94**	
		0.55	3.48–3.80	
Average A_v	0.10	0.55	3.96–4.21	
		0.60	**3.80–4.06**	
		0.65	3.63–3.92	
	0.06	0.45	3.90–4.12	
		0.50	**3.75–3.99**	
		0.55	3.59–3.86	
Maximum A_v	0.10	0.55	3.98–4.22	
		0.60	**3.81–4.08**	
		0.65	3.65–3.93	
	0.06	0.45	3.93–4.12	
		0.50	**3.78–3.99**	
		0.55	3.63–3.86	

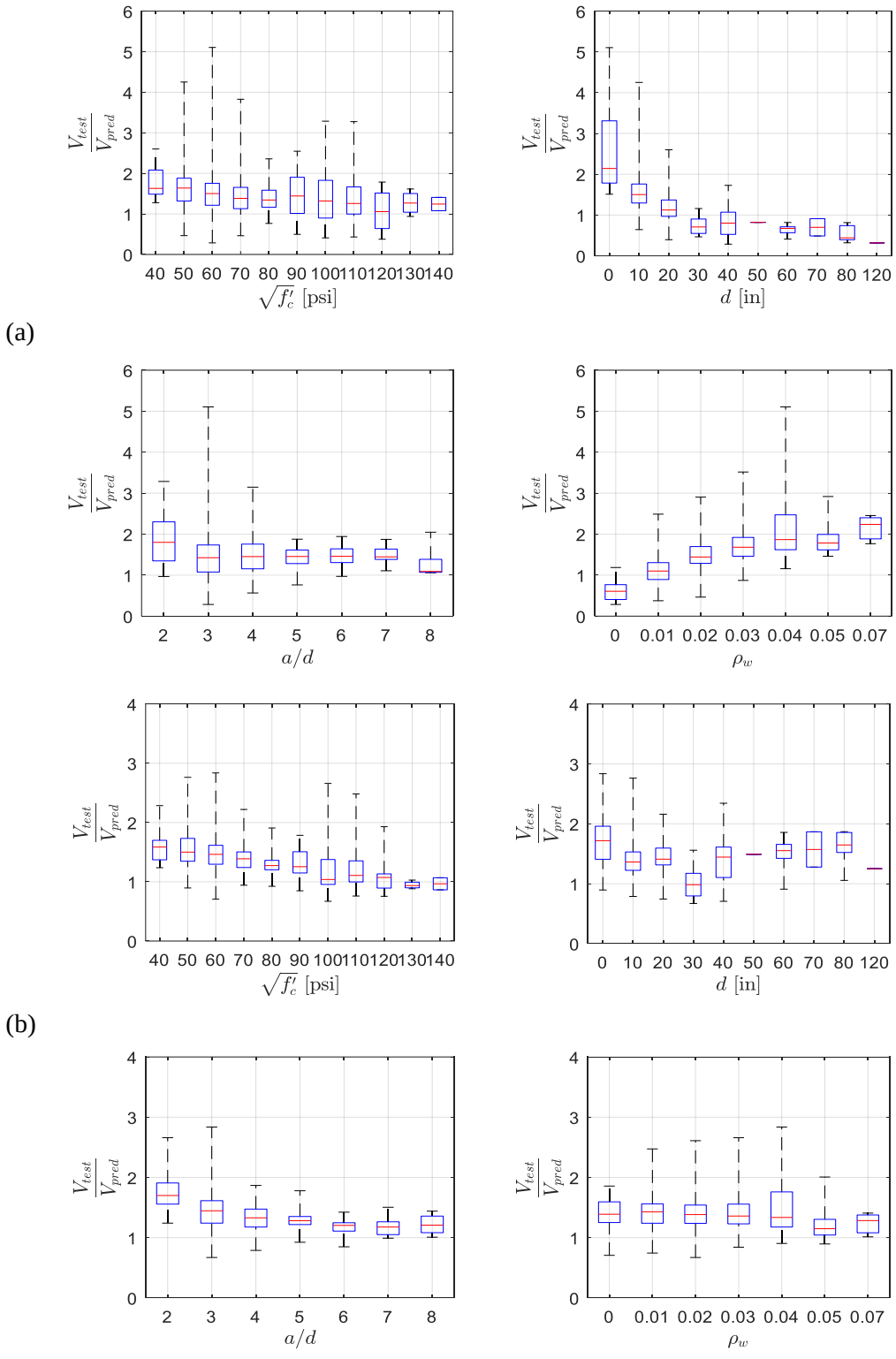

Fig. 3.1–Performance of one-way shear predictive equations in beams without web reinforcement: (a) ACI 318-14; and (b) ACI 318-19

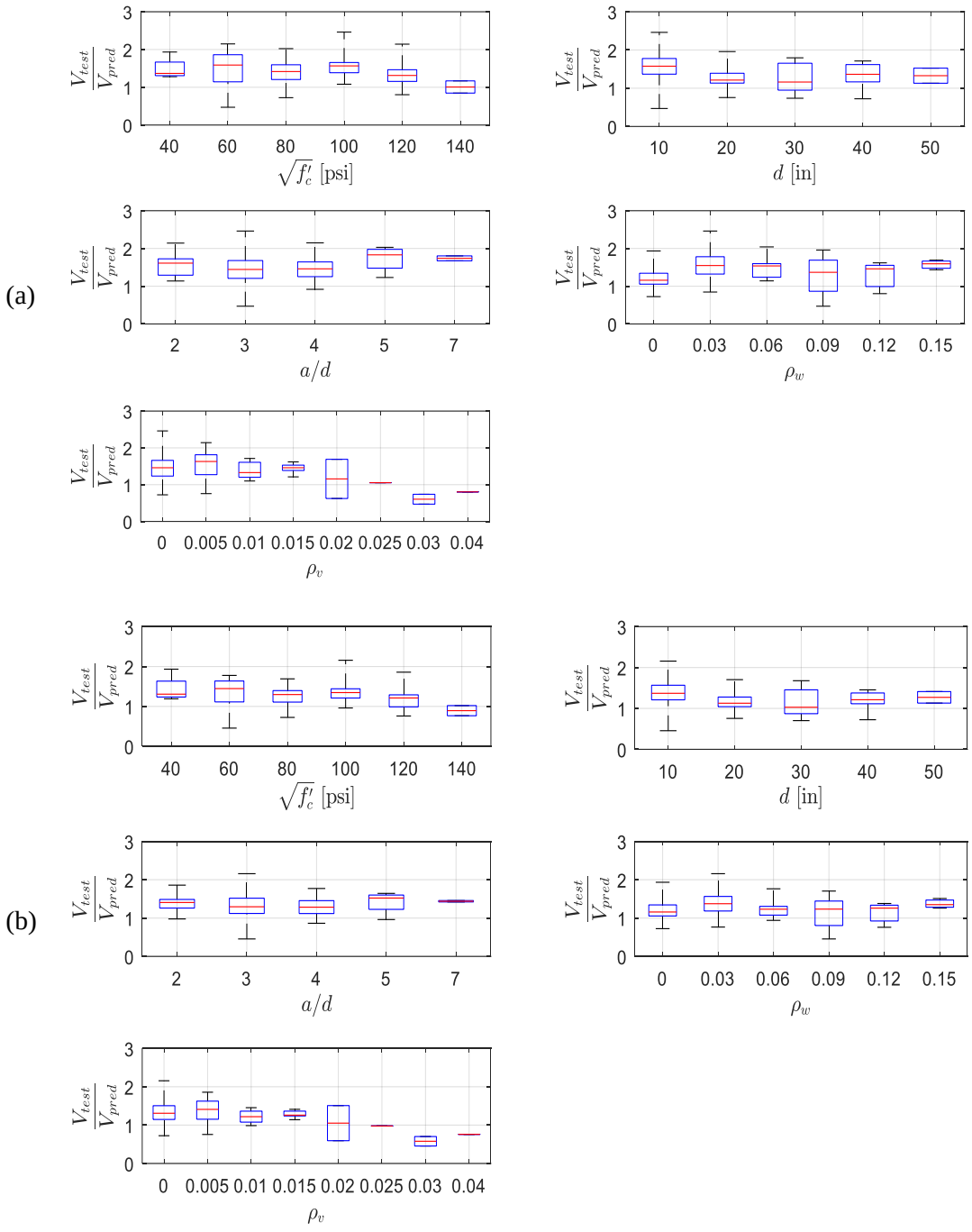

Fig. 3.2–Performance of one-way shear predictive equations in beams with web reinforcement: (a) ACI 318-14; and (b) ACI 318-19

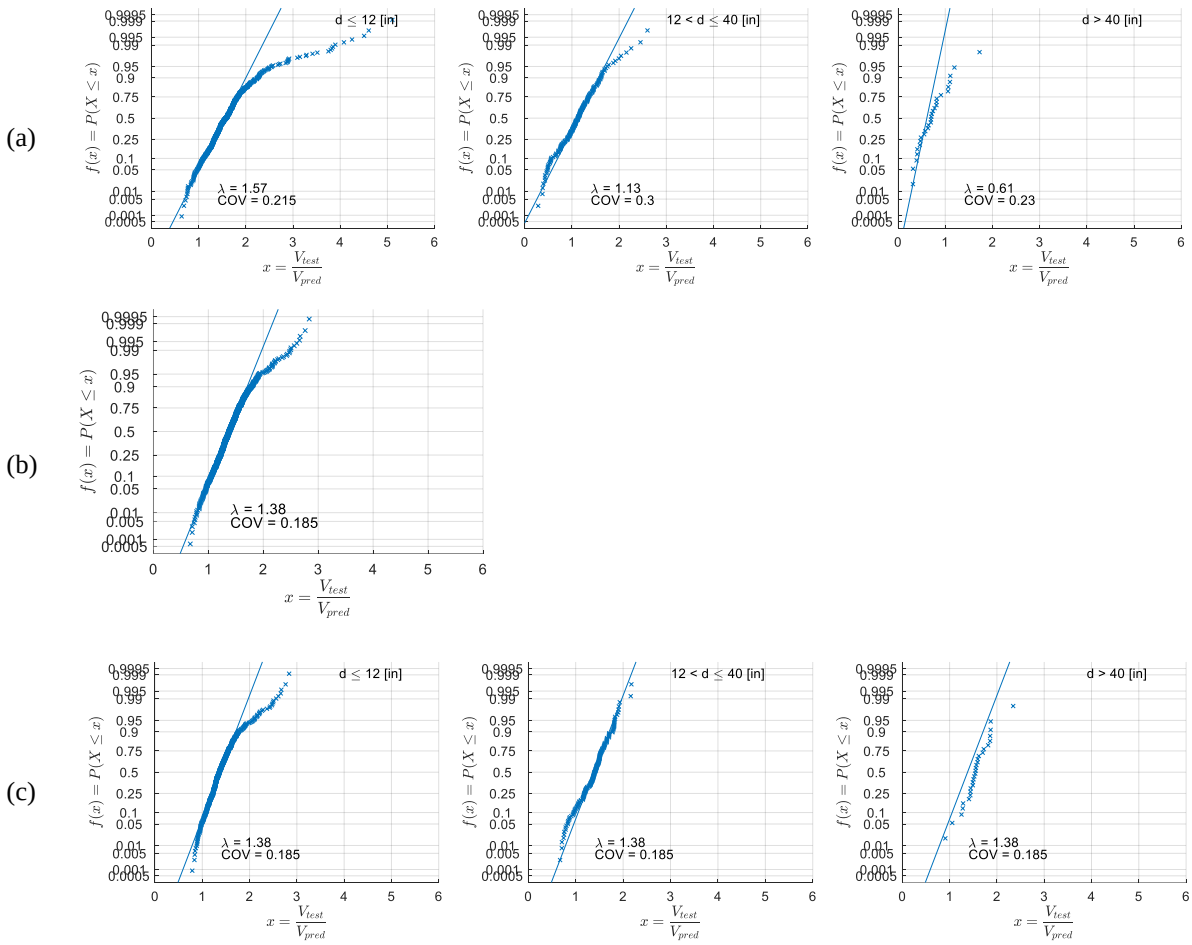

Fig. 3.3–Normal distribution fit for professional factor for members without web reinforcement: (a) ACI 318-14 simplified grouped by depth; (b) ACI 318-19 all data; and (c) ACI 318-19 grouped by depth

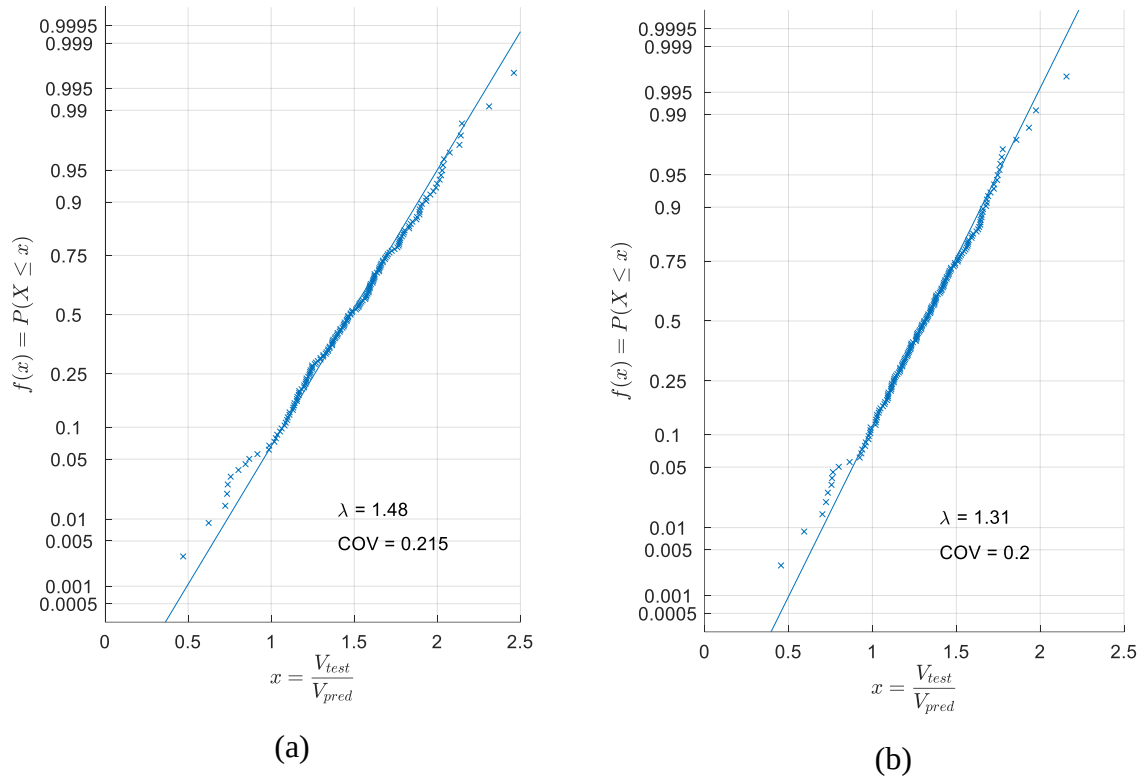

Fig. 3.4–Normal distribution fit for professional factor for members with web reinforcement: (a) ACI 318-14 simplified; and (b) ACI 318-19

Chapter 4

STRENGTH REDUCTION FACTORS FOR THE ACI 318-19 STRUT-AND-TIE METHOD FOR DEEP BEAMS

ABSTRACT

The strut-and-tie approach has gained importance in reinforced concrete design practice in the U.S. in the last two decades. This method has proven suitable for designing shear-critical structures where beam theory is not applicable. However, the strength reduction factors specified for the strut-and-tie method have not been calibrated based on the structural reliability approach. Therefore, the reliability of members designed according to these provisions is unknown.

The reliability of deep beams designed using the strut-and-tie method according to *ACI 318 building code requirements for structural concrete* is determined using simulations. Statistical parameters for load components, material uncertainty, and fabrication uncertainty are based on published literature. The analytical uncertainty was characterized based on available test results.

As results of this study, reliability-based strength reduction factors are suggested, current inconsistencies in the design of deep beams are highlighted, and recommendations to address them are given.

Keywords: reliability; strut-and-tie; reinforced concrete; design

4.1 INTRODUCTION

Since 2002, the *ACI 318 Building code requirement for structural concrete* requires that deep beams are designed using either nonlinear analysis or using the strut-and-tie method (STM)[1]. The strut-and-tie approach has proven very useful for designing shear-critical structures where beam theory does not apply, e.g., pile caps, corbels, beams with holes, anchorage zones, and the focus of this study, deep beams. The classical beam theory does not apply to deep beams because the assumption of plane sections remain plane after loading is not valid due to significant shear deformations. The strut-and-tie modeling approach represents a complex stress field of a concrete structure as an equivalent truss, with elements in compression (struts), elements in tension (ties), and the truss joints are called nodal zones (or nodes). The strength of struts and nodal zones control the dimensions of the concrete member, while the tie forces determine the amount of reinforcement required to resist the external loads. The main assumptions in STM are: (1) equilibrium must be satisfied; (2) the centroid of each component and the lines of action of the applied loads must coincide at joints, and (3) failure occurs when a strut or node crushes or when a tie reaches its yielding capacity, so a mechanism is formed (for statically determined truss models). The STM requires the designer to identify one possible load path for each load combination and assure that none of the components of the load path is overloaded.

The STM was formally published by Schlaich et al.[2], and it was introduced to the U.S. practice in the 1st edition of *AASHTO LRFD Bridge Design Specifications*[3], later it was included in Appendix A of ACI 318-02[1] for building design. ACI 318-14[4] moved the STM to be part of the main body, and ACI 318-19[5] updated several aspects of strut-and-tie design. This shows that strut-and-tie modeling approach has gained attention and importance in practice. Theoretical background on strut-and-tie modeling is provided by Schlaich et al.[2,6]; ACI 445R[7]; Collins and

Mitchell[8]; FIP[9]; MacGregor et al.[10]; Menn[11]; Muttoni et al.[12]; while several examples of application have been presented by Rogowsky and MacGregor[13]; Colorito et al.[14]; Martin et al.[15]; Reineck[16]; Reineck and Novak[17]; and Kuchma et al.[18] Experimental research on deep beams and comparison with strut-and-tie shear strength predictions can be found in the literature[13,19–31]. Most of the experimental research has found ACI 318 provisions conservative or very conservative, except for Garay-Moran and Lubell[29] who tested deep beams with high-strength longitudinal reinforcement with and without web transverse reinforcement. Comparison among code provisions and test results have resulted in proposals for improvements to update ACI 318[32,33] and some have already been implemented. The main changes in ACI 318-19[5] STM provisions are: (1) the inclusion of a confinement factor that increases the effective compressive strength of struts and nodal zones when subjected to triaxial compression; (2) the strut coefficient was updated; (3) a size effect factor, consistent with the one specified for the new one-way shear model[34] based on fracture mechanics[35], was added to the maximum ultimate shear force limitation; and (4) modifications in the minimum distribution reinforcement were incorporated. Alternative design procedures based on the strut-and-tie approach can be found in published literature[28,31,36–39].

The load and resistance factors (resistance factors are also called strength reduction factors) for sectional strength in the ACI 318 building code requirements were calibrated based on a probabilistic approach[40–42]. Nevertheless, the resistance factors specified for the design using STM have not been calibrated; instead, they were adopted from the shear design provisions without further analysis; hence, the safety level of designs based on STM is unknown. In general, as load factors are related to the level of uncertainty in the load sources, the resistance factors should reflect the difference in variation in the yield stress of the reinforcing bars, which defines the tie strength, and the compressive strength of concrete, which controls the strut and nodal zones

strength. Although, experimental research has shown that the failure mode of deep beams is somehow ductile when the longitudinal reinforcement and stirrups yield before shear failure occurs, yet this has happened under laboratory conditions where material strength and dimensions are well controlled. *In-situ* conditions are uncertain, material properties and dimensions are random variables, the concrete compressive strength is significantly more variable than the yielding stress of steel, as well as, the dimensions of cast-in-place concrete members is much more variable than the steel bar dimensions which are under strict fabrication tolerances. Therefore, inconsistencies in safety and in failure mode are suspected because all resistance factors for strut-and-tie model components are $\phi = 0.75$.

An assessment of STM provisions in ACI 318-19[5] with regard to its reliability and likelihood of ductile failure mode is described in this paper. The analysis includes (1) determination of the current safety margin in terms of reliability index of individual components and the deep beam system, (2) selection of target reliability index, and (3) presentation of alternatives for strength reduction factors.

4.2 RESEARCH SIGNIFICANCE

The contributions of this study are the determination of the current safety margin of deep beams designed according to ACI 318-19[5] STM provisions, in terms of reliability indexes, and the development of strength reduction factors for strut, nodal zones, and ties with consideration of failure modes.

4.3 ACI 318-19 PROVISIONS FOR THE STRUT-AND-TIE METHOD

Chapter 23 of ACI 318-19[5] applies to the design of structural members, or region of members, where loads or geometric discontinuities cause a nonlinear distribution of longitudinal strains within the cross section, which therefore includes deep beams. For each applicable factored load combination, the design strength of each strut, tie, and nodal zone are to be equal or greater than the ultimate load as stated in **Eq. (1)**:

$$F_{us} \le \phi F_{ns} \; ; \; F_{ut} \le \phi F_{nt} \; ; \; F_{un} \le \phi F_{nn} \tag{1}$$

where F_{us} , F_{ut} , and F_{un} are the factored force in a strut, in a tie, and on a nodal face, respectively; F_{ns} , F_{nt} , and F_{nn} are the nominal strength of a strut, a tie, and at a face of a nodal zone, respectively; and ϕ is the resistance factor or strength reduction factor. ACI 318-19[5] provisions specify ϕ = 0.75 for struts, ties, and nodes. The strength of each component in a strut-and-tie model are defined in the following subsections.

4.3.1 Strut strength

The nominal compressive strength of a strut is defined differently for reinforced struts and unreinforced struts as indicated in **Eq. (2)**:

$$\begin{aligned} F_{ns} &= f_{ce} A_{cs} \quad \text{for unreinforced struts} \\ F_{ns} &= f_{ce} A_{cs} + A_s' f_s' \quad \text{for reinforced struts} \end{aligned} \tag{2}$$

where A_{cs} is the cross-sectional area at the end of the strut under consideration; A_s' is the area of compression reinforcement along the length of strut; f_s' is the stress in the compression reinforcement of the strut at the nominal axial strength of the strut, which is permitted to take it

equal to the yielding stress of the steel; and f_{ce} is the effective compressive strength of concrete in a strut in accordance with **Eq. (3)**:

$$f_{ce} = 0.85\beta_c\beta_s f_c^{'} \tag{3}$$

where β_c is the strut and node confinement modification factor that accounts for the effect of concrete confinement when the resisting concrete area is larger than the loaded area, which definition is the same as the one used for bearing strength (the effect of confinement in strut-and-tie models has been studied by Tuchscherer et al.[27] and Breen et al.[43]). β_s is called strut coefficient, and it is a factor used to account for the effect of tensile stress presence and cracking reinforcement on the effective compressive strength of the concrete in a strut; $\beta_s = 1.0$ for strut with uniform cross-sectional area along the length; $\beta_s = 0.75$ for struts located in a region of a member where the width of the compressed concrete at mid-length if the strut can spread laterally if minimum strut reinforcement is provided; other cases are specified in ACI 318-19[5] code.

4.3.2 Node strength

The nodal compressive strength of a nodal zone is taken as **Eq. (4)**:

$$F_{nn} = f_{ce}A_{nz} \tag{4}$$

where A_{nz} is the area of the nodal face under consideration which is perpendicular to the line of action of F_{us} ; if F_{us} is not perpendicular to the nodal face, then shear stresses at the face need to be considered. Mohr's circle can be used to find the principal compressive stress on the nodal face,

or equivalently, the concept of the extended nodal zone can also be applied; f_{ce} is the effective compressive strength of concrete at a face of a nodal zone in accordance with **Eq. (5)**:

$$f_{ce} = 0.85\beta_c\beta_n f_c^{'} \tag{5}$$

where β_c is the strut and node confinement modification factor previously described in 4.3.1; β_n is the nodal zone coefficient, a factor used to account for the effect the anchorage of ties on the effective compressive strength of a nodal zone. $\beta_n = 1.0$ if the nodal zone is bounded by struts, bearing areas, or both; $\beta_n = 0.80$ if the nodal zone is anchoring one tie; and $\beta_n = 0.60$ if the nodal zone is anchoring two or more ties.

4.3.3 Tie strength

The tie strength can be calculated as follows when nonprestressed reinforcement is used:

$$F_{nt} = A_{ts} f_y \tag{6}$$

where A_{ts} is the area of reinforcement in a tie; and f_y is the yield stress of the reinforcement.

4.4 RELIABILITY ANALYSIS

The objective of reliability analysis is to incorporate the uncertainties involved in load and resistance in the design process to determine a probabilistic safety margin. There are many sources of uncertainty inherent to the design of concrete structures. Therefore, random variables are inevitable in structural design; therefore, absolute safety or zero probability of failure cannot be achieved. Consequently, structural members must be designed to serve their functions with a finite probability of failure[44]. To explain the concept of the random variable, consider an experiment that

is performed repeatedly, with all conditions maintained as precisely constant as possible. If the measured results are identical in each repetition, then the variable that is being measured is said to be deterministic. On the contrary, if the outcomes vary, the variable is called random or stochastic.

The structural reliability approach—a probabilistic approach—has been extensively used to calibrate design procedures in modern structural design codes to achieve an upfront selected safety margin[40,41,45–49]. This section describes the fundamentals of reliability analysis, and it provides the statistical models used for this analysis.

4.4.1 Fundamentals of reliability analysis

Consider the design formula in load and resistance factor design (LRFD) format, **Eq. (7)**:

$$1.2D_n + 1.6L_n \leq \phi R_n \tag{7}$$

where D_n, L_n, and R_n, are the nominal values of the dead load effect, live load effect, and the component corresponding resistance, respectively; and ϕ is the strength reduction factor. The strength limit state function to consider is stated in **Eq. (8)**:

$$g = R - (D + L) \tag{8}$$

where D, L, and R are random variables corresponding to the dead load effect, live load effect, and the corresponding resistance, respectively. A positive value of g represents satisfactory performance, and a negative value of g corresponds to failure. If g is assumed normally distributed, the probability of failure can be written as **Eq. (9)**:

$$P_F = P\left(g < 0\right) = \Phi\left(-\frac{\mu_g}{\sigma_g}\right) \tag{9}$$

where μ_g is the mean of g; σ_g is the standard deviation of g; and Φ is the standard normal cumulative distribution function. For convenience, the safety is measured in terms of the reliability index (β), which is defined in **Eq. (10)**:

$$\beta = \frac{\mu_g}{\sigma_g} \tag{10}$$

thus, the reliability index (β) is a function of the probability of failure (p_f), and as the probability of failure decreases the reliability index increases.

The acceptable safety margin, in terms of a reliability index, must be established upfront in order to calibrate strength reduction factors, this value is called target reliability index. The target reliability index for individual beams or girders for strength limit states have been selected as $\beta_T = 3.5$ in previous reliability-based calibrations[41]. This is equivalent to a probability of failure $p_f = 0.233\times10^{-3}$. Lower values of reliability index are specified for service limit state since the consequences of exceedance a service limit state are not nearly as dangerous as the reach of a strength limit state. Consequently, larger values of reliability index are desired for structural members which failure could represent severe consequences. In addition, larger values of reliability index are preferred for strength limit states that correspond to non-ductile failures, as is the case of shear failure of deep beams.

4.4.2 Load models

The statistical models for load effects were taken from previous reliability-based calibrations[45,50]. **Table 4.1** provides the statistical parameters used to simulate dead and live load in this analysis in

terms of the bias factor (λ, ratio mean-to-nominal), coefficient of variation (*COV*, ratio standard deviation to mean), and distribution type.

4.4.3 Resistance model

The load-carrying capacity of a structural element is a random variable due to various categories of uncertainties, e.g., material properties, fabrication tolerances, and analysis simplifications. Each category is represented by a statistical distribution, and therefore the resistance can be expressed as **Eq. (11)**:

$$R = R_n MFP \tag{11}$$

where R_n is the nominal value of resistance; M is the material factor, which is a distribution that represents the uncertainty in material properties; F is the fabrication factor, which is a distribution that represents the uncertainty in dimensions; and P is the analysis or professional factor, which accounts for uncertainties in the analytical model itself. The resistance of each component in a strut-and-tie model is simulated considering the following random variables (uncertain quantities): concrete compressive strength, reinforcement yield stress, width of the beam, and area of reinforcing steel. It is assumed that the strength of concrete in the actual structural component is less than the specified compressive strength by 10 percent[51]. For the analysis of the system reliability, the analysis uncertainty and the uncertainty in the forces at each truss member are also considered. The statistical parameters used for each random variable are based on published literature[40,44] and are summarized in **Table 4.2**. From the reliability analysis point of view, the main interest is to quantify the probability of overload and understrength; hence, the lower tail of the resistance distribution is of essential importance.

4.4.4 Uncertainty in the analysis model

The professional factor can be defined based on comparing test results and predictions based on the analytical method. Park and Kuchma[36] calculated strengths of deep beams based on ACI 318-05[52] using the strut-and-tie specifications and compared against the measured capacity of the 214 deep beam test results from eight different sources[19–26]. The essence of the ACI 318 STM provisions has not changed since it was first included in ACI 318-02[1], thus this information is useful to determine a probabilistic model that captures the uncertainty in the analysis model. Park and Kuchma[36] provide ratios between the measured shear at failure to predicted shear strength (V_{test}/V_{pred}). The cumulative distribution function (CDF) of V_{test}/V_{pred} is plotted for each source of experimental data on normal probability scale in **Fig. 4.1a**. Normal distributions were fitted to the lower tail of each source dataset with good agreement. Thus, the bias factor ranges from λ = 1.24–2.60 and the coefficient of variation ranges from COV = 0.10–0.31. Researchers[30,36] have recognized that the conservatism of these predictions decreases as the concrete strength increases. **Fig. 4.2** shows V_{test}/V_{pred} ratios as a function the concrete compressive strength in a scatter plot and a box plot. The central mark inside the box indicates the median, and the bottom and top edges of the box indicate the 25th and 75th percentiles, respectively. The whiskers indicate the most extreme data points, i.e., minimum and maximum. Consequently, two categories for professional factor were defined: normal-strength concrete $f'_c \leq$ 6,000 psi, and high-strength concrete $f'_c >$ 6,000 psi. The CDFs and the fitted normal distributions are shown in **Fig. 4.1b**, these distributions are used as the professional factors (see **Table 4.2**) for reliability analysis.

As the strut-and-tie model (load-path) is defined by the designer based on geometric assumptions, the forces in struts, nodal zones, and ties might differ from the true member forces. Considering the geometry and loading of the example provided by Reineck[16], the location of the

top strut of the STM was varied by $\pm$4 in. and the location of the tie was varied $\pm$2 in. Thus, the forces calculated in the members can change a maximum of *0.8P*. Using the 3σ rule, the uncertainty in the load path definition is assumed as normally distributed, and therefore *0.8P* is the difference between $\mu - 3\sigma$ and $\mu + 3\sigma$. Thus, the coefficient of variation is estimated as *COV* = 0.133. Larger elements might have a larger variation; therefore, λ = 1.0 and *COV* = 0.20 were assumed for further analysis.

4.4.5 System reliability index

Strut-and-tie models frequently are statically determinate trusses. Therefore, these systems can be classified as a series system, because if anyone of the truss members fails, the truss will not be able to carry the load without collapse. For a system in series, the system reliability index is bounded by two extremes, the lower bound is the probability of failure when all elements are fully correlated, and the upper bound is the probability of failure when all components are statistically independent, as shown in **Eq. (12)**[44]:

$$\max\{P_i\} \le P_F \le 1 - \prod_{i=1}^{n}(1 - P_i) \qquad (12)$$

where P_i is the probability of failure of the individual member *i*; and *n* is the total number of members in the system. The reliability analysis performed in this work is carrying on considering fully correlated concrete members (strut and nodes), yet uncorrelated with the steel reinforcement (ties).

4.5 CURRENT SAFETY MARGIN OF DEEP BEAMS DESIGNED WITH STM

4.5.1 Reliability index of individual components

The first step for analyzing the reliability of a deep beam is to determine the reliability index of individual components of the system, i.e., strut, nodal zone, and tie. Monte Carlo simulations are performed to determine the probability of failure of each component of the strut-and-tie model. Then, the reliability index can be approximated using **Eq. (9)** and **Eq. (10)**. The uncertainties in struts and nodal zones are the same, so the reliability of those components are also the same. Thus, the reliability index of individual components for load ratios, $D_n/(D_n+L_n)$, ranging from 0.3 to 0.7 are shown in **Fig. 4.3.** One can observe that the reliability index for a tie is much larger than for struts and nodal zones. The reliability indices obtained for different sizes of bars are very consistent, then a unique distribution can reasonably be used for further simulations to represent the material uncertainty of reinforcing steel, i.e., λ = 1.13 and COV = 0.03, same as in Nowak et al.[42]. The reader can notice that for $D_n/(D_n+L_n) \geq 0.6$ the reliability index of ties is not reported. This is because it required a huge number of simulations to obtain accurate results; nevertheless, the reliability index for $D_n/(D_n+L_n) = 0.7$ should be close to 6. Different is the case of reliability indices of struts and nodes, where the lowest is obtained for f'_c = 3,000 psi and f'_c = 12,000 psi. These two cases are used in further analyses as reference for normal strength concrete and high strength concrete, respectively.

4.5.2 Target reliability index and performance

The selection of target reliability indexes is a key step in reliability-based calibration. The target must be upfront in order to calibrate strength reduction factors. As it is traditionally done, this

target is defined based on past satisfactory practice. In addition, this study also defines a set of target reliability indexes based on considerations for reducing the likelihood of brittle failures.

The previous calibration of ACI 318 building code requirements defined a target reliability index of $\beta_T = 3.5$ for the shear ultimate limit state for slender beams[41]. It is of interest to determine the current reliability index of a system designed according to ACI 318-19[5] STM specifications, so the safety margin of current practice is known and used as a reference for calibration of strength reduction factors.

Failure in struts or nodal zones due to high compressive stress is an undesired brittle type failure. Nevertheless, if the reinforcement is adequately developed, and ties yield before concrete fails, the failure mode is reasonably ductile. Hence, within the elements of a strut-and-tie model, the reliability index of the tie should be the lowest of all components; so that reinforcement is likely to yield before concrete is crushed or splits, which is also a crucial assumption in the development of the strut-and-tie model.

For a load ratio of 0.5, the reliability index for individual members of deep beams was found to be $\beta = 3.0$ for struts and nodal zones for members built with normal strength concrete, and $\beta = 3.3$ for members built with high strength concrete. The reliability of ties was found to be $\beta = 5.0$. The reliability index of the system (which includes the uncertainty in the load path definition and analysis model) was found to be $\beta = 4.0$ and $\beta = 3.2$ for normal strength concrete and high strength concrete, respectively (see first section of **Tables 4.3-4.4**).

In reference to **Table 4.3**, for normal strength concrete, the simulations also have shown that out of all the scenarios considered (100 million simulations), the tie resistance is lesser than strut and node resistances in 61 percent of the cases simulated. Within the scenarios that represented a failure of the system, none of the cases was controlled by tie failure. Similarly, **Table**

4.4 informs that for high strength concrete, the tie resistance is lesser than strut and node resistances in only 11 percent of all the cases simulated. And, within the scenarios that represented a failure of the system, only 0.3 percent of the cases were controlled by tie failure.

This analysis selects strength reduction factors in such a way that the individual reliability index of the tie is close to the reliability index of struts and nodes. The resistance factors also should provide a system reliability index greater or equal than current design practice.

4.5.3 Reliability of a generic strut-and-tie deep beam design

Consider the simply supported deep beam carrying two concentrated loads and the corresponding STM shown in **Fig. 4.4a** and **Fig. 4.4b.** Since the load path is a statically determine truss, theoretically, the failure of one individual element causes the failure of the system, thus **Eq. (12)** is applicable. **Table 4.3** and **Table 4.4** summarizes the results of the simulation for several sets of resistance factors for a load ratio of 0.5, for normal strength concrete, and for high strength concrete, respectively. The results included are the individual and system reliability index, the percentage of cases where the tie resistance controlled the design (whole simulation set), and the percentage of cases where the tie resistance controlled the failure mode (failure cases set).

4.5.4 Suggested resistance factors for deep beam design

For normal strength concrete, resistance factors ϕ = 0.65 for strut and nodal zones and ϕ = 1.0 for ties are recommended. Those resistance factors lead to a higher system reliability index than current practice. Also, the likelihood of a ductile failure mode is increased from zero to 18 percent. For high strength concrete, resistance factors ϕ = 0.65 for strut and nodal zones and ϕ = 0.9 for ties provide more consistent designs increasing the system reliability index from β = 3.2 to β =

3.4. **Fig. 4.5** shows the system reliability index for the suggested resistance factor for load ratios from 0.3 to 0.7.

4.6 DISCUSSION

The reliability indices of deep beams for normal-strength concrete and high-strength concrete are significantly different due to the dissimilar levels of conservatism within the analysis model itself. The ACI 318-19[5] STM is overly conservative for normal-strength concrete, and conservative for high-strength concrete. It is recommended to improve STM specifications to accomplish a uniform level of conservatism for a wide range of concrete compressive strength. The dependency of the concrete effective compressive strength (f_{ce}) on the concrete compressive strength has been featured in other STM provisions[9,53]. Several alternatives for defining f_{ce} have been proposed, e.g., f_{ce} depending on the principal tensile strain perpendicular to the principal compressive stress[54,55]; f_{ce} depending on the square root of the concrete compressive strength[56]; f_{ce} that decreases as the compression strength increases[57]. Recent work has proposed new equations for estimating the effective compressive strength of struts and nodal zones including the influence of the concrete compressive strength, the span-to-depth ratio, and the tensile strain perpendicular to the strut[31,58–61].

There are inconsistencies in the reliability level associated with the design of deep beams based on STM provisions in ACI 318-19[5]. The current reliability of deep beams designed according to STM is not consistent with the previous sectional strength calibration of ACI 318[41]. The results of this study indicate that the reliability of deep beams built with normal-strength concrete designed by ACI 318-19[5] STM provisions (β_{sys} = 4.0) exceeds the acceptable range of reliability defined in the previous calibration of the ACI 318 building code requirements (β_T =

3.5); however, there is an unacceptably high probability of an undesired failure mode. For high-strength concrete, the reliability of deep beams (β_{sys} = 3.2) is below the accepted range due to the lower level of conservatism in the design method. The most likely failure mode is also undesirable.

Several combinations of strength reduction factors were considered aiming for a system reliability index at least as high as the current practice reliability, assuring that the component reliability index of ties is lower or equal then the reliability index of struts and nodes. For normal-strength concrete, resistance factors ϕ = 0.65 for strut and nodal zones and ϕ = 1.0 are suggested. These factors give a system reliability index of β = 4.2, which exceeds the current practice reliability index (β = 4.0). For high-strength concrete, resistance factors ϕ = 0.65 for strut and nodal zones and ϕ = 0.9 are suggested. These factors give a system reliability index of β = 3.4, which is larger than the reliability index of the current practice (β = 3.2) and it is almost as high as the classical target β_T = 3.5. Resistance factors ϕ = 0.50 and ϕ = 0.75 for struts/nodes and ties, respectively, need to be used to achieve a system reliability index of β = 4.1, so the current practice reliability index of deep beams made of normal-strength concrete is achieved.

It is advised to address the lower level of conservatism in high-strength concrete designs in the design method. It is suggested to decrease the conservatism for normal-strength concrete and increase it for high-strength concrete. Then, reliability-based calibration should be re-visited.

4.7 CONCLUSIONS

The reliability of deep beams designed in accordance with ACI 318-19[5] strut-and-tie method was studied. Reliability analysis was carried out using simulations based on existing statistical models of load components, material uncertainty, and fabrication uncertainty. The uncertainty in the strut-and-tie analytical model was characterized based on experimental data found in the published literature and engineering judgment. Strength reduction factors are suggested to increase the likelihood of observing ductile failure modes and to maintain or improve the current reliability of deep beams.

The results obtained in this study led to the following conclusions:

1. The strut-and-tie method in ACI 318-19[5] to determine the shear strength of deep beams is overly conservative for normal-strength concrete, and conservative for high-strength concrete.
2. The current reliability of deep beam designed according to the ACI318-19[5] strut-and-tie provisions is not consistent with the previous calibration of ACI 318 building code requirements for sectional strength.
3. The current strength reduction factors favor undesired non-ductile failure modes.

In order to decrease the likelihood of undesired failure modes, yet obtaining the same or higher reliability than current deep beam designs, the following is recommended:

1. For members made of normal-strength concrete ($f'_c \leq 6{,}000$ psi), the reliability-based calibration performed suggests updating the strength reduction factors to $\phi = 0.65$ for struts and nodal zones, and $\phi = 1.0$ for ties.

2. For members made of high-strength concrete ($f'_c > 6{,}000$ psi), the reliability-based calibration performed suggests updating the strength reduction factors to $\phi = 0.65$ for struts and nodal zones and $\phi = 0.90$ for ties.

4.8 FURTHER RESEARCH

A reliability-based calibration of the strength reduction factors pertinent to struts, ties, and nodal zones that include more shear-critical structural members is recommended. Similar work is warranted for pile caps, corbels, beams with holes, anchorage zones, dapped end beams, and walls with openings. Therefore, the creation and maintenance of relevant databases would be of interest.

This research dealt only with deep beams under vertical loading with a direct strut load path. Reliability analysis of reinforced concrete members design with the strut-and-tie method to resist wind and earthquake loads is also required. Updated databases for developing a consensus professional factor is also needed, as well as improvements in the specifications that allow a uniform level of conservatism in the analysis method itself.

A different professional factor for struts, nodal zones, and ties would be ideal to be able to determine accurately the system reliability index of members designed with STM, especially for more complex strut-and-tie models. Strains measured at struts and ties that later can be interpreted to determine forces at members are required for such a goal.

REFERENCES

1. ACI Committee 318. “Building code requirements for structural concrete (ACI 318-02); and commentary (ACI 318R-02),” Farmington Hills, MI, American Concrete Institute, 2002.
2. Schlaich, J., Schafer, K., and Jennewein, M. “Toward a Consistent Design of Structural Concrete,” *PCI Journal*, V. 32, No. 3, 1987, pp. 74–150.
3. AASHTO. “LRFD Bridge Design Specifications,” 1st edition, Washington, D.C., American Association of State Highway and Transportation Officials, 1994.
4. ACI Committee 318. “Building code requirements for structural concrete: (ACI 318-14); and commentary (ACI 318R-14),” Farmington Hills, MI, American Concrete Institute, 2014.
5. ACI Committee 318. “Building code requirements for structural concrete: (ACI 318-19); and commentary (ACI 318R-19),” Farmington Hills, MI, American Concrete Institute, 2019.
6. Schlaich, J., and Schafer, K. “Design and detailing of structural concrete using strut-and-tie models,” *The structural engineer*, V. 69, No. 6, 1991, pp. 113–25.
7. ACI Committee 445R. “ASCE/ACI Joint Committee 445 Recent Approaches to Shear Design of Structural Concrete, ACI 445R-99,” 1999.
8. Collins, M. P., and Mitchell, D. “Prestressed concrete structures,” v. vol. 9, Prentice Hall Englewood Cliffs, NJ, 1991.
9. FIP Commission 3. “Practical design of structural concrete,” *The International Federation for Structural Concrete: FIB*, 1999.
10. Wight, J. K., and MacGregor, J. G. “Reinforced concrete: mechanics and design,” 6th edition, New Jersey, Pearson Education, 2012.
11. Menn, C. “Prestressed concrete bridges,” 1997.
12. Muttoni, A., Schwartz, J., and Thürlimann, B. “Design of concrete structures with stress fields,” Springer Science & Business Media, 1996.
13. Rogowsky, D. M., and MacGregor, J. G. “Design of Reinforced Concrete Deep Beams,” *Concrete International*, V. 8, No. 8, 1986, pp. 49–58.
14. Colorito, A. B., Wilson, K. E., Bayrak, O., et al. “Strut-and-Tie Modeling (STM) for Concrete Structures, Design Examples,” 2017.
15. Martin, B. T., Sanders, D. H., Wassef, W., et al. “Verification and implementation of strut-and-tie model in LRFD bridge design specifications,” *NCHRP Project*, 2007, pp. 20–07.
16. Reineck, K.-H. “SP 208 (2002): Examples for the Design of Structural Concrete with Strut-and-Tie Models. Reineck, K,” *H. Editor, ACI SP-208, ACI, Farmington Hills, MI*, 2002.
17. Reineck, K.-H., and Novak, L. C. “Further Examples for the Design of Structural Concrete with Strut-and-Tie Models,” *ACI SP-273 (2010), ACI, Farmington Hills, MI*, 2010.
18. Kuchma, D. A., Yindeesuk, S., Nagle, T., et al. “Experimental Validation of Strut-and-Tie Method for Complex Regions,” *ACI Structural Journal*, V. 105, No. 5, 2008.
19. Smith, K. N., and Vantsiotis, A. S. “Shear strength of deep beams,” *ACI Journal Proceedings*, V. 79, No. 3, 1982, pp. 201–213.
20. Kong, F.-K., Robins, P. J., and Cole, D. F. “Web reinforcement effects on deep beams,” *ACI Journal Proceedings*, V. 67, No. 12, 1970, pp. 1010–1017.

21. Clark, A. P. “Diagonal tension in reinforced concrete beams,” *ACI Journal Proceedings*, V. 48, No. 10, 1951, pp. 145–156.
22. Oh, J. K., and Shin, S. W. “Shear Strength of Reinforced High-Strength Concrete Deep Beams,” *ACI Structural Journal*, V. 98, No. 2, 2001, pp. 164–73.
23. Aguilar, G., Matamoros, A. B., Parra-Montesinos, G., et al. “Experimental evaluation of design procedures for shear strength of deep reinforced concrete beams,” *ACI Structural Journal*, V. 99, No. 4, 2002, pp. 539–48.
24. Quintero-Febres, C. G., Parra-Montesinos, G., and Wight, J. K. “Strength of struts in deep concrete members designed using strut-and-tie method,” *ACI Structural Journal*, V. 103, No. 4, 2006, p. 577.
25. Tan, K.-H., Kong, F.-K., Teng, S., et al. “High-strength concrete deep beams with effective span and shear span variations,” *ACI Structural Journal*, V. 92, No. 4, 1995, pp. 395–405.
26. Anderson, N. S., and Ramirez, J. A. “Detailing of stirrup reinforcement,” *ACI Structural Journal*, V. 86, No. 5, 1989, pp. 507–515.
27. Tuchscherer, R., Birrcher, D., Huizinga, M., et al. “Confinement of deep beam nodal regions,” *ACI Structural Journal*, V. 107, No. 6, 2010, p. 709.
28. Hwang, S.-J., Lu, W.-Y., and Lee, H.-J. “Shear Strength Prediction for Deep Beams,” *ACI Structural Journal*, 2000, p. 10.
29. Garay-Moran, J. de D., and Lubell, A. S. “Behavior of Deep Beams Containing High-Strength Longitudinal Reinforcement,” *ACI Structural Journal*, V. 113, No. 1, 2016.
30. Ismail, K. S., Guadagnini, M., and Pilakoutas, K. “Shear Behavior of Reinforced Concrete Deep Beams,” *ACI Structural Journal*, V. 114, No. 1, 2016.
31. Chen, H., Yi, W.-J., and Hwang, H.-J. “Cracking strut-and-tie model for shear strength evaluation of reinforced concrete deep beams,” *Engineering Structures*, V. 163, 2018, pp. 396–408.
32. Tuchscherer, R. G., Birrcher, D. B., and Bayrak, O. “Strut-and-tie model design provisions,” *PCI journal*, V. 56, No. 1, 2011, p. 155.
33. Tuchscherer, R. G., Birrcher, D. B., Williams, C. S., et al. “Evaluation of existing strut-and-tie methods and recommended improvements,” *ACI Structural Journal*, V. 111, No. 6, 2014, p. 1451.
34. Kuchma, D. A., Wei, S., Sanders, D. H., et al. “Development of the One-Way Shear Design Provisions of ACI 318-19 for Reinforced Concrete,” *ACI Structural Journal*, V. 116, No. 4, 2019.
35. Bažant, Z. P., Yu, Q., Gerstle, W., et al. “Justification of ACI 446 code provisions for shear design of reinforced concrete beams,” *ACI Structural Journal*, V. 104, No. 5, 2007, pp. 601–10.
36. Park, J., and Kuchma, D. A. “Strut-and-Tie Model Analysis for Strength Prediction of Deep Beams,” *ACI Structural Journal*, V. 104, No. 6, 2007, pp. 657–66.
37. Tseng, C.-C., Hwang, S.-J., and Lu, W.-Y. “Shear Strength Prediction of Reinforced Concrete Deep Beams with Web Openings,” *ACI Structural Journal*, V. 114, No. 6, 2017.
38. Russo, G., Venir, R., and Pauletta, M. “Reinforced Concrete Deep Beams- Shear Strength Model and Design Formula,” *ACI Structural Journal*, V. 102, No. 3, 2005, pp. 429–37.
39. Yang, K.-H., and Ashour, A. F. “Strut-and-Tie Model Based on Crack Band Theory for Deep Beams,” *Journal of Structural Engineering*, V. 137, No. 10, 2011, pp. 1030–8.

40. Nowak, A. S., and Szerszen, M. M. “Calibration of Design Code for Buildings (ACI 318) Part 1: Statistical Models for Resistance,” *Ann Arbor*, V. 1001, 2003, pp. 48109–2125.
41. Szerszen, M. M., and Nowak, A. S. “Calibration of Design Code for Buildings (ACI 318) Part 2: Reliability Analysis and Resistance Factors,” *Ann Arbor*, V. 1001, 2003, pp. 48109–2125.
42. Nowak, A. S., Rakoczy, A. M., and Szeliga, E. K. “Revised statistical resistance models for r/c structural components,” *Special Publication*, V. 284, 2012, pp. 1–16.
43. Breen, J. E. “Anchorage zone reinforcement for post-tensioned concrete girders,” v. vol. 356, Transportation Research Board, 1994.
44. Nowak, A. S., and Collins, K. R. “Reliability of structures,” 2nd edition, Boca Raton, FL, CRC Press, 2013.
45. Nowak, A. S. “NCHRP report 368: Calibration of LRFD Bridge Design Code,” Washington, D.C, Transportation Research Board, National Research Council, 1999.
46. Nowak, A. S., and Lind, N. C. “Practical code calibration procedures,” *Canadian Journal of Civil Engineering*, V. 6, No. 1, 1979, pp. 112–9.
47. Nowak, A. S., and Ritter, M. A. “Load and Resistance Factor Design Code for Wood Bridges,” n.d., p. 8.
48. Paikowsky, S. G. “LRFD design and construction of shallow foundations for highway bridge structures,” v. vol. 651, Transportation Research Board, 2010.
49. Paikowsky, S. G., Birgisson, B., McVay, M., et al. “NCHRP report 507: Load and resistance factor design (LRFD) for deep foundations,” Washington, D.C., Transportation Research Board, National Research Council, 2004.
50. Ellingwood, B., Galambos, T. V., MacGregor, J. G., et al. “Development of a Probability Based Load Criterion for American National Standard A 58,” *NBS Special Report 577, U. S. Department of Commerce, National Bureau of Standards*, 1980.
51. Bartlett, F. M., and MacGregor, J. G. “Variation of In-Place Concrete Strength in Structures,” *Materials Journal*, V. 96, No. 2, 1999.
52. ACI Committee 318. “Building code requirements for structural concrete (ACI 318-08); and commentary (ACI 318R-08),” Farmington Hills, MI, American Concrete Institute, 2008.
53. AASHTO. “LRFD Bridge Design Specifications,” 8th edition, Washington, DC, American Association of State Highway Transportation Officials, 2017.
54. Collins, M. P., and Mitchell, D. “Shear and Torsion Design of Prestressed and Non-prestressed Concrete Beams,” 1980.
55. Vecchio, F. J., and Collins, M. P. “Predicting the response of reinforced concrete beams subjected to shear using modified compression field theory,” *ACI Structural Journal*, V. 85, No. 3, 1988, pp. 258–268.
56. Ramirez, J. “A truss analysis of the shear and torsional strength of beams.” PhD, University of Texas, Austin, Texas, United States, 1984.
57. Nielsen, M. P., Braestrup, M. W., Jensen, B. C., et al. “Concrete plasticity, beam shear–shear in joints–punching shear,” *Special Publication*, 1978, pp. 1–129.
58. Shuraim, A. B., and El-Sayed, A. K. “Experimental verification of strut and tie model for HSC deep beams without shear reinforcement,” *Engineering Structures*, V. 117, 2016, pp. 71–85.

59. Su, R. K. L., and Looi, D. T. W. “Revisiting Unreinforced Strut Efficiency Factor,” *ACI Structural Journal*, V. 113, No. 2, 2016.
60. Mohamed, K., Farghaly, A. S., and Benmokrane, B. “Strut Efficiency-Based Design for Concrete Deep Beams Reinforced with Fiber-Reinforced Polymer Bars,” *ACI Structural Journal*, V. 113, No. 4, 2016.
61. Ismail, K. S., Guadagnini, M., and Pilakoutas, K. “Strut-and-Tie Modeling of Reinforced Concrete Deep Beams,” *Journal of Structural Engineering*, V. 144, No. 2, 2018, p. 04017216.

Table 4.1–Statistical parameters of the load components

Item	λ	*COV*	Distribution	Source
Dead Load from cast-in-place component	1.05	0.10	Normal	Ellingwood et al.[50] Nowak[45]
50 years maximum building live load	1.00	0.18	Extreme type I	Nowak and Szerszen[36] Nowak and Collins[44]

Table 4.2–Statistical parameters of random variables involved in the resistance model

Material factor		λ	*COV*	Distribution	Source
f_c' (psi)	3,000	1.31	0.170	Normal	Nowak et al.[42]
	4,000	1.24	0.150		
	5,000	1.19	0.135		
	6,000	1.15	0.125		
	7,000	1.13	0.115		
	8,000	1.11	0.110		
	10,000	1.09	0.110		
	12,000	1.08	0.110		
f_y = 60,000 psi	# 3	1.18	0.040	Lognormal	Nowak et al.[42]
	# 4	1.13	0.030		
	# 5	1.12	0.020		
	# 6	1.12	0.020		
	# 7	1.14	0.030		
	# 8	1.13	0.025		
	# 9	1.14	0.020		
	# 10	1.13	0.020		
	# 11	1.13	0.020		
	# 14	1.14	0.020		

Fabrication factor	λ	*COV*		
Width cast-in- place beam	1.01	0.040	Normal	Ellingwood et al.[50]
Area of reinforcement	1.00	0.015		Nowak et al.[42]

Analysis factor	λ	*COV*		
Normal-strength concrete	1.76	0.142		
High-strength concrete	1.31	0.145	Normal	This study
Member forces	1.00	0.200		

Table 4.3–Component and system reliability of deep beams for normal-strength concrete

Component	ϕ	β_i	System results	
Strut	0.75	3.0	$R_t<R_s=R_{nz}$ whole	61%
Node	0.75	3.0	$R_t<R_s=R_{nz}$ failure	0
Tie	0.75	5.0	β_{sys}	4.0
Strut	0.75	3.0	$R_t<R_s=R_{nz}$ whole	88%
Node	0.75	3.0	$R_t<R_s=R_{nz}$ failure	1%
Tie	0.90	4.0	β_{sys}	4.0
Strut	0.75	3.0	$R_t<R_s=R_{nz}$ whole	95%
Node	0.75	3.0	$R_t<R_s=R_{nz}$ failure	6%
Tie	1.00	3.4	β_{sys}	4.0
Strut	0.65	3.4	$R_t<R_s=R_{nz}$ whole	96%
Node	0.65	3.4	$R_t<R_s=R_{nz}$ failure	3%
Tie	0.90	4.0	β_{sys}	4.2
Strut	0.65	3.4	$R_t<R_s=R_{nz}$ whole	99%
Node	0.65	3.4	$R_t<R_s=R_{nz}$ failure	18%
Tie	1.00	3.4	β_{sys}	4.2

Table 4.4–Component and system reliability of deep beams for high-strength concrete

Component	ϕ	β_i	System results	
Strut	0.75	3.3	$R_t<R_s=R_{nz}$ whole	11%
Node	0.75	3.3	$R_t<R_s=R_{nz}$ failure	0.3%
Tie	0.75	5.0	β_{sys}	3.2
Strut	0.75	3.3	$R_t<R_s=R_{nz}$ whole	87%
Node	0.75	3.3	$R_t<R_s=R_{nz}$ failure	70%
Tie	1.00	3.4	β_{sys}	2.9
Strut	0.65	3.9	$R_t<R_s=R_{nz}$ whole	92%
Node	0.65	3.9	$R_t<R_s=R_{nz}$ failure	78%
Tie	0.90	4.0	β_{sys}	3.4
Strut	0.60	4.3	$R_t<R_s=R_{nz}$ whole	87%
Node	0.60	4.3	$R_t<R_s=R_{nz}$ failure	58%
Tie	0.80	4.7	β_{sys}	3.8
Strut	0.50	5.1	$R_t<R_s=R_{nz}$ whole	98%
Node	0.50	5.1	$R_t<R_s=R_{nz}$ failure	93%
Tie	0.75	5.0	β_{sys}	4.1

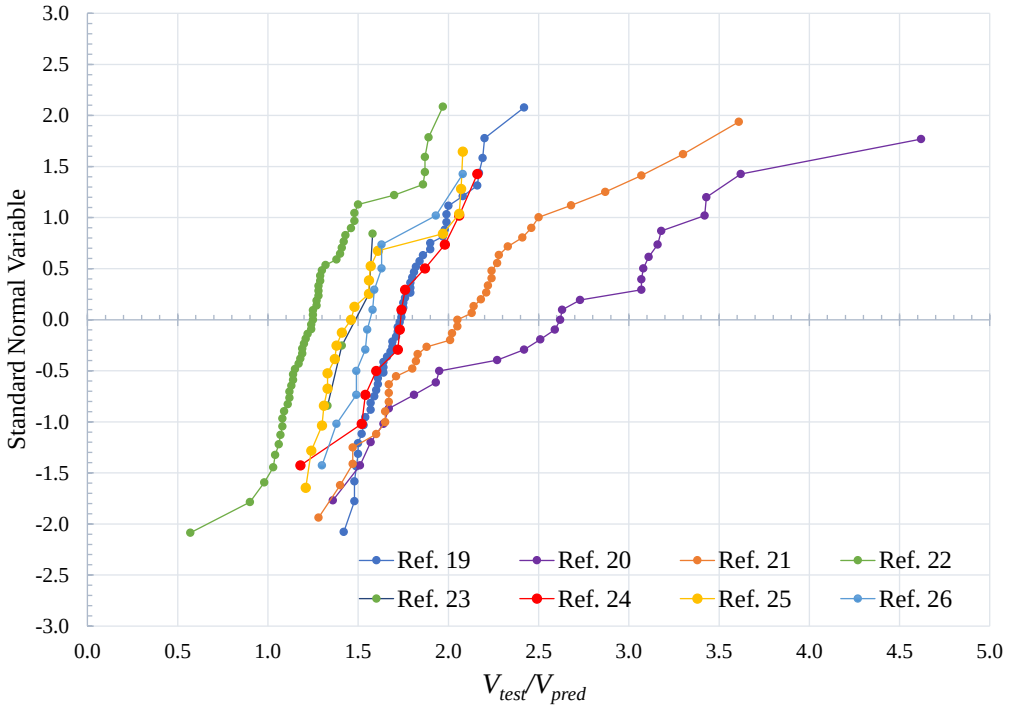

(a)

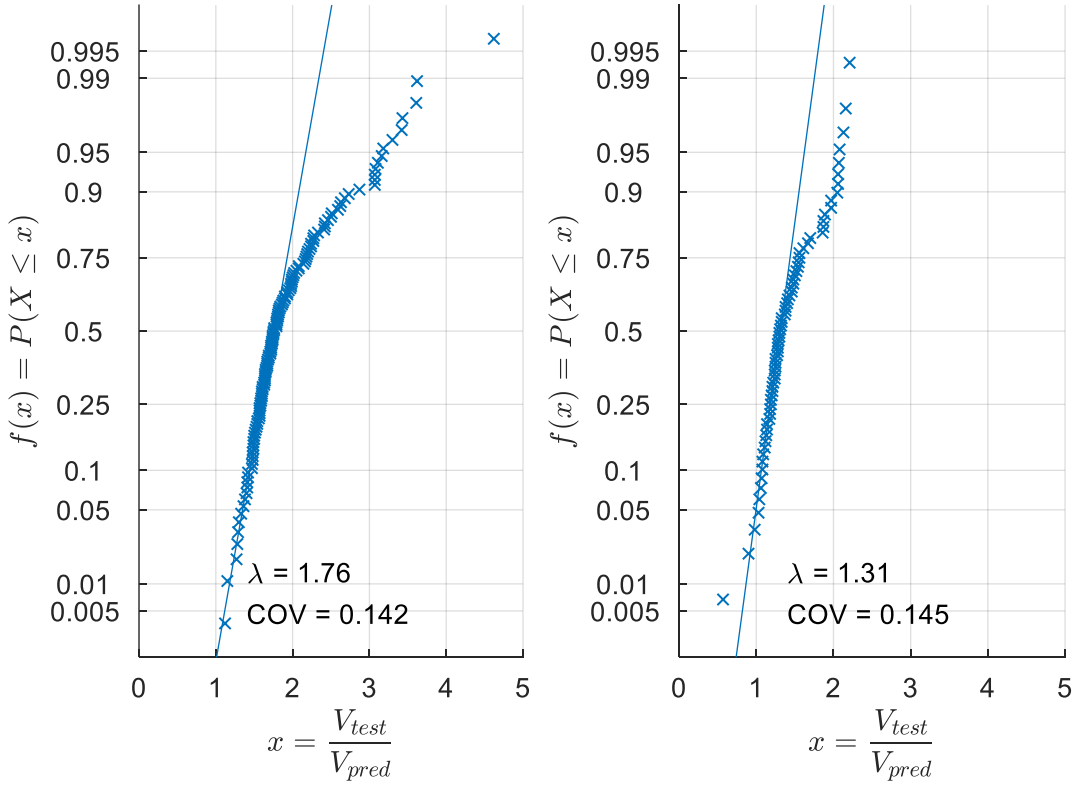

(b) (c)

Fig. 4.1–V_{test}/V_n Cumulative distribution functions on normal probability scale. (a) based on source; (b) dataset for $f'_c \leq 6{,}000$ psi; and (c) dataset for $f'_c > 6{,}000$ psi

(a)

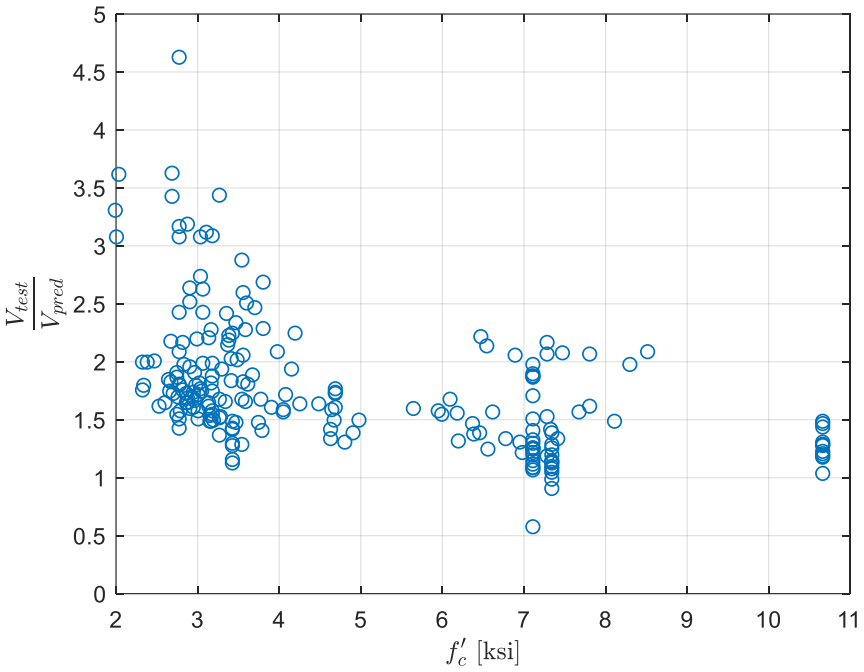

(b)

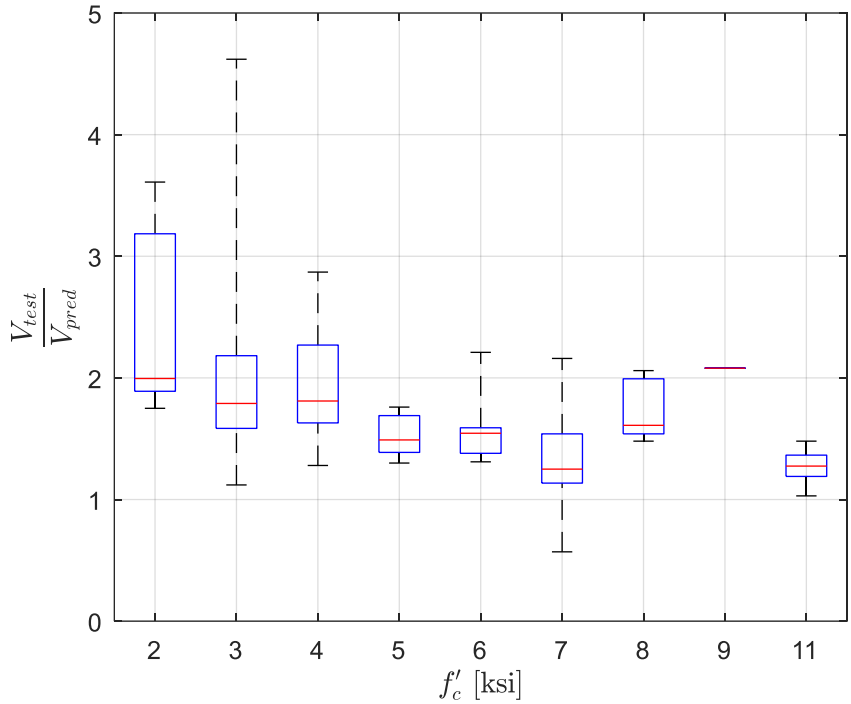

Fig. 4.2–V_{test}/V_n based on f'_c presented in (a) scatter plot and (b) box plot

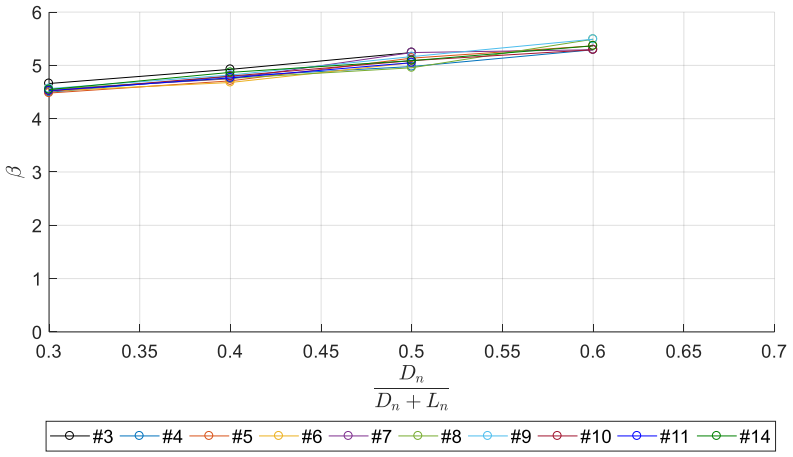

(a)

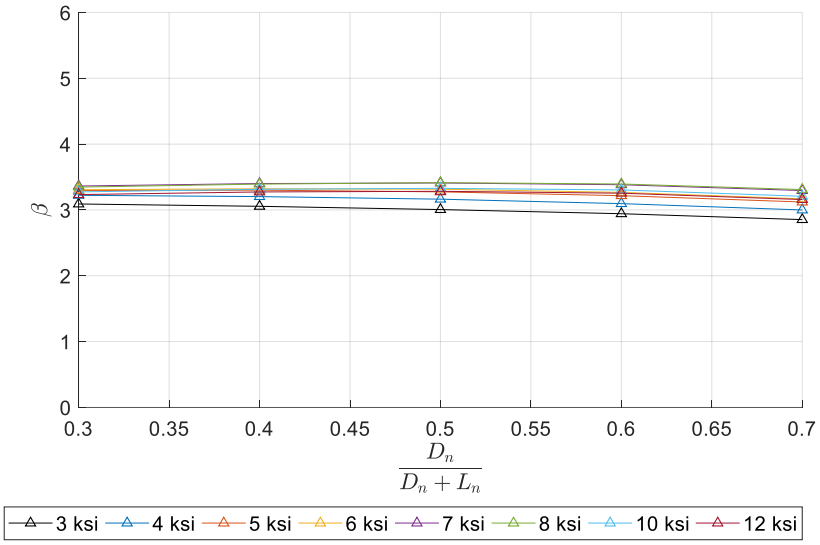

(b)

Fig. 4.3–Reliability of individual components: (a) ties and (b) struts and nodal zones

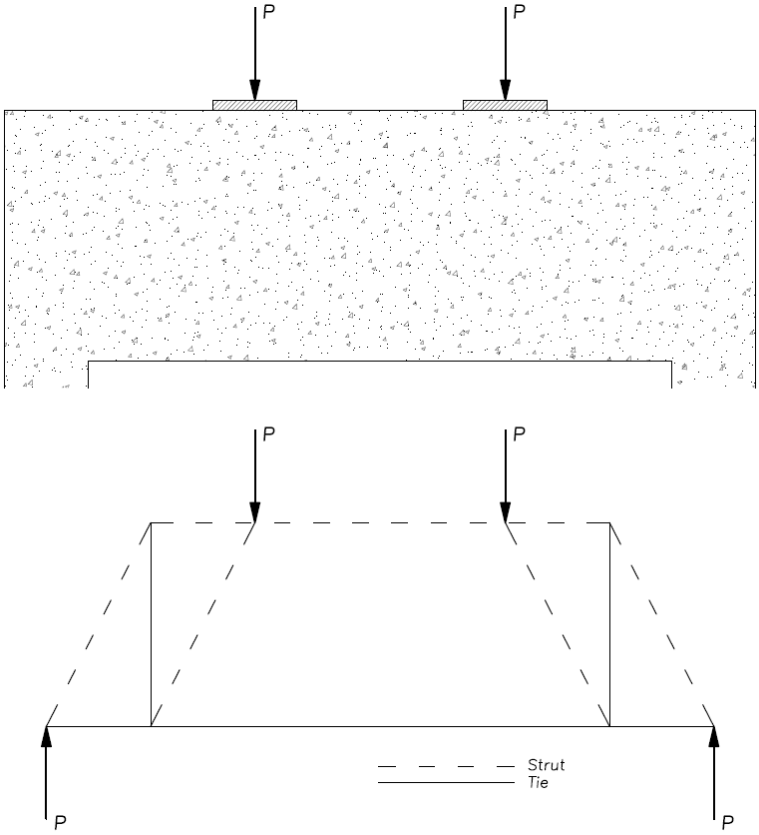

Fig. 4.4–Generic deep beam and strut-and-tie model

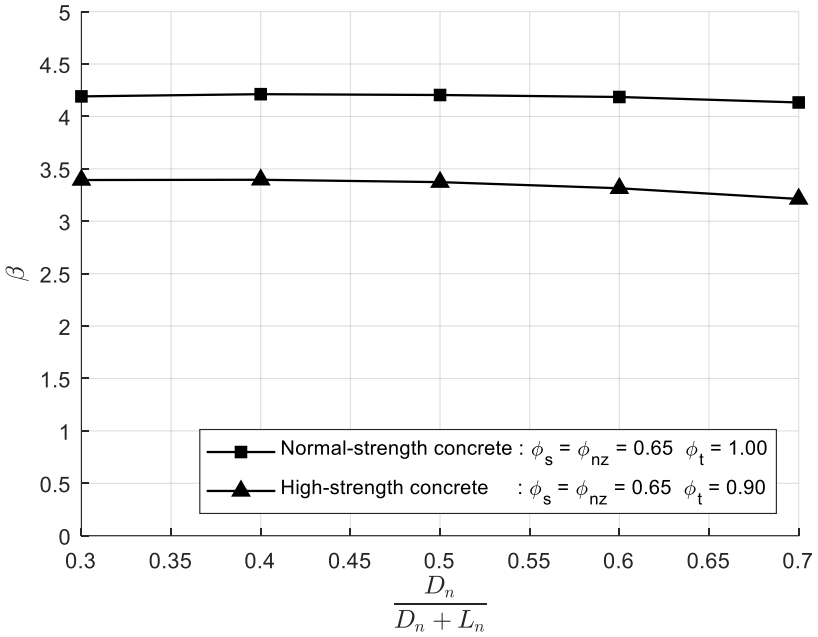

Fig. 4.5–Ssystem reliability index for the suggested resistance factors

Chapter 5

CONCLUDING REMARKS

Motivated by the recent research on one-way shear strength, strut-and-tie method, and changes in design provision for reinforced concrete structures, this dissertation explores the one-way shear strength of slender and deep concrete members under the umbrella of reliability analysis. Available databases were reviewed and used to quantify uncertainties in material properties and analysis methods. Statistical tools were used to investigate the accuracy of recently published methods for one-way shear strength, as well as the accuracy of the strut-and-tie modeling approach. Reliability analysis was extensively used to study the safety margins of concrete members and to calibrate strength reduction factors for available design procedures. The contributions of this research are listed as follows:

1. The accuracy of a selection of methods currently available to estimate the one-way shear strength of reinforced concrete members is informed in this research. Hence, engineers can use these results for selecting the method that fits better their purpose according to the intended application.

2. Statistical models for analysis uncertainty based on available experimental data (data-driven professional factor) were developed for ACI 318 one-way shear equations; statistical models for one-way shear resistance were developed for ACI 318 one-way shear equations, and updated strength reduction factors for one-way shear design were proposed.

3. The current probabilistic safety margin of deep beams designed according to ACI 318 strut-and-tie provisions was determined. Strength reduction factors for strut, nodal zones, and ties with

consideration of failure mode were suggested.

The findings of the work presented in this dissertation and its future extensions are a contribution to advance the state-of-practice on one-way shear design for slender and deep reinforced concrete members. These results are expected to be useful for reinforced concrete designers and for code developers.

APPENDIX A: NOTATION

NOTATION Chapter 2

a = shear span, i.e., distance from center of the concentrated load to center of support for simply supported members.
AP = acceptable predictions (within 20%)
A_s = area of longitudinal tension reinforcement
A_v = area of shear reinforcement within spacing s
A_{vmin} = minimum area of shear reinforcement within spacing s.
b = width of compression face of member
b_{veff} = effective width for shear strength
b_w = web width of member
c = distance from extreme compression fiber to neutral axis
COV = coefficient of variation (ratio standard deviation to mean)
d = distance from extreme compression fiber to centroid of longitudinal tension steel
d_{agg} = maximum specified size of coarse aggregate
E_s = modulus of elasticity of reinforcement and structural steel
f_c' = compressive strength of concrete
f_r = modulus of rupture of concrete
f_y = yielding strength for reinforcement
f_{yt} = yielding strength for transversal reinforcement (web reinforcement, or shear reinforcement)
h = overall height or depth of member
λ = modification factor to reflect the reduced mechanical properties of light-weight concrete relative to normal-weight concrete of the same compressive strength
M_n = nominal flexural strength at section
M_u = factored moment at section
R^2 = coefficient of determination
$RSME$ = root of squared mean error
s = center-to-center spacing of transverse reinforcement
V_c = nominal shear strength provided by concrete
V_n = nominal shear strength
V_s = nominal shear strength provided by shear reinforcement (web reinforcement)
V_{exp} = Shear force at failure from a test, or experimental shear force
V_{pred} = Shear force at failure predicted by a given method
V_{pred}* = Shear force at failure predicted by a given method normalized to fit as good as possible
V_u = factored shear force at section
ϕ = strength reduction factor

ρ = population coefficient of correlation

ρ_s = ratio of A_s to bd

ρ_v = ratio of A_v to sd

ρ_w = ratio of A_s to $b_w d$

NOTATION Chapter 3

a = shear span, i.e., distance from center of the concentrated load to center of support for simply supported members.
A_v = area of shear reinforcement within spacing s
b = width of compression face of member
b_w = web width of member
COV = coefficient of variation defined as the standard deviation-to-mean ratio
d = distance from extreme compression fiber to centroid of longitudinal tension steel
D = statistical distribution of dead load effect
D_n = nominal dead load effect
F = Fabrication factor. The statistical distribution that represents the variability in the resistance of a structural component due to uncertainty in member dimensions
f_c' = compressive strength of concrete
f_r = modulus of rupture of concrete
f_y = yielding strength for reinforcement
f_y = specified yield strength reinforcement
g = limit state function
L = statistical distribution of live load effect
L_n = nominal live load effect
M = material factor. The statistical distribution that represents the variability in the resistance of a structural component due to uncertainty in material properties
N_u = ultimate axial load acting on a beam cross section
P = professional or analysis factor. The statistical distribution that represents the uncertainty in the resistance of a structural member due to analysis simplification or assumptions.
P_F = probability of exceeding a limit state or probability of failure
R = statistical distribution of strength of a structural component
R_n = nominal strength of a structural component
R_{pred} = Predicted value or resistance
s = center-to-center spacing of transverse reinforcement
V_c = nominal shear strength provided by concrete
V_{exp} = Shear force at failure from a test, or experimental shear force
V_n = nominal shear strength
V_{pred} = Shear force at failure predicted by a given method
V_s = nominal shear strength provided by shear reinforcement (web reinforcement)
V_{test} = measure shear strength from a test
β = reliability index
β_T = target reliability index

ϕ = strength reduction factor or resistance factor

$\Phi(x)$ = standard cumulative normal distribution

λ = bias factor defined as the mean-to-nominal ratio

λ = modification factor to reflect the reduced mechanical properties of lightweight concrete relative to normal-weight concrete of the same compressive strength

ρ_w = ratio of A_s to $b_w d$

σ_x = standard deviation random variable x

μ_x = mean of random variable x

NOTATION Chapter 4

A_{cs} = cross-sectional area of a strut perpendicular to the axis of the strut
A_{nz} = area of a face of a nodal zone or a section through a nodal zone
A_s' = area of compression reinforcement
A_{ts} = area of nonprestressed reinforcement in a tie
COV = coefficient of variation defined as the standard deviation-to-mean ratio
D = statistical distribution of dead load effect
D_n = nominal dead load effect
F = fabrication factor. Statistical distribution that represents the variability in the resistance of a structural component due to uncertainty in member dimensions
f_{ce} = effective compressive strength of the concrete in a strut or a nodal zone
F_{nn} = nominal strength at face of a nodal zone
F_{ns} = nominal strength of a strut
F_{nt} = nominal strength of a tie
f_s' = compressive stress in reinforcement under factored loads
F_{un} = factored (ultimate) force on the face of a node
F_{us} = factored (ultimate) compressive force in a strut
F_{ut} = factored (ultimate) tensile force in a tie
f_y = specified yield strength for nonprestressed reinforcement
g = limit state function
λ = bias factor defined as the mean-to-nominal ratio
L = statistical distribution of live load effect
L_n = nominal live load effect
M = material factor. Statistical distribution that represents the variability in the resistance of a structural component due to uncertainty in material properties
P = professional or analysis factor. Statistical distribution that represents the uncertainty in the resistance of a structural member due to analysis simplification or assumptions.
P_F = probability of exceed a limit state or probability of failure
P_i = probability of failure of an individual component in a system
R = statistical distribution of strength of a structural component
R_n = nominal strength of a structural component
R_{nz} = statistical distribution of strength of a nodal zone
R_s = statistical distribution of strength of a strut
R_t = statistical distribution of strength of a tie
V_n = nominal shear strength predicted from strut-and-tie method
V_{test} = measure shear strength from a test
β = reliability index
β_c = confinemet modification factor

β_i = reliability index of an individual component in a system

β_n = nodal zone coeficient

β_s = strut coefficent

β_{sys} = reliability index of the system

ϕ = resistance factor

$\Phi(x)$ = standard cumulative normal distribution

σ_g = standard deviation of limit state distribution

μ_g = mean of limit state distribution

APPENDIX B: EVALUATION PLOTS FOR MEMBERS WITHOUT WEB REINFORCEMENT

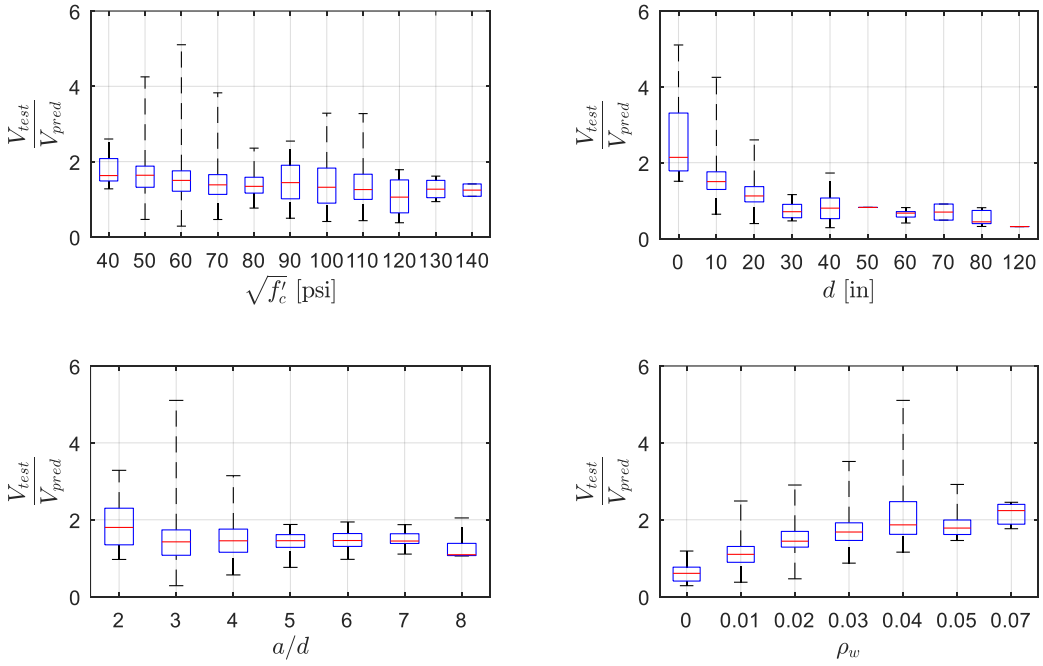

Fig. B1–V_{exp}/V_{pred} ratio for ACI 318-14 simplified

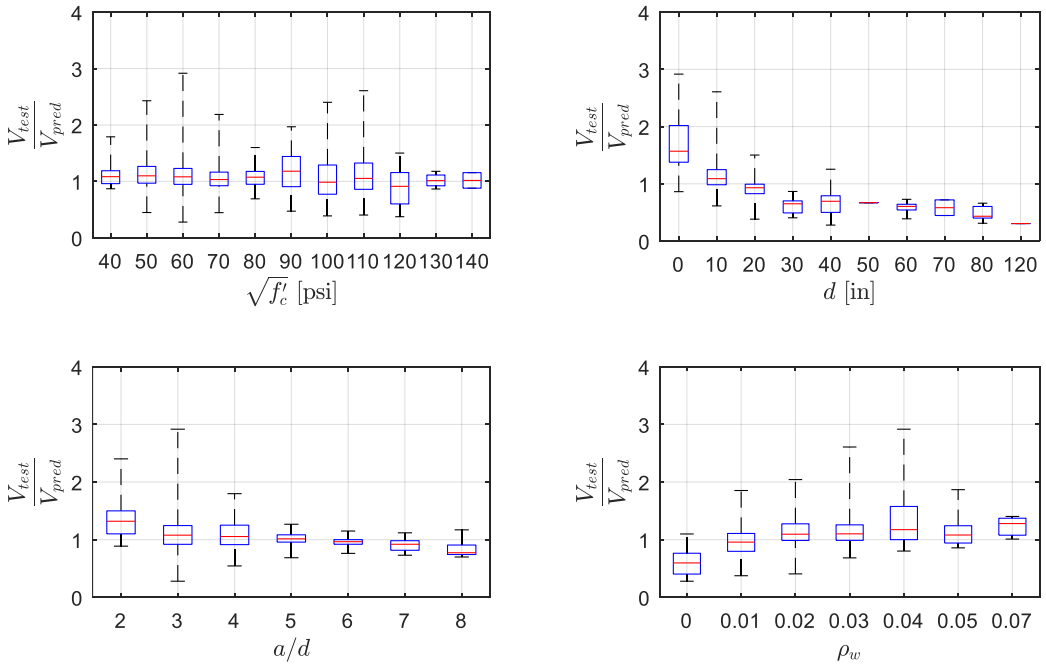

Fig. B2–V_{exp}/V_{pred} ratio for ACI 318-14 detailed

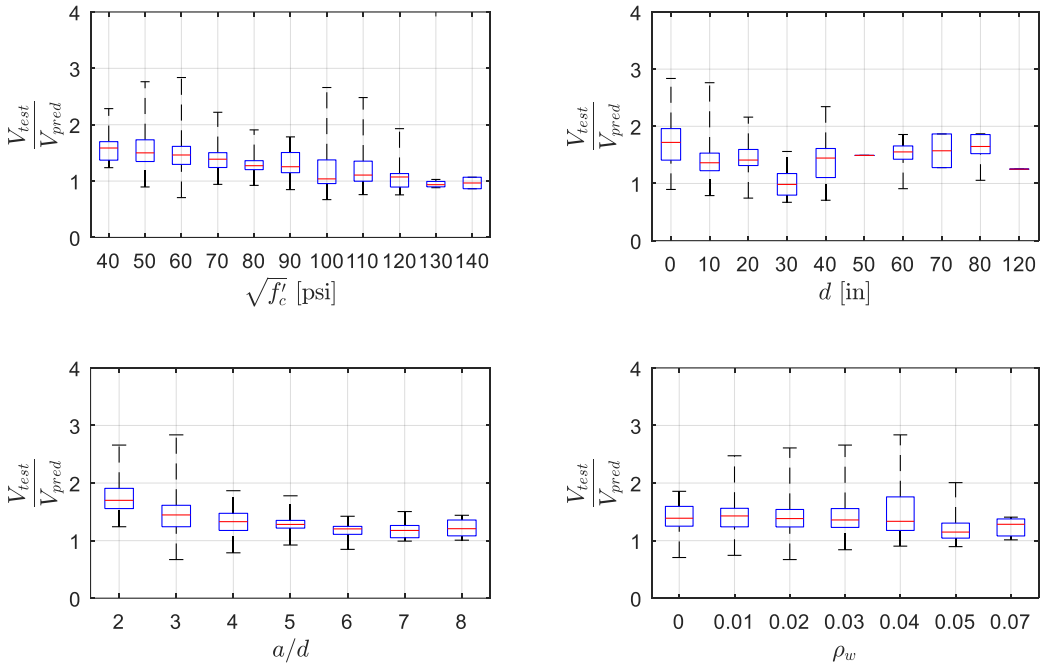

Fig. B3–V_{exp}/V_{pred} ratio for ACI 318-19

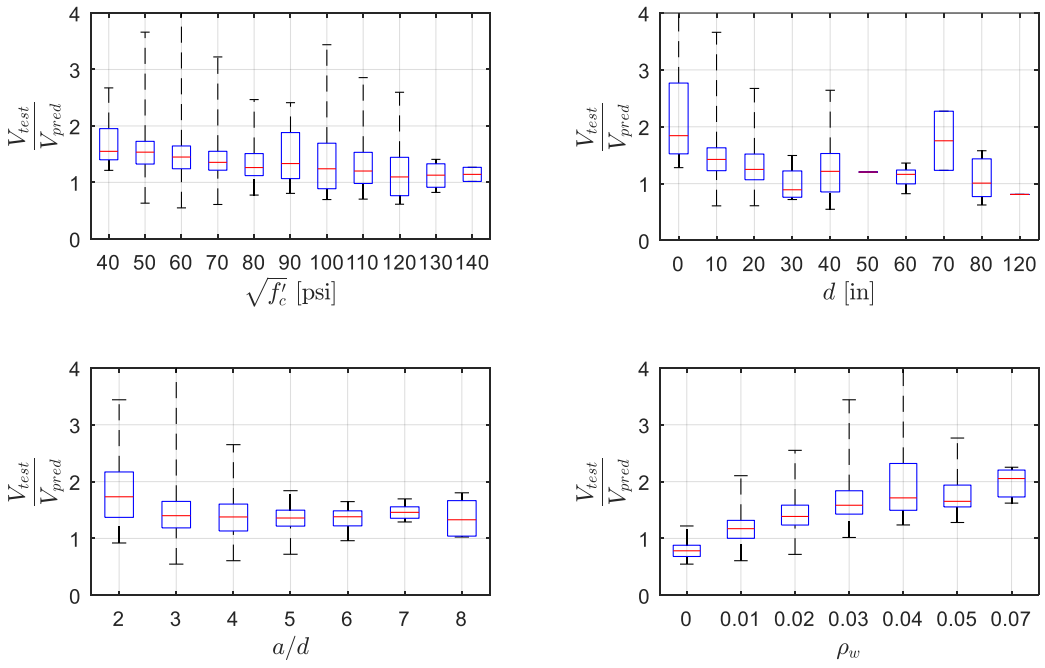

Fig. B4–V_{exp}/V_{pred} ratio for Bentz and Collins simplified method

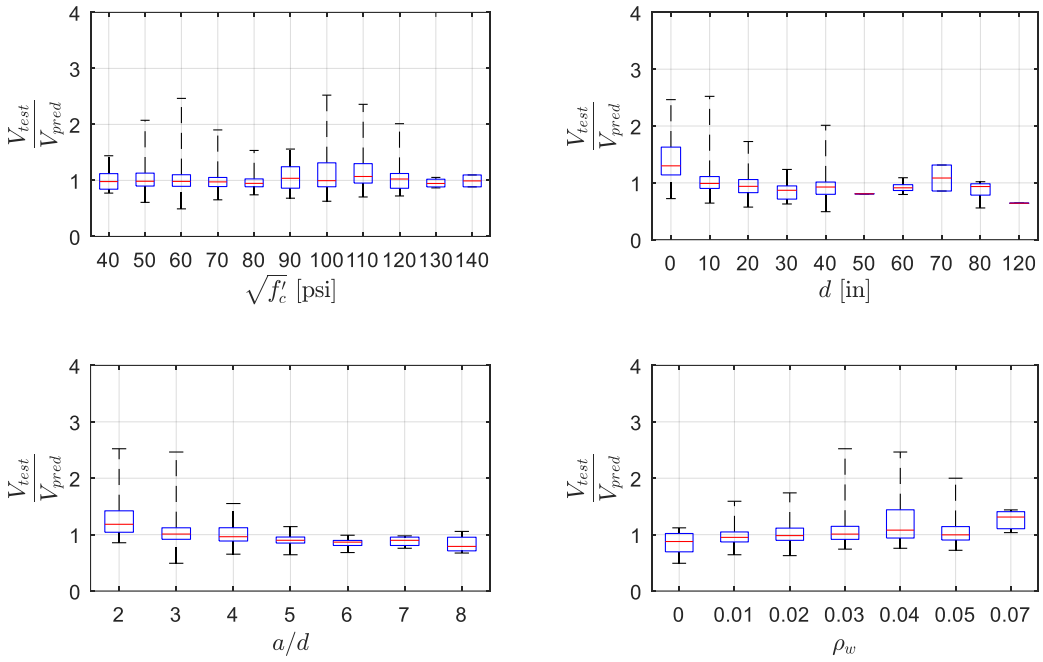

Fig. B5–V_{exp}/V_{pred} ratio for Bentz and Collins detailed method

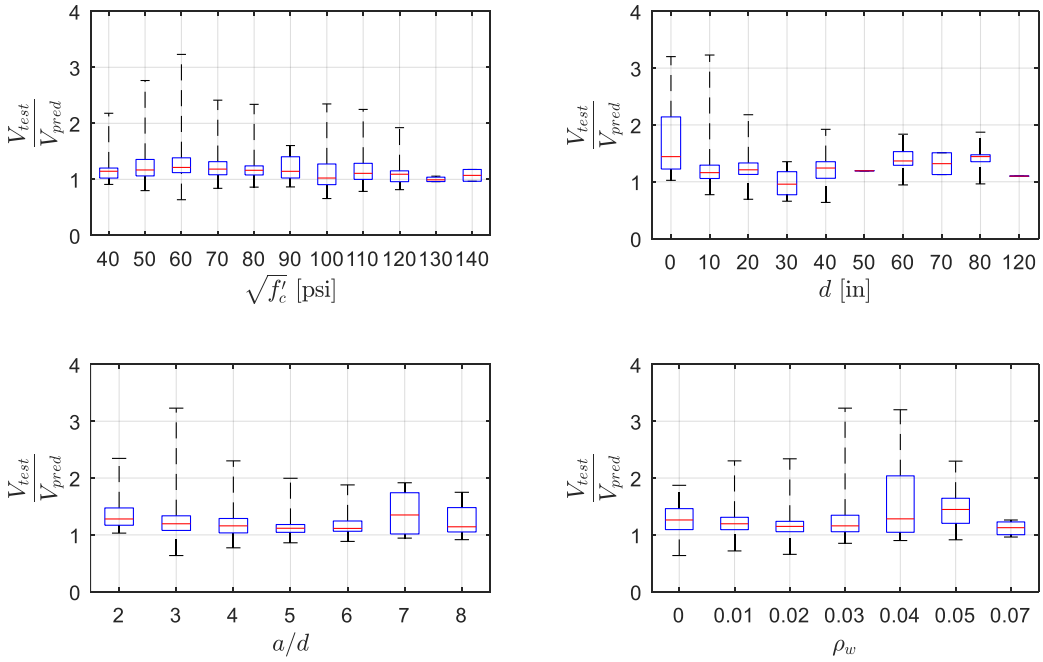

Fig. B6–V_{exp}/V_{pred} ratio for Cladera et al. method

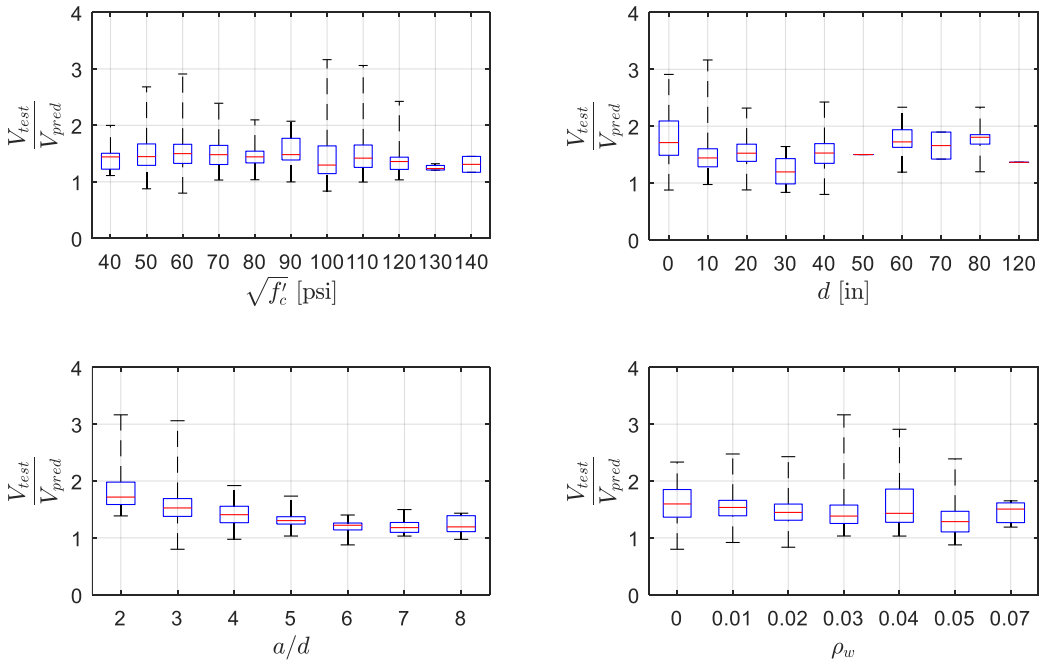

Fig. B7–V_{exp}/V_{pred} ratio for Frosch et al. method

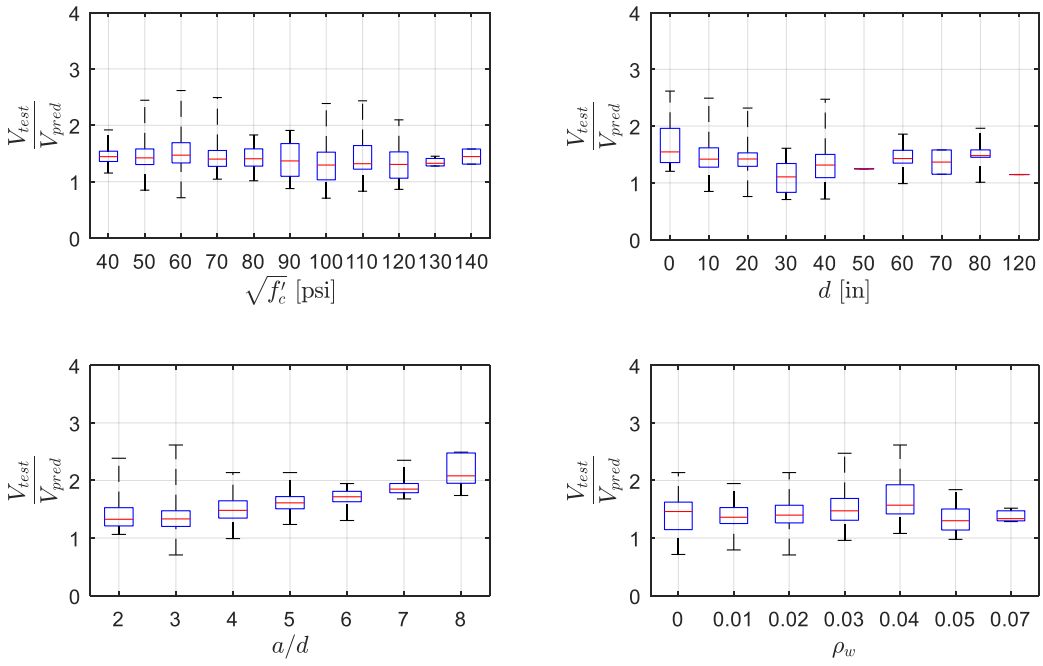

Fig. B8–V_{exp}/V_{pred} ratio for Li et al. method

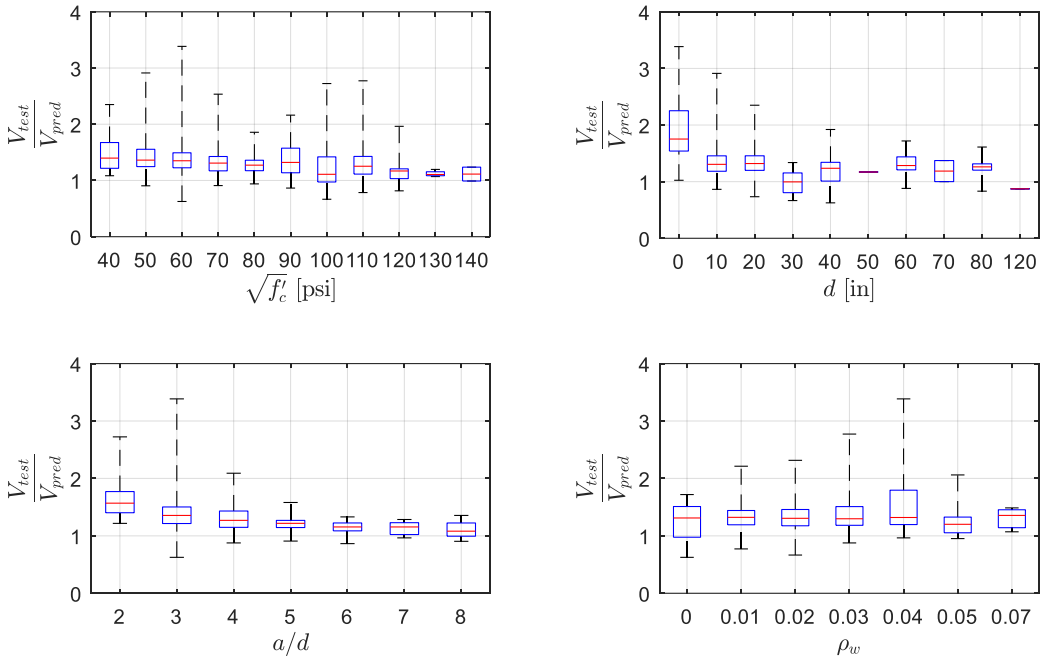

Fig. B9–V_{exp}/V_{pred} ratio for Park and Choi method

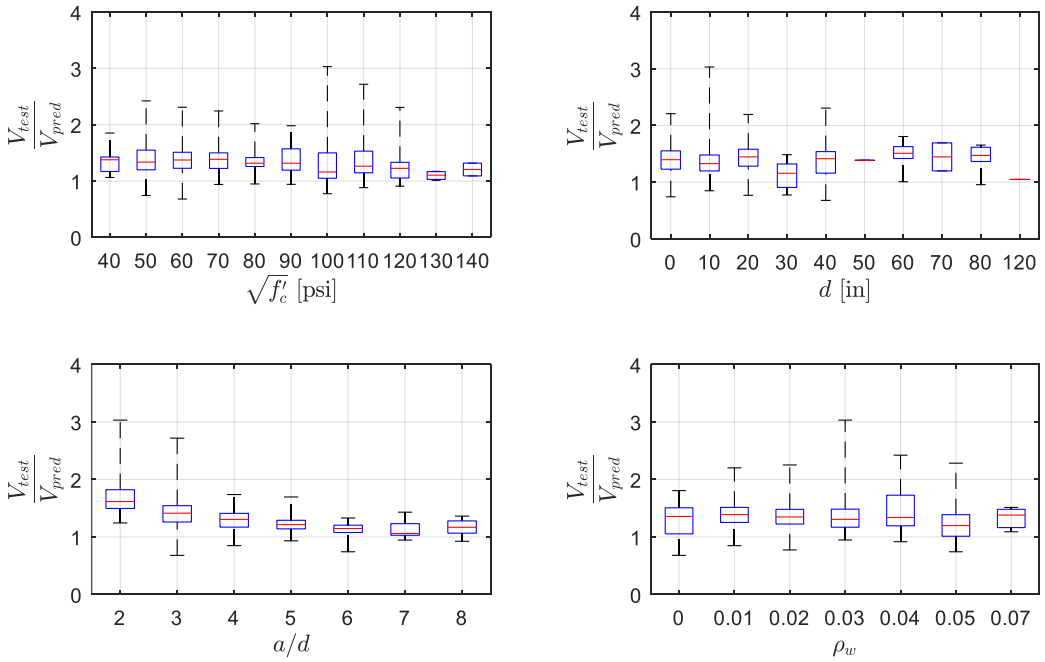

Fig. B10–V_{exp}/V_{pred} ratio for Reineck method

APPENDIX C: EVALUATION PLOTS FOR MEMBERS WITH WEB REINFORCEMENT

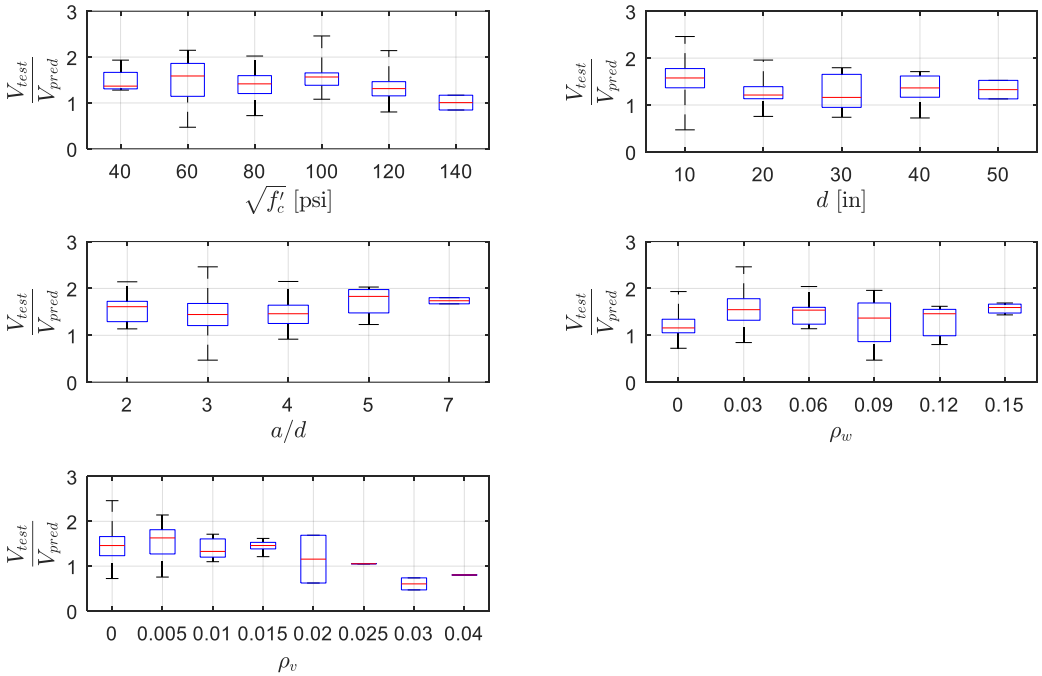

Fig. C1–V_{exp}/V_{pred} ratio for ACI 318-14 simplified

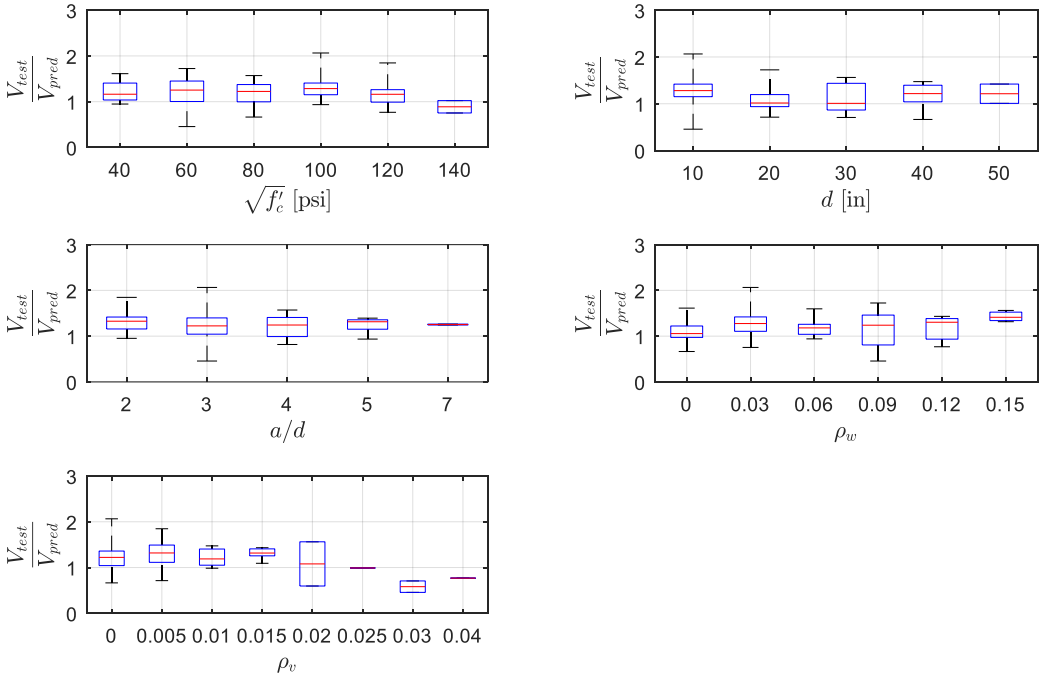

Fig. C2–V_{exp}/V_{pred} ratio for ACI 318-14 detailed

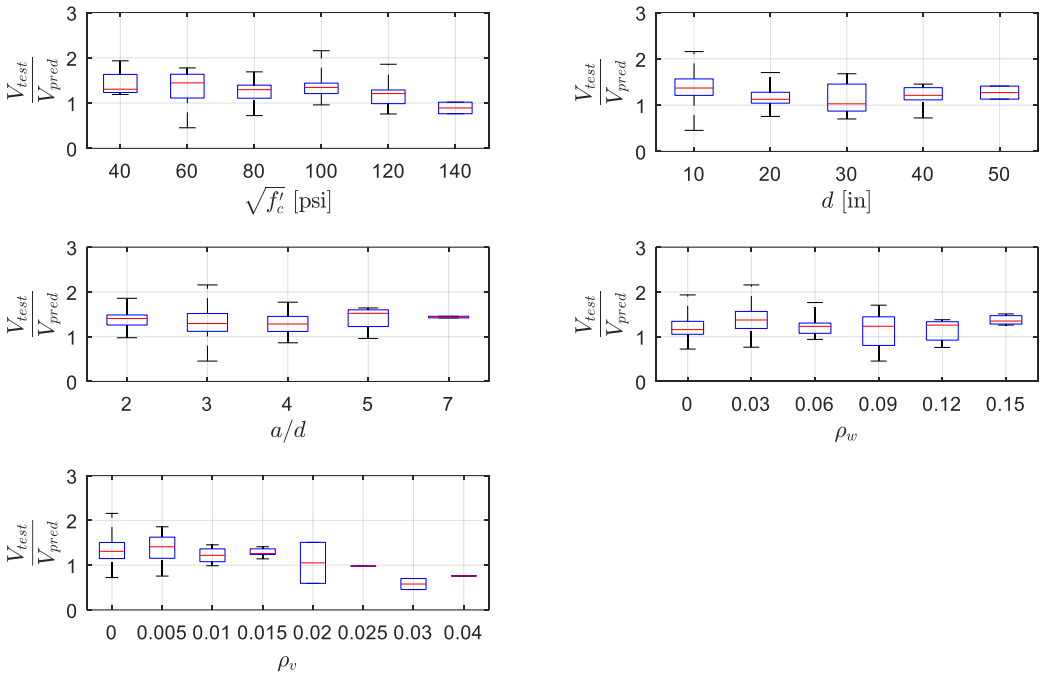

Fig. C3–V_{exp}/V_{pred} ratio for ACI 318-19

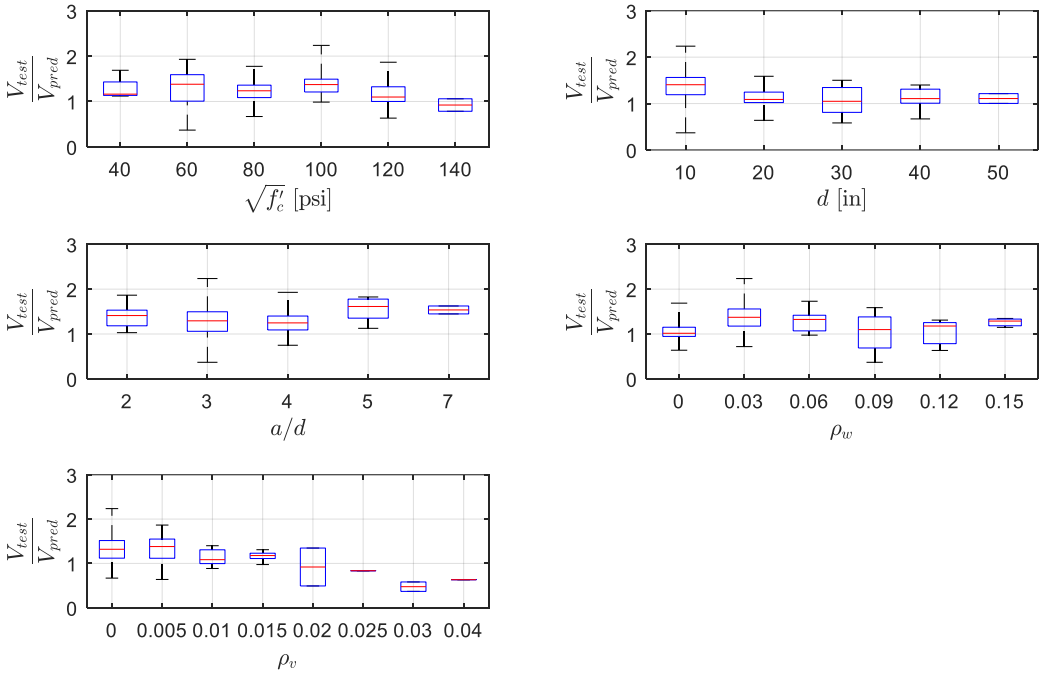

Fig. C4–V_{exp}/V_{pred} ratio for Bentz and Collins simplified method

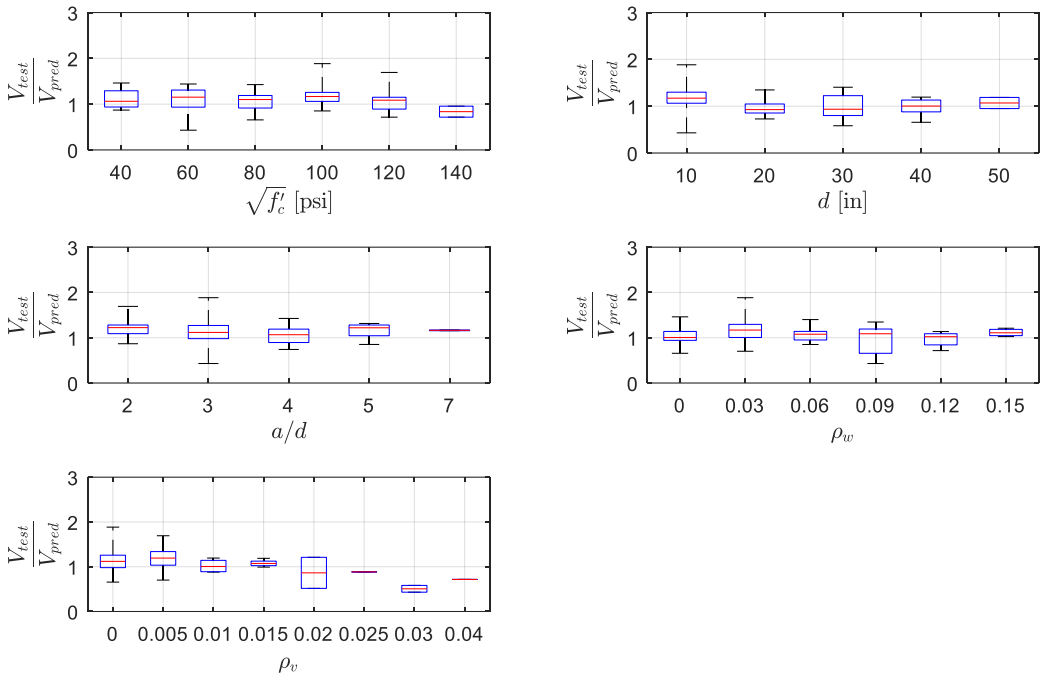

Fig. C5–V_{exp}/V_{pred} ratio for Bentz and Collins detailed method

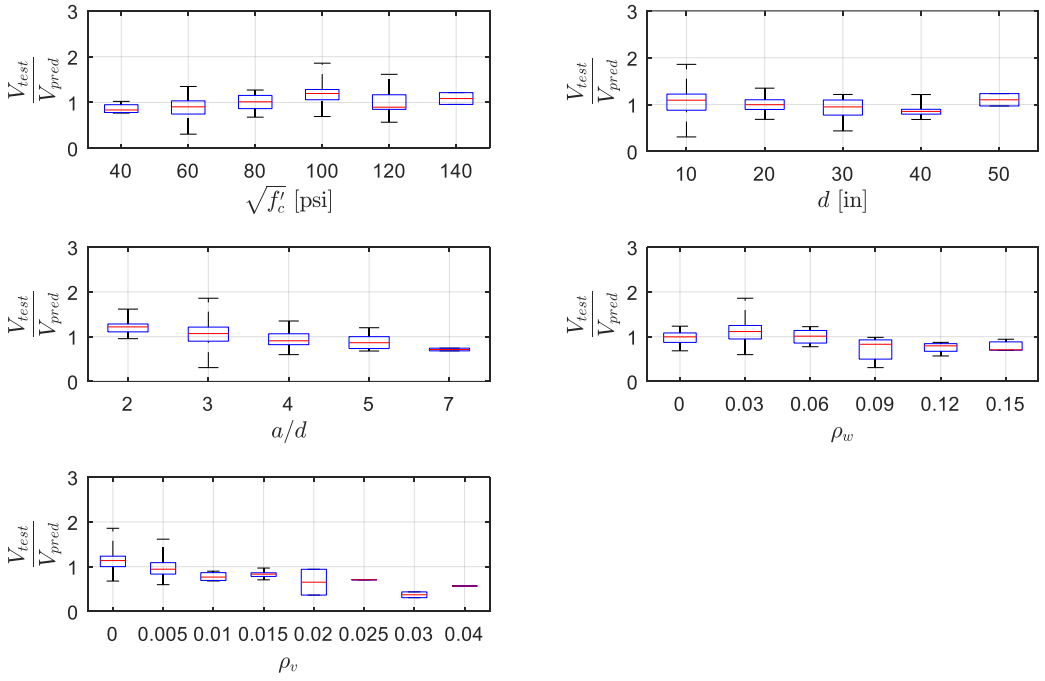

Fig. C6–V_{exp}/V_{pred} ratio for Cladera et al. method

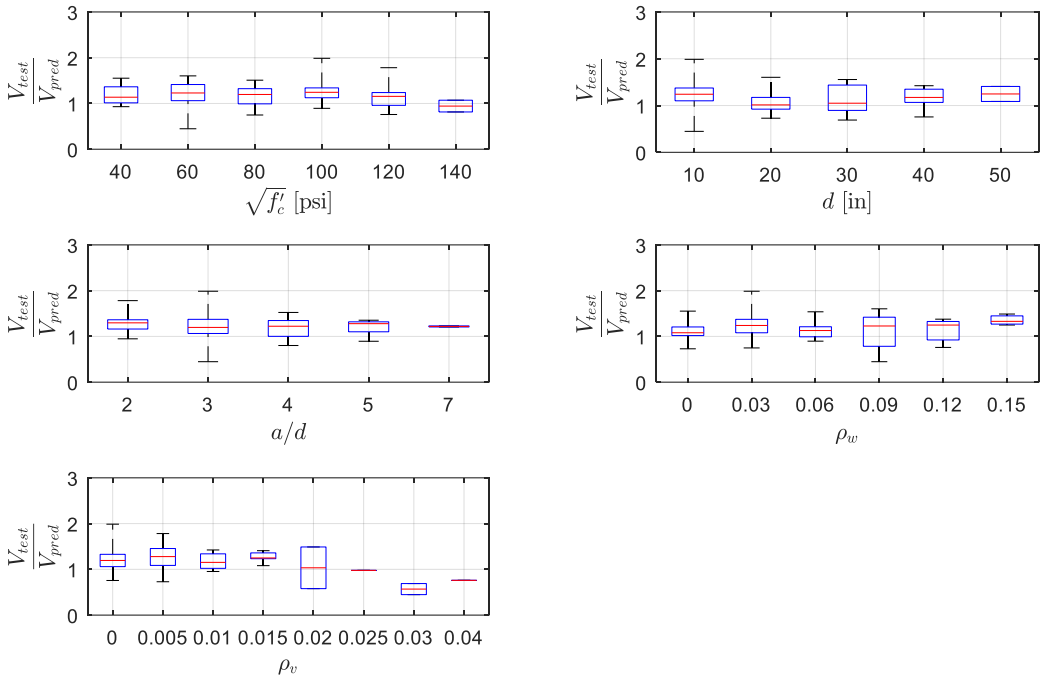

Fig. C7–V_{exp}/V_{pred} ratio for Frosch et al. method

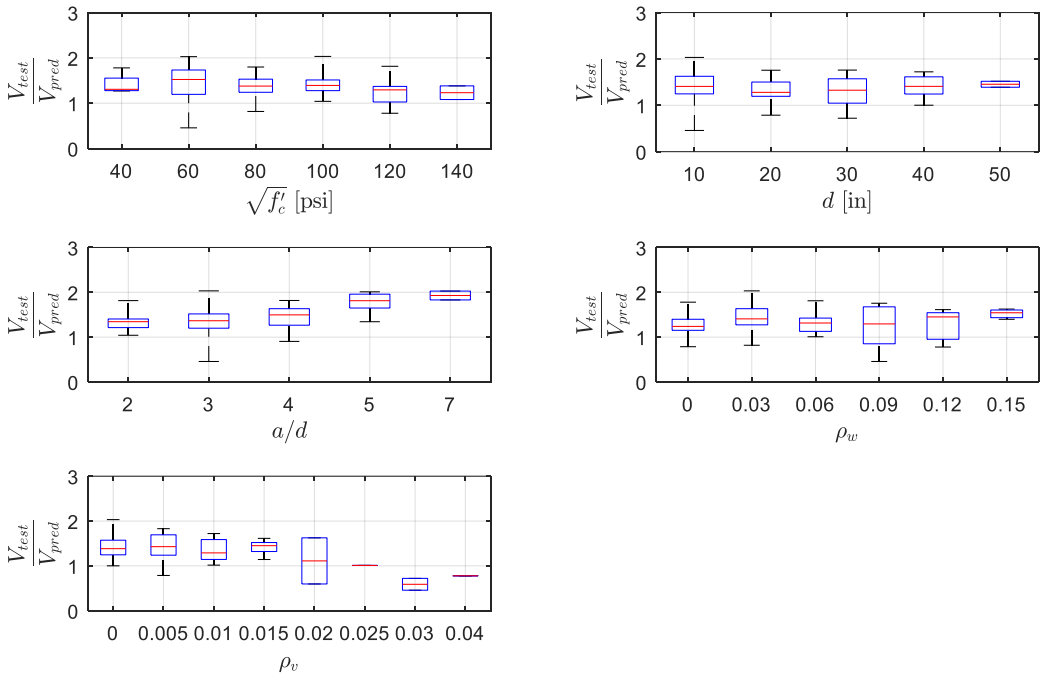

Fig. C8–V_{exp}/V_{pred} ratio for Li et al. method

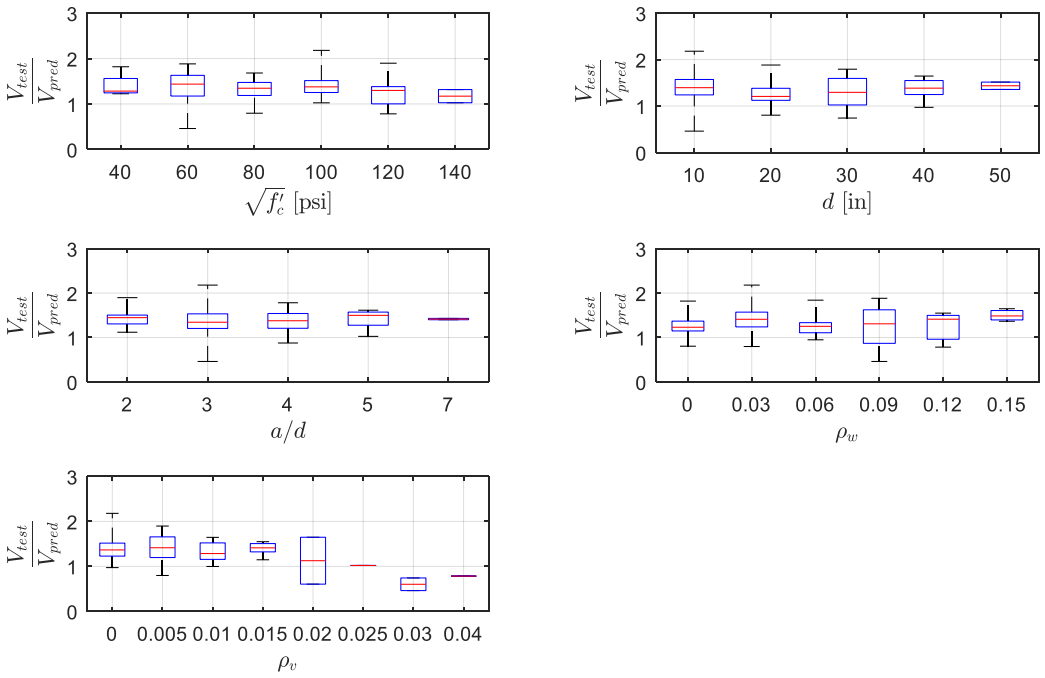

Fig. C9–V_{exp}/V_{pred} ratio for Park and Choi method

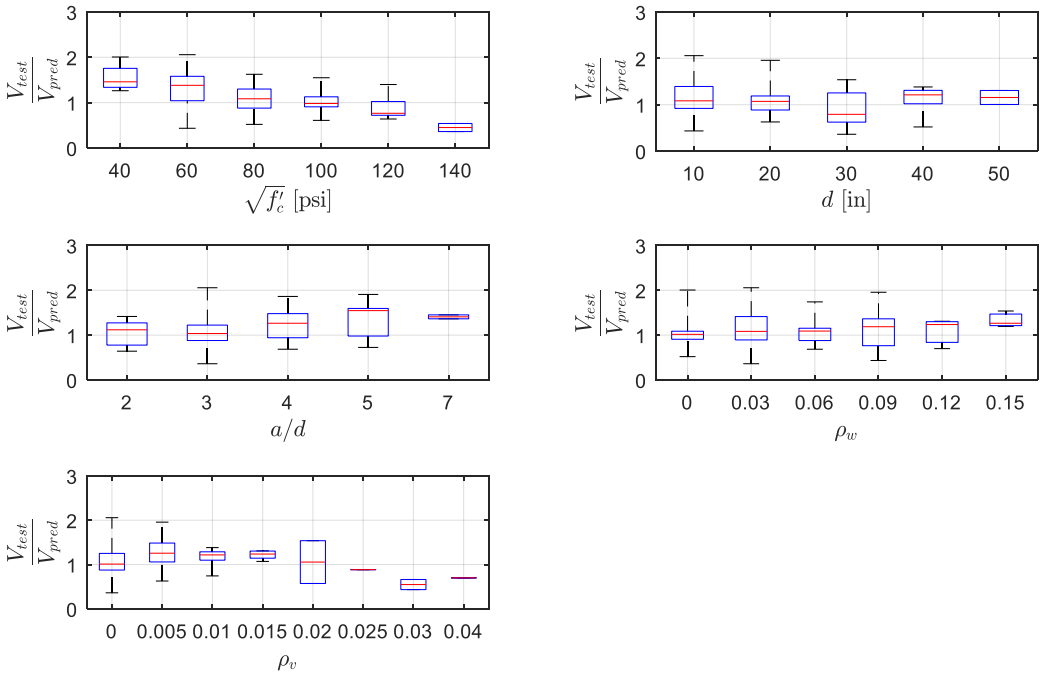

Fig. C10–V_{exp}/V_{pred} ratio for Reineck method